

# Conditional In Vivo Expression of the Fusion Kinase ITK-SYK

Konstanze Marie Pechloff

Dissertation zur Erlangung des akademischen Grades  
Doktor der Naturwissenschaften (Dr. rer. nat.)  
der Fakultät für Biologie  
der Ludwig-Maximilians-Universität München

München, 2012

Wesentliche Teile dieser Arbeit sind in folgender Publikation veröffentlicht:

Pechloff, K., Holch, J., Ferch, U., Schweneker, M., Brunner, K., Kremer, M., Sparwasser, T., Quintanilla-Martinez, L., Zimmer-Strobl, U., Streubel, B., Gewies, A., Peschel, C., and Ruland, J., "The Fusion Kinase ITK-SYK Mimics a T Cell Receptor Signal and Drives Oncogenesis in Conditional Mouse Models of Peripheral T Cell Lymphoma," *The Journal of Experimental Medicine*, Vol. 207, No.5, 2010, pp. 1031–1044.

Erstgutachter: PD Dr. Daniel Krappmann

Zweitgutachter: Prof. Dr. Heinrich Leonhardt

Promotionsgesuch eingereicht: 20.11.2012

Tag der mündlichen Prüfung: 25.06.2013

Ich versichere hiermit an Eides statt, dass die vorliegende Dissertation selbständig und ohne unerlaubte Hilfe angefertigt wurde. Weiterhin erkläre ich, dass die Dissertation nicht ganz oder in wesentlichen Teilen einer anderen Prüfungskommission vorgelegt worden ist und dass ich mich nicht anderweitig einer Doktorprüfung ohne Erfolg unterzogen habe.

München, den 20.11.2012

Konstanze M. Pechloff

# Acknowledgments

First of all, I would like to thank my advisor Prof. Dr. med. Jürgen Ruland for welcoming me into his thriving research group, as well as for providing me with his expertise and support throughout the years. I would also like to thank PD Dr. Daniel Krappmann for his endorsement and for representing this thesis at the Department of Biology of the Ludwig-Maximilians Universität München. Furthermore, I would like to thank Prof. Dr. Heinrich Leonhardt, Prof. Dr. Ruth Brack-Werner, Prof. Dr. Charles N. David, Prof. Dr. Angelika Böttger, and Prof. Dr. Dirk Eick for constituting the thesis committee. I would equally like to thank Prof. Dr. med. Christian Peschel and Prof. Dr. med. Heinz Höfler for providing access, respectively, to the research facilities of the III. Medizinischen Klinik des Klinikums rechts der Isar and the Institute of Pathology of the Technischen Universität München.

Daily lab-life is always facilitated through a functional network of peers. In this regard, I would like to thank all of my current and former colleagues for their encouragement, constructive discussions and support. I would especially like to thank Dr. Olaf Groß and Dr. Thomas Patzelt for introducing me to the work processes. Furthermore, I am grateful to all who have collaborated within the particular research project: Julian Holch, Dr. Uta Ferch, Dr. Marc Schweneker, Katja Meiners, Susanne Weiss, PD Dr. Leticia Quintanilla-Martinez de Fend, PD Dr. med. Marcus Kremer, PD Dr. Marc Schmidt-Supprian, Prof. Dr. med. univ. Berthold Streubel, Prof. Dr. Tim Sparwasser and PD Dr. Ursula Zimmer-Strobl. A special thank you goes out to Kristina Brunner for her reliable and excellent technical support in the lab as well as in mouse husbandry. In this regard, I would also like to thank the animal caretaker team of the Center of Preclinical Research of the Technischen Universität München. I am especially grateful to Dr. Andreas Gewies for his guidance, both as a colleague and as a friend. I would like to thank him as well as Julian Holch, Sebastian Kuhn and Dr. Melanie Kimm for providing valuable commentary on the underlying manuscript. I would further like to thank all members of the AG Duyster, the former AG Bernhard, AG Krackhard, AG Haas/Poeck, AG Jost and AG Groß for the cordial intergroup working environment.

Lastly, I want to express my deepest gratitude to my parents Jakob and Elisabeth Pechloff and to my brother Alexander for their love and support toward this goal.

# Zusammenfassung

Unspezifizierte periphere T-Zell-Lymphome (uPTZL) stellen eine Untergruppe der hoch aggressiven Non-Hodgkin-Lymphome dar, die durch eine hohe Rezidivanfälligkeit und eine schlechte Langzeitüberlebensrate gekennzeichnet sind. Die Heterogenität der uPTZL und deren weitgehend unverstandene molekulare Pathogenese erschweren die Etablierung spezifischer therapeutischer Ansätze. Berthold Streubel et al. [178] war es möglich, innerhalb der uPTZL das wiederkehrende Translokationsereignis  $t(5;9)(q33;q22)$  zu identifizieren, was zur Expression einer neuen Fusionskinase, ITK-SYK, führt. Sowohl ITK als auch SYK sind gut charakterisierte Tyrosinkinase und wichtige Bestandteile Antigenrezeptor-vermittelter Signaltransduktion. Die zellulären Folgen der ITK-SYK Aktivierung hingegen sind ungeklärt.

Ziel der vorliegenden Arbeit war es, den Einfluss von ITK-SYK auf T- bzw. B-Zellen zu untersuchen und der Frage nachzugehen, ob ein ursächlicher Zusammenhang zwischen der Expression der Fusionkinase und der Entstehung einer malignen T-Zell proliferativen Erkrankung besteht. *In vitro* Experimente zeigten, dass ITK-SYK konstitutiv mit T-Zell *lipid rafts* assoziiert ist und zur aktivierenden Phosphorylierung der T-Zell Rezeptor (TZR) proximalen Signalmoleküle PLC $\gamma$ 1, SLP-76 und LAT führt. Zusätzlich induzierte ITK-SYK die Aktivierung von AKT und der MAPKinasen p38 und ERK1. Letztendlich zeigten ITK-SYK exprimierende T-Zellen Merkmale akuter Aktivierung, wie die Expression des Oberflächenmarkers CD69 und die Sekretion des T-Zell stimulierenden Zytokins IL-2. Die Tatsache, dass anti-CD3/CD28 stimulierte T-Zellen ähnliche Aktivierungsmerkmale aufwiesen wie ITK-SYK exprimierende T-Zellen, führte zur Hypothese, dass ITK-SYK in der Lage ist, Aspekte eines TZR/kostimulatorischen Signals zu immitieren. Zur Untersuchung des onkogenen Potentials der Fusionskinase wurden konditionale transgene Mauslinien generiert, die mittels des Cre/loxP Rekombinasesystems eine Zelltyp-spezifische Expression von ITK-SYK ermöglichen. Tatsächlich entwickelten Mäuse mit T-Zell spezifischer ITK-SYK Expression Krankheits Symptome wie Apathie, gekrümmte Haltung mit einer abdominalen Umfangsvergrößerung, die anatomisch durch eine ausgeprägte Splenomegalie zu erklären war. Die Tiere starben in einem mittleren Alter von 21 Wochen. Periphere ITK-SYK exprimierende T-Zellen expandierten in der Maus und zeigten einen aktivierten Phänotyp, der sich durch eine Zellgrößen-

zunahme sowie der Expression des Aktivierungsmarkers CD44 und des Verlustes von CD62L, auszeichnete. Histologische Analysen zeigten ferner, dass die T-Zellen positiv für den Proliferationsmarker Ki-67 waren. Ihr klonales, infiltratives Wachstum in lymphoide und nicht-lymphoide Organe sowie ihre Transplantierbarkeit charakterisierte die lymphoproliferative Erkrankung als malignes PTZL. Interessanterweise zeigte eine B-Zell spezifische Expression der Fusionkinase keine Auswirkung auf B-Zell Entwicklung oder B-Zell Aktivierung. Da ITK-SYK spezifisch in *lipid rafts* von T-Zellen, jedoch nicht von B-Zellen detektierbar war, ist es möglich, dass der phänotypische Unterschied auf einer fehlenden Membranrekrutierung von ITK-SYK basiert. Diese *in vivo* Beobachtung wäre in Einklang mit den *in vitro* durchgeführten Mutationsanalysen, die gezeigt haben, dass sowohl die enzymatische Aktivität als auch die korrekte Membranpositionierung nötig ist, um das aktivierende Potential von ITK-SYK zu vermitteln.

Zusammenfassend lässt sich sagen, dass in dieser Arbeit Mausmodelle für Zelltypspezifische Expression der Fusionskinase ITK-SYK generiert wurden und somit erstmals der ursächliche Zusammenhang zwischen *in vivo* Expression der Fusionskinase und der Entstehung eines PTZLs gezeigt werden konnte. Anhand dieser Mausmodelle sollte es möglich sein, die Bedeutung individueller Signalmoleküle bzw. Signalwege in der ITK-SYK vermittelten Pathogenese von PTZL zu untersuchen. Basierend auf diesen Erkenntnissen könnten neue therapeutische Ansätze angedacht und präklinisch im Mausmodell untersucht werden.

# Abstract

Peripheral T cell lymphomas (PTCL), not otherwise specified (NOS), belong to the category of the most aggressive non-Hodgkin Lymphomas (NHL). They are associated with a high mortality rate, minimal effectiveness of conventional chemotherapy, and only 10-30% longterm survival. The molecular pathogenesis of this heterogenous group of lymphomas is not well understood, and pre-clinical animal models for the disease are lacking. Recently, the chromosomal translocation t(5;9)(q33;q22) was identified as a recurrent and specific genomic alteration in a subgroup of PTCL-NOS. This translocation fuses the spleen tyrosine kinase (SYK) gene to the interleukin-2 (IL-2)-inducible T cell kinase (ITK) gene, leading to the expression of the fusion tyrosine kinase ITK-SYK. Both, ITK and SYK are required for normal antigen-induced lymphocyte activation, however, the molecular and cellular consequences of ITK-SYK expression in lymphocytes are unknown.

By combining *in vitro* analysis with the generation of conditional mouse models expressing the fusion kinase ITK-SYK in a cell-type specific manner, it is shown that ITK-SYK associates constitutively with lipid rafts in T cells and triggers antigen independent phosphorylation of T cell receptor (TCR) proximal proteins such as SLP-76, LAT, and PLC $\gamma$ 1. These events lead to constitutive activation of downstream AKT, ERK and p38 MAP kinase pathways and induce acute cellular outcomes that correspond to regular TCR ligation, including upregulation of CD69 and production of Interleukin-2 *in vitro*, as well as deletion of thymocytes and activation of peripheral T cells *in vivo*. Ultimately, conditional expression of ITK-SYK in mice induces malignant PTCLs with 100% penetrance carrying features reminiscent of the human disease. The work at hand provides data demonstrating that ITK-SYK constitutively engages antigen receptor signaling pathways in T cells, eventually culminating in the development of malignant PTCLs. Therefore *in vivo* evidence is provided that constitutively enforced antigen receptor signaling can, in principle, act as a powerful oncogenic driver in lymphoma pathogenesis. Moreover, a clinically relevant model of PTCL was generated. It can serve as a valuable tool in identifying and verifying compounds for treatment strategies against PTCL.

# Contents

Acknowledgements . . . . .	iv
Zusammenfassung . . . . .	v
Abstract . . . . .	vii
Contents . . . . .	viii
List of Figures . . . . .	xi
Abbreviations . . . . .	xiii
<b>1 Introduction</b>	<b>1</b>
1.1 Adaptive Immunity . . . . .	1
1.1.1 Features . . . . .	1
1.1.2 T Cell and B Cell Development . . . . .	2
1.1.3 T Cell and B Cell Activation . . . . .	3
1.2 Antigen Receptor Signaling . . . . .	4
1.2.1 T Cell Receptor Signaling . . . . .	4
1.2.2 B Cell Receptor Signaling . . . . .	10
1.2.3 The IL-2 Inducible T Cell Kinase . . . . .	10
1.2.4 The Spleen Tyrosine Kinase . . . . .	12
1.3 Peripheral T Cell Lymphoma Not Otherwise Specified . . . . .	15
1.3.1 Definition, Incidence, and Etiology . . . . .	15
1.3.2 Clinical Presentation and Therapeutic Approaches . . . . .	16
1.3.3 Phenotypic Characterization . . . . .	17
1.3.4 Genetic Characterization . . . . .	18
1.4 Translocation t(5;9)(q33;q22) and the Fusion Kinase ITK-SYK . . . . .	19
<b>2 Research Objective</b>	<b>21</b>
<b>3 Materials</b>	<b>23</b>
3.1 Reagents . . . . .	23
3.2 Employed Antibodies . . . . .	23
3.2.1 Westernblot Analysis . . . . .	23
3.2.2 Stimulation Experiments . . . . .	23

3.2.3	Flowcytometry: Extracellular Staining Panel . . . . .	24
3.2.4	Flowcytometry: Intracellular Staining Panel . . . . .	25
3.2.5	Immunohistochemistry . . . . .	25
3.3	Employed Primer . . . . .	25
3.3.1	ITK-SYK cDNA and Mutant Generation . . . . .	25
3.3.2	Southern Probe Amplifikation . . . . .	26
3.3.3	Genotyping . . . . .	26
3.3.4	Genescan Analysis . . . . .	26
<b>4</b>	<b>Methods</b>	<b>28</b>
4.1	Work with Nucleic Acids . . . . .	28
4.1.1	Determination of Nucleic Acid Concentration . . . . .	28
4.1.2	Agarose Gelectrophoresis . . . . .	28
4.1.3	Polymerase Chain Reaction . . . . .	29
4.1.4	Reverse Transcriptase-Polymerase Chain Reaction . . . . .	29
4.1.5	Genescan Analysis . . . . .	30
4.1.6	Molecular Cloning . . . . .	31
4.1.7	Southernblot Analysis . . . . .	32
4.2	Work with Proteins . . . . .	33
4.2.1	Westernblot Analysis . . . . .	33
4.2.2	Lipid Raft Preparations . . . . .	34
4.3	Work with Retroviruses . . . . .	35
4.3.1	Retroviral Expression Vectors . . . . .	35
4.3.2	Retroviral Transduction . . . . .	36
4.4	Work with Eukaryotic Cells . . . . .	37
4.4.1	Basic Cell Culture . . . . .	37
4.4.2	Embryonic Stem Cell Culture . . . . .	38
4.4.3	Embryonic Stem Cell Electroporation and Selection . . . . .	38
4.4.4	Cell Purification . . . . .	39
4.4.5	Cell Stimulation . . . . .	40
4.4.6	Enzyme-linked Immunosorbent Assay . . . . .	41
4.4.7	Flow Cytometry . . . . .	41
4.5	Work with Mice . . . . .	42
4.5.1	Mouse Husbandry . . . . .	42
4.5.2	Generation of ROSA26 <sup>loxSTOPlox-ITK-SYK</sup> Mice . . . . .	42
4.5.3	Mouse Breeding Approaches . . . . .	43
4.5.4	Genotyping . . . . .	43
4.5.5	Transplantation . . . . .	44
4.5.6	Histology . . . . .	44

4.6	Statistical Analysis . . . . .	45
<b>5</b>	<b>Results</b>	<b>46</b>
5.1	ITK-SYK Expression Leads to T Cell Activation <i>In Vitro</i> . . . . .	46
5.2	Mouse Model for Conditional ITK-SYK Expression . . . . .	52
5.2.1	Targeting the ROSA26 Locus . . . . .	52
5.2.2	Cell Type Specific Expression of ITK-SYK . . . . .	55
5.2.3	ITK-SYK Can Imitate a TCR Signal <i>In Vivo</i> . . . . .	56
5.2.4	ITK-SYK Does Not Affect BCR Signaling <i>In Vivo</i> . . . . .	61
5.3	Peripheral T Cell Lymphoma in ITK-SYK Expressing Mice . . . . .	66
5.3.1	ITK-SYK Expression in T Cells Results in a Fatal Lymphoproliferative Disease with Neoplastic Character . . . . .	66
5.3.2	Sporadic ITK-SYK Expression in Single T Cells is Able to Induce T Cell Lymphomas in ITK-SYK <sup>CD19-Cre</sup> mice . . . . .	74
<b>6</b>	<b>Discussion</b>	<b>79</b>
6.1	ITK-SYK: Investigating a Novel Fusion Protein . . . . .	79
6.2	<i>In Vitro</i> Implications of Aberrant ITK-SYK Signaling . . . . .	80
6.3	Structural Aspects of ITK-SYK and its Potential Mode of Action . . . . .	82
6.4	Pathological Outcome of ITK-SYK Expression . . . . .	86
<b>7</b>	<b>Summary and Outlook</b>	<b>90</b>
	<b>Bibliography</b>	<b>93</b>

# List of Figures

1.1	The TCR/CD3 and BCR/Ig complex composition. . . . .	6
1.2	Key TCR signaling events. . . . .	9
1.3	Schematic view of the ITK protein domain structure. . . . .	11
1.4	Schematic view of the SYK protein domain structure. . . . .	13
1.5	Schematic view of ITK, SYK, and the fusion kinase ITK-SYK. . .	19
5.1	Schematic view of the fusion kinase ITK-SYK and its mutants. .	47
5.2	ITK-SYK induces signaling events similar to a TCR signal <i>in vitro</i>	49
5.3	ITK-SYK induces cellular outcomes similar to a TCR signal <i>in vitro</i> . . . . .	51
5.4	Successful targeting of the ROSA26 locus. . . . .	54
5.5	Breeding scheme. . . . .	55
5.6	Conditional expression of ITK-SYK in T cells or B cells <i>in vivo</i> . .	56
5.7	ITK-SYK induces loss of thymocytes in ITK-SYK <sup>CD4-Cre</sup> mice. .	58
5.8	ITK-SYK induces loss of peripheral T cells in ITK-SYK <sup>CD4-Cre</sup> mice. . . . .	59
5.9	ITK-SYK expressing T cells exhibit an activated phenotype <i>in vivo</i> . . . . .	60
5.10	ITK-SYK expressing T cells proliferate but do not undergo apoptosis <i>in vivo</i> . . . . .	61
5.11	B cell-intrinsic ITK-SYK expression does not affect B cell development. . . . .	63
5.12	Lacking B cell activation and T cell specific recruitment of ITK-SYK into lipid rafts. . . . .	65
5.13	Conditional expression of ITK-SYK in T cells induces a fatal lymphoproliferative disease. . . . .	68
5.14	Severe organ infiltration caused by abnormal T cell expansion in ITK-SYK <sup>CD4-Cre</sup> mice. . . . .	69
5.15	Selective expansion of distinct T cell clones in affected ITK-SYK <sup>CD4-Cre</sup> mice. . . . .	72

5.16 Proliferation and infiltration of ITK-SYK expressing T cells upon transplantation. . . . .	73
5.17 ITK-SYK <sup>CD19-Cre</sup> mice develop a lymphoproliferative disease. . .	76
5.18 ITK-SYK <sup>CD19-Cre</sup> mice display organ infiltration by activated T cells. . . . .	77
5.19 Selective expansion of distinct T cell clones in ITK-SYK <sup>CD19-Cre</sup> mice. . . . .	78
6.1 Model of ITK-SYK induced TCR signaling. . . . .	85

# Abbreviations

<b>Instance</b>	<b>Expansion</b>
A	deoxyadenylate
AF647	Alexa Fluor <sup>®</sup> 647
AgR	antigen receptor
AITL	angiimmunoblastic T cell lymphoma
ALCL	anaplastic large cell lymphoma
ALK	anaplastic lymphoma receptor tyrosine kinase
AKT	v-akt murine thymoma viral oncogene homolog
AP-1	activator protein 1
APC	antigen presenting cell/ allophycocyanin
ASCT	allogeneic stem cell transplantation
ATP	adenosine triphosphate
BCL	B cell lymphoma/leukemia
BCR	B cell receptor
BLK	B lymphoid tyrosine kinase
BLNK	B cell linker
BM	bone marrow
bp	base pair
BSA	bovine serum albumine
BTK	bruton agammaglobulinemia tyrosine kinase
°C	degree Celsius
C	deoxycytidylate (nucleotide)/ cysteine (amino acid)
CARD	caspase recruitment domain
CARMA1	CARD-containing protein 11
CD	cluster of differentiation
cDNA	complementary deoxyribonucleic acid
CHAPS	3-[(3-cholamidopropyl)dimethylammonio]-1-propanesulfonate
CHOP	cyclophosphamide, doxorubicine, vincristine, prednisone
CIAP	calf intestine alkaline phosphatase

<b>Instance</b>	<b>Expansion</b>
CML	chronic myeloid leukemia
Cre	protein recombinase of the phage P1
DAG	diacylglycerol
DEPC	diethylpyrocarbonate
DMEM	Dulbecco's Modified Eagle Medium
DN	double negative
dNTP	deoxyribonucleoside triphosphate
DP	double positive
dp-ITAM	double phosphorylated immunoreceptor tyrosine-based activation motif
DTT	dithiothreitol
E	ecotroph
<i>E. coli</i>	<i>Escherichia coli</i>
EDTA	ethylenediaminetetraacetic acid
eGFP	enhanced green fluorescent protein
EGTA	ethyleneglycoltetraacetic acid
ELISA	enzyme-linked immunosorbent assay
ERK	extracellular signal-regulated protein kinase
ESC	embryonic stem cell
FACS	fluorescence activated cell sorting
FAM	6-carboxyfluorescein
FB	FACS buffer
FBS	fetal bovine serum
FC	feeder cells
FDA	Food and Drug Administration
FO	follicular
FRT	flippase recombination enzyme recognition target
fwd	forward
FYN	FYN oncogene related to SRC, FGR, YES
G	deoxyguanylate
GADS	GRB2-related adaptor protein 2
GC	germinal center
GEF	guanine nucleotide exchange factor
GTP	guanosine triphosphate
GM1	monosialotetrahexosylganglioside 1
GRB2	growth factor receptor-bound protein 2
h	hour

<b>Instance</b>	<b>Expansion</b>
HA	hemagglutinin
HDAC	histone deacetylase
H&E	hematoxylin and eosin
HRP	horseradish peroxidase
IFN	interferon
Ig	immunoglobulin
I $\kappa$ B	inhibitor of kappa B
IKK	inhibitor of kappa B kinase
IL	interleukine
IP3	inositol (1,4,5)-trisphosphate
IRES	internal ribosomal entry site
IRF	interferon regulatory factor
ITK	IL-2 inducible T cell kinase
J	Joule
JAK	Janus kinase
JNK	c-Jun amino-terminal kinase
K	lysine
kb	kilobase
KD	kinase dead
kDa	kilodalton
KID	kidney
LAT	linker for activation of T cells
LCK	lymphocyte-specific protein tyrosine kinase
LIF	leucemic inhibitory factor
LIV	liver
LN	lymph node
LNG	lung
LYN	v-yes-1 Yamaguchi sarcoma viral related oncogene homolog
loxP	locus of crossover in P1 bacteriophage
MALT1	mucosa associated lymphoid tissue lymphoma translocation gene 1
MAPK	mitogen-activated protein kinase
MEK	MAPK/ERK kinase
MES	2-(N-morpholino)ethanesulfonic acid
MHC	major histocompatibility complex
MIG	MSCV-based vector with IRES-eGFP element
min	minute

<b>Instance</b>	<b>Expansion</b>
ml	mililiter
mRNA	messenger RNA
MSCV	murine stem cell virus
mTOR	mammalian target of rapamycin
mut	mutated
MZ	marginal zone
NEO	neomycin cassette
NFAT	nuclear factor of activated T cells
NF $\kappa$ B	nuclear factor kappa B
NHL	non-Hodgkin lymphoma
NK	natural killer
nm	nanometer
nM	nanomolar
OD	optical density
o/n	over night
pA	polyadenylation signal sequence
PAGE	polyarylamid gelelectrophoresis
PBS	phosphate buffered saline
PC	peritoneal cavity
PCR	polymerase chain reaction
PE	phycoerythrin
PE-Cy5	phycoerythrin cyanin
PDGFR	platelet-derived growth factor receptor
PDK1	pyruvate dehydrogenase kinase, isozyme 1
pen	penicillin
PFA	paraformaldehyde
PH	pleckstrin homology
pH	potentia hydrogenium
PI	propidium iodide
PI3K	phosphatidylinositol 3-kinase
PIP2	phosphatidylinositol (4,5)-bisphosphate
PIP3	phosphatidylinositol (3,4,5)-trisphosphate
PKB	protein kinase B
PKC	protein kinase C
PLC $\gamma$ 1	phospholipase C gamma 1
POP	performance optimized polymer

<b>Instance</b>	<b>Expansion</b>
PTCL-NOS	peripheral T cell lymphoma, not otherwise specified
PVDF	polyvinylidene difluoride
R	arginine
RACE	rapid amplification of cDNA ends
RasGRP	ras guanyl releasing protein 1
RE	restriction endonuclease
Rec	recombinant
rev	reverse
RFU	relative fluorescent unit
RNA	ribonucleic acid
rpm	revolutions per minute
RT	room temperature
RT	Reverse Transcriptase
R26	Rosa26
s	second
SA	splice acceptor site
SH	SRC homology
SDS	sodium dodecylsulfate
SLP	SH2 domain containing leukocyte protein
SP	single positive
SPL	spleen
SRC	v-src sarcoma viral oncogene homolog
SSC	saline sodium citrate
STAT	signal-transducer and activator of transcription
strep	streptomycin
SYK	spleen tyrosine kinase
T	thymidylate (nucleotide)/ threonine (amino acid)
t	translocation
TAE	tris acetate EDTA
TAK1	TGF-beta activated kinase 1
TEC	tyrosine kinase expressed in hepatocellular carcinoma
TCR	T cell receptor
TMB	3,3',5,5'-tetramethylbenzidine
TRAF6	TNF receptor-associated factor 6
U	unit
UV	ultraviolet

<b>Instance</b>	<b>Expansion</b>
V	volt
v	volume
VAV1	vav 1 guanine nucleotide exchange factor
w	weight
WT	wildtype
Y	tyrosine
ZAP-70	zeta-chain associated protein kinase 70
$\mu\text{g}$	microgramm
$\mu\text{l}$	microliter
$\mu\text{M}$	micromolar

# Chapter 1

## Introduction

### 1.1 Adaptive Immunity

#### 1.1.1 Features

Triggering cellular responses to pathogenic intruders or nonself structures arising from within the organism itself requires crosstalk between immune cells and functional signaling within the involved cells. The immune system can be roughly divided into two branches: the innate and the adaptive immune response. Distinct in their timing and ways of attacking, however, the adaptive and the innate immune cells are interdependent and work together in their joint endeavor for protection [90].

The major players of the adaptive immune response are T cells and B cells. One common feature of both lymphocytes is their surface expression of a clonotypic antigen receptor. These multiprotein complexes termed the T cell receptor (TCR) and the B cell receptor (BCR) are specialized in antigen recognition and are the starting point from where signal transduction is initiated. A network of transmembrane and intracellularly located proteins and other molecules are responsible for relaying the signal from the antigen receptor (AgR) towards the nucleus, inducing cellular outcomes as distinct as cell survival, proliferation, differentiation or cell death. In the case of an activating scenario, naive mature lymphocytes expand clonally upon antigen encounter and develop into effector cells, taking part in clearing the pathological situation [90]. Yet, adaptive immune cells can become subject to transforming processes, potentially leading up to the development of lymphoid leukemia or lymphoma [98, 162, 5].

Since both developing and activated T cells and B cells are the subject of investigation as to whether *de novo* expression of the previously described fusion kinase ITK-SYK [178] mediates lymphomagenesis, fundamentals on both cell types will first be given. Additionally, the main concepts and players in the signaling pathways emerging downstream of the TCR and the BCR complex will be outlined. On this basis, the results in

the work at hand will be discussed and interpreted.

### 1.1.2 T Cell and B Cell Development

Both T cells and B cells develop from common lymphoid progenitors generated in the bone marrow. While B cell development is continued in the same environment, early T cell progenitors colonize the thymus to complete their development [90].

T cell development is characterized by a chemokine-driven migration of T cell progenitors throughout anatomically distinct thymic regions [180]. During this process, maturation and selection of thymocytes occurs, eventually leading to the release of naive mature T cells to colonize secondary lymphatic organs [127]. The majority of T cells present in secondary lymphoid organs are  $\alpha\beta$  T cells, referring to the expression of a TCR $\alpha$  and TCR $\beta$  chain. During development,  $\alpha\beta$  T cells have to master several selection steps. First, successful TCR $\beta$  gene rearrangement with subsequent preTCR complex formation has to occur at the stage of double negative (DN) thymocytes, as are defined by their lack of CD4 and CD8 coreceptor expression. Having passed this so called beta selection, DN thymocytes initiate CD4 and CD8 gene expression and mature to the double positive (DP) state. After successful rearrangement of the TCR $\alpha$  gene locus, surface expression of both the TCR $\alpha$  and the TCR $\beta$  chain takes place. Together with the already expressed CD3 molecules, a full TCR complex is formed and transferred onto the cell surface [31]. According to an avidity model, DP thymocytes which successfully, yet weakly, recognize self peptides bound to major histocompatibility complexes (MHCs), are positively selected, thus rescued from apoptosis and mature to the single positive (SP) state, either expressing the CD4 or the CD8 coreceptor [31]. In the case of a high avidity interaction between the TCR and MHC/self peptide complexes, however, DP thymocytes undergo negative selection and die [31]. Rescued naive mature SP T cells leave the thymus and colonize secondary lymphatic tissues.

In accordance to T cells, maturing B cells are screened for successful immunoglobulin (Ig) heavy and light chain expression, as well as for their potential risk of recognizing self antigens [103]. In brief, B cell progenitors evolve to a pro B cell state by rearranging their heavy chain Ig locus. Upon successful signaling from a pre-BCR complex, pro B cells mature to the pre B cell state. At this stage, the light chain Ig locus is rearranged which leads to the expression of a full BCR complex on the cell surface, obtaining the status quo of an immature B cell [103]. The BCR complex now consists of a surface IgM molecule associated with the signaling relevant Ig $\alpha$  and Ig $\beta$  molecules. By interacting with stromal cells, immature B cells are exposed to self antigens. B cells expressing AgRs which do not show self peptide recognition receive a survival signal and mature. Recognition of self antigen, however, leads either to its death by apoptosis, a state of unresponsiveness or the cell is offered one more round of Ig light chain rearrangement in the hopes of

passing negative selection [103]. Hence, successfully selected immature B cells enter the periphery to evolve to mature IgM, IgD expressing recirculating B cells. Within the spleen, the majority of B cells develop into Follicular (FO) B cells. These cells are recirculating compared to a minority of B cells residing in a specific area within the spleen, thus referred to as marginal zone B cells [103].

For both lymphocytes, signaling from the AgR, either in its preliminary or its complete state, seems to direct T cell [126] and B cell fates [65]. Investigations of several knockout or mutant mouse strains have shown that the lack of AgR-associated immunoreceptor tyrosine-based activation motif (ITAM)-carrying CD3 or Ig chains as well as the lack of molecules involved in AgR signaling lead to impaired T cell or B cell development at specific stages. Amongst the signaling components are the receptor proximal Rous sarcoma oncogene (SRC) kinase family and the spleen tyrosine kinase (SYK) family as well as a set of scaffold proteins implementing signal relay [126, 65]. The importance of individual molecules for correct TCR or BCR signaling in mature cells will be described in Subsection 1.2.1 and Subsection 1.2.2, respectively.

### 1.1.3 T Cell and B Cell Activation

Upon successful development, lymphocytes recirculate through secondary lymphoid organs in a mature but still naive state and await proper antigen stimulation, inducing proliferation and eventual effector cell differentiation. B cells become antibody producing plasma cells, T cells become T helper cells, cytotoxic T cells, or regulatory T cells [90]. Additionally, activation may also lead to the development of memory T cells and B cells, which enable a faster immune response upon secondary antigen encounter [90].

Focusing on cytotoxic and helper T cells, the initial signal for activation is provided by TCR-mediated recognition of MHC-coupled antigen on antigen presenting cells (APCs) such as macrophages, dendritic cells or B cells [90]. This interaction is accompanied by binding of the T cell coreceptor CD8 or CD4 to its respective MHC class I or class II molecule [90]. However, it is not until costimulation is shared between the two communicating cells that full T cell activation is reached [90]. The best investigated costimulatory molecule expressed on T cells is the CD28 receptor, which interacts with the B7 family members CD80 and CD86. Both molecules are upregulated on activated APCs [70]. Without costimulation, cells either die or enter a state of unresponsiveness known as anergy [90].

Proliferating T cells undergo several changes affecting, e.g., their cell size, surface marker expression and cytokine secretion. Upon antigen encounter and costimulation, T cells have been shown to lose the naive homing receptor L-selectin (CD62L) [143], whereas other proteins involved in cell adhesion are upregulated, e.g., the hyaluronate receptor CD44 [27]. Upregulation of the C-type lectin CD69 has been linked to a state of

early cellular activation [73], as has the secretion of the auto-/paracrine acting cytokine Interleukin-2 (IL-2) [172]. Coherently, upregulation of the IL-2 receptor  $\alpha$  chain (CD25) occurs [30], enabling surface expression of a high affinity trimeric IL-2 receptor complex [112]. It has been shown that CD28 receptor signaling enhances IL-2 production, thereby promoting cell survival and proliferation [19]. Ambivalent in its outcome, however, IL-2 signaling may also induce apoptosis upon TCR stimulation, which is known as activation induced cell death (AICD) [111, 47].

Similar to the T cell, B cell activation necessitates antigen recognition by the BCR. Antigen mediated receptor crosslinking and interaction of the coreceptor complex (CD19/21/81) with complement proteins (C3d/C3dg) induces antigen uptake, processing and presentation of MHC bound peptides on the B cells surface [90]. For the majority of B cells, the necessary costimulatory input is provided through interaction with T helper cells of the same antigenic specification. T cell recognition of the MHC/antigen complex along with CD40L/CD40 interaction and cytokine production mediates B cell proliferation and further differentiation [90]. Besides cellular blasting, a classical feature of activated B cells is the upregulation of CD80 and CD86 molecules [70], thus in return providing the precedingly mentioned costimulatory signal needed for T cell activation.

## 1.2 Antigen Receptor Signaling

### 1.2.1 T Cell Receptor Signaling

Having described the extracellular events leading up to T cell and B cell activation, the focus will now be set on the intracellular events mediating signal transduction. Albeit distinct in their antigen recognition and cellular function, T cells and B cells share common features of signal transduction [90]. Within this Subsection, principles of TCR signaling will be outlined. Subsection 1.2.2 will then complement the picture for AgR signaling in B cells.

In its most reduced version, TCR signaling can be divided into three different phases: signal initiation, signal amplification and signal diversification [106]. Although various studies have elucidated the role of individual molecules in TCR signal transduction, the question on how the interaction between the TCR/coreceptor and the MHC/antigen complex conveys signal initiation has not been clarified yet [117]. The concepts of receptor clustering upon MHC/peptide interactions as well as conformational changes of the TCR-associated CD3 chains are likely to play a role in signal initiation [171]. These events are thought to increase both proximity and accessibility of the TCR complex to intracellular signal transducers [171]. Another principle for promoting molecular proximity is compartmentalization. Signaling components such as kinases or scaffold proteins have

been shown to preferentially reside in lipid rafts. These are enriched membrane areas with a high density of sphingolipids in its exoplasmic leaflet and phospholipids with saturated fatty acids in its inner leaflet [168]. These tightly packed membrane areas are recognized as essential mobile signaling platforms within the membrane bilayer [168]. Besides the affinity of non receptor signaling components, an increased affinity towards lipid rafts has also been seen for the TCR complex itself upon ligand interaction [130]. Eventual raft aggregation accompanies T cell synapse formation, an area of close contact between the T cell and the APC, where its signal outcome is thought to be determined [51].

Despite the remaining question on how signal initiation is accomplished, it is certain that TCR ligation results in the activation of the SRC family of protein tyrosine kinases, such as the lymphocyte specific protein tyrosine kinase (LCK) and the FYN oncogene related to SRC, FGR, YES (FYN) [117]. As the main initiating kinase, LCK, phosphorylates the commonly shared ITAM amino acid sequence utilized in signal initiation [188]. LCK mediated phosphorylation occurs at two distinctly spaced tyrosine residues in the ITAM core sequence: YxxL/I-X<sub>6-8</sub>-YxxL/I [147]. Each TCR complex provides ten ITAMs located in the receptor associated CD3 chains, namely the CD3 $\epsilon/\gamma$ , CD3 $\epsilon/\delta$  heterodimers and the CD3 $\zeta/\zeta$  homodimer (Figure 1.1). The raft associated LCK is fully activated upon both dephosphorylation by the CD45 phosphatase [153] and trans-autophosphorylation at the activation loop tyrosine residue within its kinase domain [200]. As soon as kinase proximity to the TCR complex is provided, either through raft clustering [50] or CD4/CD8 coreceptor interaction [185] LCK conveys its enzymatic function. Hence, double phosphorylated ITAMs (dp-ITAMs) allow accumulation of the zeta-chain (TCR) associated protein kinase of 70kDa (ZAP-70) at the CD3 interface. This interaction is achieved by the tandem SRC homology 2 (SH2) domain binding motif, which is characteristic for the SYK family of non receptor tyrosine kinases [22]. Upon binding, ZAP-70 leaves its autoinhibitory state, exposing two linker tyrosine residues for LCK mediated phosphorylation, rendering the kinase active [11]. Increased ZAP-70 activity can be further achieved through trans-autophosphorylation or LCK mediated phosphorylation at a distinct tyrosine residue within its kinase domain [11]. Continued recruitment and activation of ZAP-70 completes an important step in signal amplification.

The scaffold proteins linker for activation of T cells (LAT) and the SH2 domain containing leukocyte protein of 76kDa (SLP-76) are the main targets of ZAP-70 [11]. Once tyrosine phosphorylated and stabilized by interacting with the growth factor receptor-bound protein 2 (GRB2)-related adaptor protein 2 (GADS), LAT and SLP-76 become the heart of an organized conglomerate of interacting proteins [115]. From this point forward, signal diversification is achieved by engaging three distinct signaling blocks, eventually affecting cell adhesion, cytoskeleton reorganization and gene expression [2]. Within the signaling block for gene regulation, three essential transcriptional factor families are known

to mediate cell proliferation through initiating IL-2 gene expression: nuclear factor of activated T cells (NFAT), activator protein 1 (AP-1) and nuclear factor kappa B (NF $\kappa$ B) [2].

All three families respond to Calcium ( $\text{Ca}^{2+}$ ) dependent signaling pathways for which phospholipase C gamma 1 (PLC $\gamma$ 1) acts as its gatekeeper. Membrane recruitment of PLC $\gamma$ 1 occurs upon pleckstrin homology (PH) domain binding to phosphatidylinositol (3,4,5)-trisphosphate (PIP3) as well as stabilization through interaction with LAT and SLP-76. Correct positioning of PLC $\gamma$ 1 ensures its proximity to the tyrosine kinase expressed in hepatocellular carcinoma (TEC) family member, the IL-2-inducible T-cell kinase (ITK). ITK conveyed tyrosine phosphorylation within the SH2-SH3 linker region renders a fully active PLC $\gamma$ 1 molecule [8]. Similar to PLC $\gamma$ 1, ITK activation is also dependent on PIP3/PH domain interaction followed by tyrosine phosphorylation by LCK, trans-autophosphorylation and SLP-76 interaction [8] (Subsection 1.2.3). Subsequently, activated PLC $\gamma$ 1 enables signal spreading by phosphatidylinositol (4,5)-bisphosphate (PIP2) hydrolysis, producing the second messengers diacylglycerol (DAG) and inositol

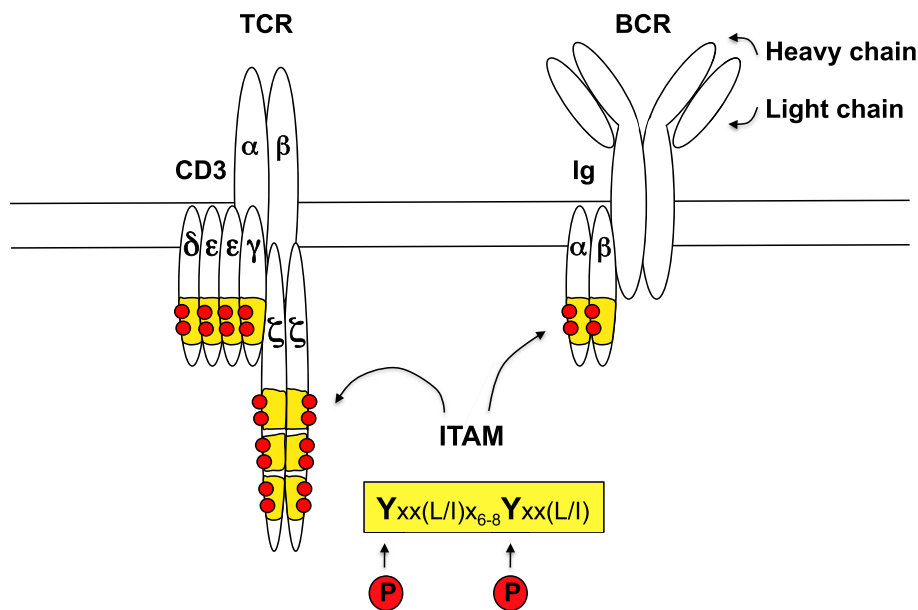


**Figure 1.1: The TCR/CD3 and BCR/Ig complex composition.** Antigen receptor (AgR) complexes of T cells and B cells share the immune receptor tyrosine based activation motif (ITAM) (in yellow), provided by their respective receptor-associated chains. For  $\alpha\beta$  T cells, the AgR complex consists of the TCR $\alpha$ /TCR $\beta$  chains, associated with the CD3 $\epsilon$ / $\gamma$ , CD3 $\epsilon$ / $\delta$  heterodimers chains, and the CD3 $\zeta$ / $\zeta$  homodimer chain. The AgR on B cells consists of two immunoglobulin (Ig) heavy and light chains for antigen recognition and the receptor associated Ig $\alpha$ / $\beta$  chains for signal transduction. SRC kinase family member mediated phosphorylation (red) of two distinctly positioned tyrosine residues establishes the classical binding motif for the SH2-tandem domain carrying SYK or ZAP-70 kinase, respectively.

(1,4,5)-trisphosphate (IP3) [149]. Soluble IP3 induces  $\text{Ca}^{2+}$  release from the endoplasmic reticulum, eventually leading to an additional  $\text{Ca}^{2+}$  influx from the extracellular space. Free cytoplasmic  $\text{Ca}^{2+}$  levels are thereby increased and available for interaction, e.g., with the  $\text{Ca}^{2+}$  receptor calmodulin [141]. Calcineurin interaction with  $\text{Ca}^{2+}$ /calmodulin induces dephosphorylation of cytoplasmic NFAT, allowing its nuclear translocation and binding to the respective IL-2 promoter regions [141].

In contrast to soluble IP3, the membrane localized second messenger DAG functions as a docking site for both the protein kinase C theta (PKC $\theta$ ) and the ras guanyl releasing protein 1 (RasGRP). The latter protein acts as guanine nucleotide exchange factor (GEF) [171]. Upon DAG binding and phosphorylation by PKC $\theta$ , RasGRP activates the small G protein Ras through the delivery of GTP [171]. Subsequently, RasGTP initiates the classical mitogen-activated protein kinase (MAPK) signaling pathway: the Raf/MAPK/ERK kinase (MEK)/extracellular signal-regulated kinase (ERK) cascade. ERK activity, as serine/threonine kinase, results in c-fos gene expression through phosphorylation of the transcription factor Elk1 [67]. Upon activation of another MAPK cascade, namely the MEK kinase (MEKK)/MEK/c-Jun amino-terminal kinases (JNK) module, c-Jun becomes phosphorylated and through dimerization with c-fos generates the transcription factor AP-1 [167]. Therefore, activation of the MAPK signaling cascades integrates AP-1 next to NFAT in a cooperative fashion, as essential transcription factor family for IL-2 gene expression. Additionally, T cell activation results in the activation of the third group of MAPKs, the p38 members [204]. Besides the described upstream mediators such as the GEF, VAV1 and the small GTPase proteins cdc42 and Rac, T cells have acquired a distinct way of p38 activation through ZAP-70 mediated phosphorylation in a MEK independent pathway [158].

Besides its more recently described role in JNK activation [16], PKC $\theta$  leads to the activation of the third important transcription factor family for IL-2 gene expression: NF $\kappa$ B [190]. Within the classical NF $\kappa$ B signaling cascade, PKC $\theta$  mediates phosphorylation of the CARD-containing protein 11 (CARMA1) at distinct linker serine residues, hypothesized to release CARMA1 from an autoinhibitory to an open conformational state [173, 123]. Subsequent multiprotein complex formation of CARMA1, B cell lymphoma/leukemia 10 (BCL10) and the mucosa associated lymphoid tissue lymphoma translocation gene 1 (MALT1) leads to the activation of the Inhibitor of kappa B Kinase (IKK)  $\alpha/\beta/\gamma$  trimeric complex. Activation occurs, on the one hand, by TNF receptor-associated factor 6 (TRAF6) complex mediated lysine (K)63-linked polyubiquitylation of the regulatory IKK $\gamma$  subunit, and, on the other hand, by TGF-beta activated kinase 1 (TAK1) mediated phosphorylation of the catalytic IKK $\beta$  subunit [194]. IKK $\beta$  in turn phosphorylates the NF $\kappa$ B bound I $\kappa$ B $\alpha$  inhibitor, marking it for K48-linked ubiquitylation and 26S proteasomal degradation. Thus, heterodimeric NF $\kappa$ B (RelA:p50) is free to translocate into the

nucleus and promote IL-2 gene expression [190].

Having outlined major signaling steps leading up to IL-2 gene expression, one important aspect has to be added. As mentioned in Subsection 1.1.3, complete T cell activation depends on the integration of the costimulatory signal [90]. CD28 is a key costimulatory receptor expressed on T cells [171]. Molecules such as PLC $\gamma$ 1, ITK, pyruvate dehydrogenase kinase, isozyme 1 (PDK1) and its substrate v-akt murine thymoma viral oncogene homolog (AKT) depend on accessible PIP3 for PH domain mediated membrane recruitment and subsequent protein activation. After CD28 interaction with CD80 or CD86 molecules expressed on activated APCs, the cytoplasmic tail of CD28 becomes tyrosine phosphorylated by LCK. This step creates a platform for phosphatidylinositol 3-kinase (PI3K) recruitment, which upon activation phosphorylates PIP2 and generates the docking motif PIP3 [171]. Thus, the CD28/PI3K module provides an important aspect in signal amplification for full T cell activation. Downregulation of signaling events occurs via lipid phosphatase or protein tyrosine phosphatase activity, in combination with protein degradation [90].

Figure 1.2 depicts key signaling steps and molecules involved in the signal transduction downstream of the TCR/CD3 complex, the coreceptors CD4/8, and the costimulatory molecule CD28 upon antigen/MHC encounter in respect to initiating T cell proliferation. Eventually, signals from various cascades are integrated through the binding of the transcriptional factor family members NF $\kappa$ B, NFAT, and AP-1 to the IL-2 promoter region, mediating T cell proliferation [84].

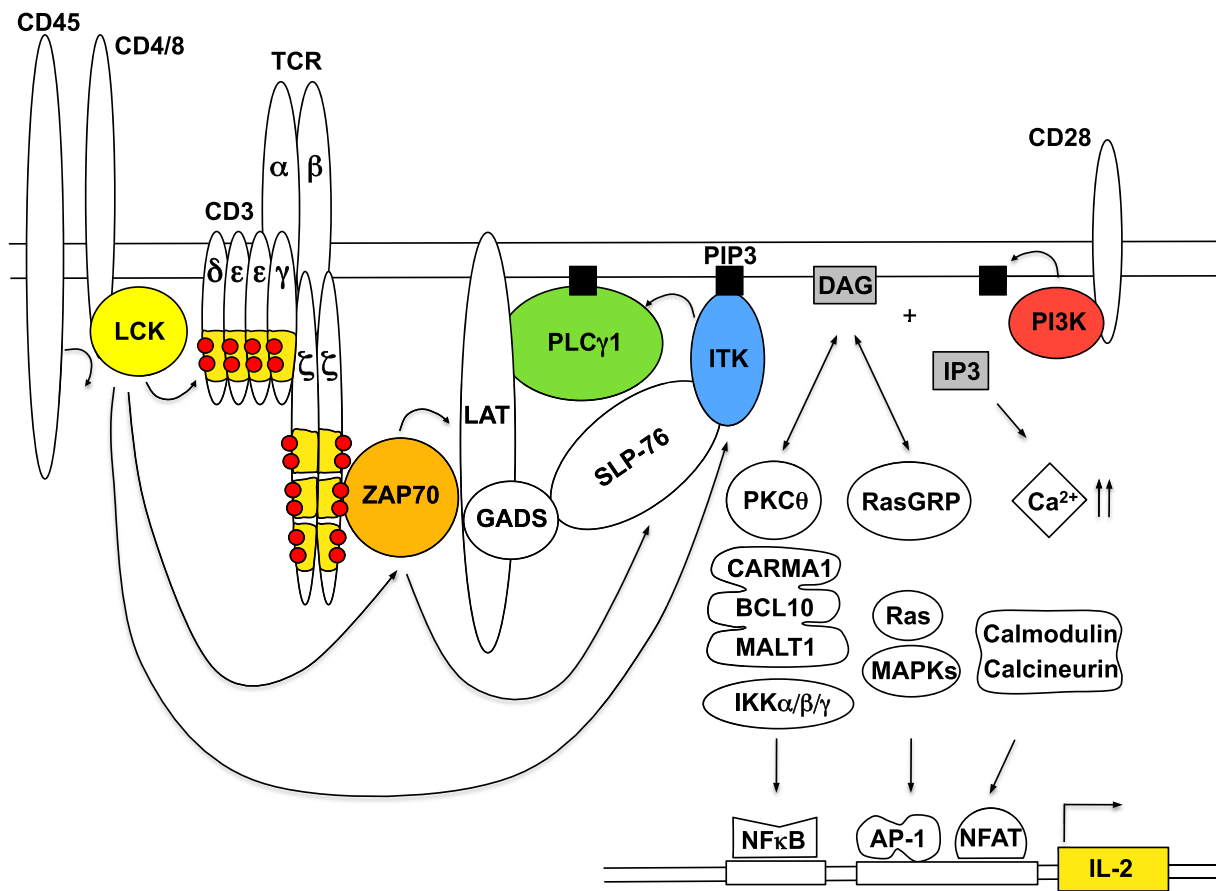


**Figure 1.2: Key TCR signaling events.** Depicted is a simplified scheme on TCR downstream signaling events leading to IL-2 gene expression. Receptor clustering is initiated by both TCR $\alpha$ ,  $\beta$  chain recognition of processed antigen and coreceptor CD4 or CD8 binding to its respective MHC molecule. Hence, the SRC kinase LCK is activated by CD45 mediated dephosphorylation and trans-autophosphorylation. Upon phosphorylation of ITAM based tyrosine residues within the CD3 molecules, ZAP-70 is recruited. ZAP-70 mediates phosphorylation of the scaffold proteins LAT and SLP-76, which enables signalosome assembly by recruitment of other proteins, such as GADS, PLC $\gamma$ 1 and ITK, into its core structure. Signal diversification is achieved by ITK dependent PLC $\gamma$ 1 activation and generation of the second messengers DAG and IP3. DAG mediated recruitment of PKC $\theta$  and RasGRP engage the NF $\kappa$ B and MAPK signaling pathways, while IP3 induces Ca<sup>2+</sup> dependent activation of Calcineurin. All three cascades come together by nuclear translocation of the key transcriptional factor families NF $\kappa$ B, AP-1 and NFAT, promoting IL-2 expression. Signal relayed by the costimulatory CD28 molecule is integrated by recruitment and activation of PI3K, generating PIP3 for PH domain mediated membrane recruitment, e.g. of PLC $\gamma$ 1 and ITK. Further information on phosphorylation events or molecular interactions is given in Subsection 1.2.1.

## 1.2.2 B Cell Receptor Signaling

Similar to the model proposed for TCR engagement, BCR signal initiation is thought to be achieved by antigen mediated BCR crosslinking, movement into lipid rafts and conformational changes of the BCR complex [53]. These steps again reflect the key issues of accessibility and proximity between the AgR and the involved signaling components as precedingly described for T cells (Subsection 1.2.1). Thus, ITAM carrying  $Ig\alpha$ ,  $\beta$  chains (Figure 1.1) are subject to SRC or SYK kinase mediated phosphorylation, which results in an increased recruitment of SYK via its tandem SH2 domain [61]. The main SRC kinases involved in BCR signaling are the v-yes-1 Yamaguchi sarcoma viral related oncogene homolog (LYN), the FYN oncogene related to SRC, FGR, YES (FYN), and the B lymphoid tyrosine kinase (BLK) [102]. Through dp-ITAM binding, SYK enters a conformationally susceptible state for further activation [9]. Upon either autophosphorylation or SRC kinase phosphorylation, SYK becomes fully activated (Subsection 1.2.4) and phosphorylates its main target: the B cell linker (BLNK) protein [60, 197]. Phosphorylated BLNK, which is homologous to SLP-76 in T cells, acts as a backbone for recruiting key signaling components, such as  $PLC\gamma 2$  and the Bruton agammaglobulinemia tyrosine kinase (BTK). In addition to PIP3 binding, BTK and  $PLC\gamma 2$  are thereby correctly positioned at the membrane for phosphorylation and further activation [102]. Interestingly, BLNK also promotes sustained SYK activity by directly interacting with a C-terminally located tyrosine residue [99]. In B cells, PI3K activity is promoted upon CD19/CD21/CD81 coreceptor complex interaction with the complement factors C3d/C3dg. Recruitment and activation of LYN, the GEF VAV1, Rac and the PI3K itself establishes PI3K activity and ensures PIP3 generation [102]. As described for TCR signaling (Subsection 1.2.1),  $PLC\gamma 2$  hydrolyses PIP2 into the second messengers DAG and IP3. IP3 induces  $Ca^{2+}$  dependent signaling pathways. DAG availability leads to  $PKC\beta$  and RasGRP3 activity, resulting in the initiation of the  $NF\kappa B$  and MAPK signaling pathways, respectively. In concert with calcineurin activity, the nuclear release of the  $NF\kappa B$ , NFAT and AP-1 transcription factor family members is engaged, regulating B cell responses [102]. As is the case in T cells, the main negative feedback mechanism include dephosphorylation of tyrosine residue and lipid structures, and ubiquitin related proteosomal degradation [90].

## 1.2.3 The IL-2 Inducible T Cell Kinase

Since studies conducted within this work at hand focus on the fusion kinase ITK-SYK [178], an overview of the individual kinases affected by the translocation event  $t(5;9)(q33;q22)$  shall be given. ITK belongs to the TEC family of non receptor tyrosine kinases [145]. Next to TEC and the resting lymphocyte kinase (RLK), ITK is the

most abundantly expressed family member in T cells [145]. Other family members include the bone-marrow tyrosine kinase gene on chromosome X (BMX) protein and BTK, latter being the main TEC kinase expressed in B cells [129]. While ITK exerts its function as TEC kinase in TCR signaling (Subsection 1.2.1), BTK does so correspondingly in BCR signaling events (Subsection 1.2.2). Knockout *in vivo* analysis in combination with *in vitro* studies depicted modulatory roles for ITK in a plethora of T cell processes such as T cell development, T cell activation, T cell cytoskeleton rearrangement and T cell effector function [8].

Structurally, ITK consists of an N-terminally located PH domain, a TEC homology domain (TH), as well as an SH3 and SH2 domain followed by the C-terminally located tyrosine kinase domain [87] (Figure 1.3). The TH domain itself is composed of a  $Zn^{2+}$ -ion binding area, referred to as the BTK homology domain, and a proline rich region (PRR) sequence motif [87]. Together, these domains constitute a platform for ITK regulation suggested to occur via intra- and intermolecular protein interaction, phosphorylation and peptide bond isomerization. The following steps have been postulated to be important for full ITK activation [145, 87]: PH domain mediated membrane recruitment through PIP3

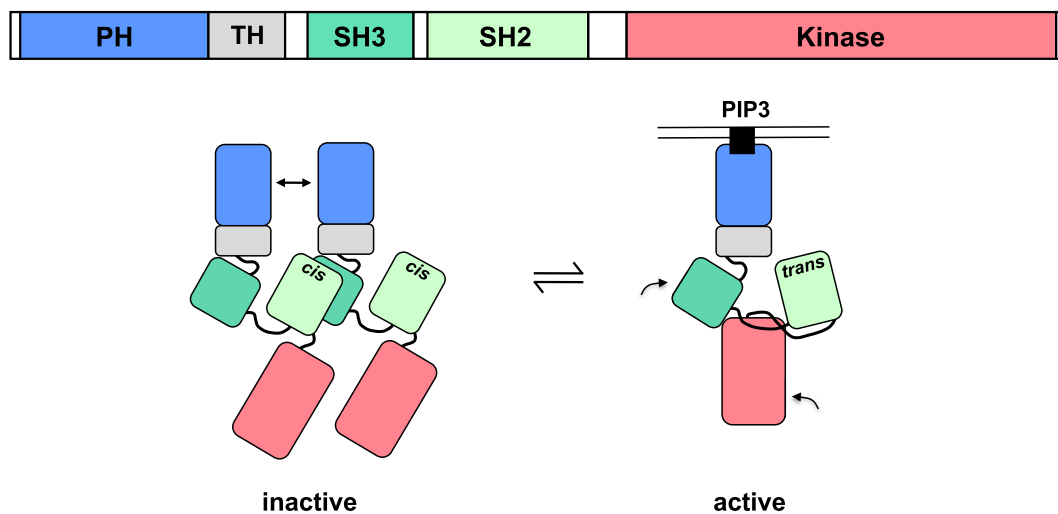


**Figure 1.3: Schematic view of the ITK protein domain structure.** ITK is characterized by its N-terminally located Pleckstrin homology (PH) domain, followed by a TEC homology (TH) domain, a SRC homology (SH)2 and SH3 domain, and an C-terminally located tyrosine kinase domain (Kinase). The following steps are implied in stabilizing ITK in its active state: PH domain mediated membrane recruitment via PIP3 binding, *cis* to *trans* isomerization of an SH2 domain located proline residue, as well as phosphorylation of the SH3 and kinase domain. On the other hand, reduced PIP3 availability and intermolecular SH3/SH2 domain interactions are discussed to promote ITK inactivation. The inactive state might be further supported by PH domain mediated oligomerization as indicated by the double-headed arrow.

binding [12], LCK mediated phosphorylation at tyrosine residue Tyr511 within the activation loop of the catalytic center [75], and isomerization from a *cis* to *trans* configuration of the proline residue Pro287 within the SH2 domain [120]. Together, these steps can be interpreted to result in a conformational change of ITK by loosening intermolecular SH3/SH2 and intramolecular SH3/PRR interactions, increasing its affinity for the activated form of the SLP-76 (pTyr145)/LAT signalosome [8]. SH2 and SH3 domain mediated interaction with SLP-76 has been shown to support ITK membrane recruitment, and to stabilize ITK activity [18, 86]. Consequently, active ITK is correctly positioned at the membrane to phosphorylate its main target PLC $\gamma$ 1 at tyrosine residue Tyr783, contributing to its activation [114, 78].

Besides target phosphorylation, ITK phosphorylates itself at tyrosine residue Tyr180 within the SH3 domain [88]. This autophosphorylation is suggested to modulate SH3 domain/protein interactions, and to promote ITK self-association through intermolecular SH3/SH2 interaction [87]. ITK oligomerization is thought to be the initial step in subsequent downregulation of ITK catalytic activity [87] and might also be supported by intermolecular PH domain interaction [80]. Next to the structural changes, ITK kinase activity is reduced through phosphoinositide phosphatases, such as the phosphatase and tensin homologue (PTEN), which simply limits PIP3 availability through dephosphorylation [166]. Protein tyrosine phosphatase activity by dephosphorylation of activation loop tyrosine residues [87] or dephosphorylating of SLP-76, as ITK interaction partner, are also discussed to contribute to ITK downregulation [8]. Next to its function as kinase, ITK has also been postulated to function as scaffold protein in recruiting the GEF VAV1 to SLP-76. Eventually, this step induces the Rac/Rho/Cdc42 MAPK signaling cascade which regulates T cell cytoskeleton rearrangement [49]. Despite its importance as TCR signaling molecule, however, to date few mutations affecting the ITK locus have been identified to be linked to the development of human lymphoproliferative diseases [81]. In terms of chromosomal aberrations, the ITK gene locus is involved in translocation t(5;9)(q33;q22) [178]. Next to ITK, the translocation affects the SYK gene locus, resulting in the expression of the fusion kinase ITK-SYK (Section 1.4). This translocation was identified in a subgroup of patients diagnosed with peripheral T cell lymphoma, not otherwise specified (PTCL-NOS) (Section 1.3).

#### 1.2.4 The Spleen Tyrosine Kinase

The SYK non receptor tyrosine kinase family consists of its original member SYK and the currently only other member described in mammals, ZAP-70 [177]. SYK is expressed in various cell types but most abundantly found in hematopoietic cells [128]. Analysis of SYK deficient mice depicted a profound role for SYK in pro to pre B cell and immature to mature B cell development, hinting at a key role in pre BCR and BCR signaling [186, 33].

Originally, the importance of SYK was restricted to signaling from classical ITAM coupled AgRs or ITAM containing Fc receptors [128]. However, SYK has been shown also to signal from non classical, so called HemITAM carrying receptors, e.g., C-type lectins, or even from non ITAM carrying receptors, such as integrins [128]. Therefore, as diverse as its involvement in signaling cascades, SYK contributes to a multitude of cellular responses, for instance, cell development, proliferation, differentiation, phagocytosis, cytotoxicity, and cell adhesion [128].

The function of SYK in adaptive immune cells is best understood for relaying BCR activation to downstream events through binding to dp-ITAMs, which are located in the  $Ig\alpha$  and  $Ig\beta$  chains (Subsection 1.2.2). Structurally, this binding is conveyed through two N-terminally located SH2 domains, which are connected by an amino acid stretch termed Interdomain A. Interdomain B, on the other hand, connects the tandem SH2 domain module with the C-terminally located tyrosine kinase domain [9] (Figure 1.4). In resting lymphocytes, the majority of SYK molecules are located in the cytoplasm in an enzymatically dormant state. Insights into the full-length crystalline structure of ZAP-70 [46] in combination with single particle electron microscopy of full length SYK [9] have proposed that SYK is kept in an autoinhibitory state by intramolecular interactions of the interdomains A and B with its kinase domain (Figure 1.4) [46, 9]. Upon dp-ITAM binding, however, the autoinhibitory conformation is disturbed, promoting SYK to enter a catalytically active

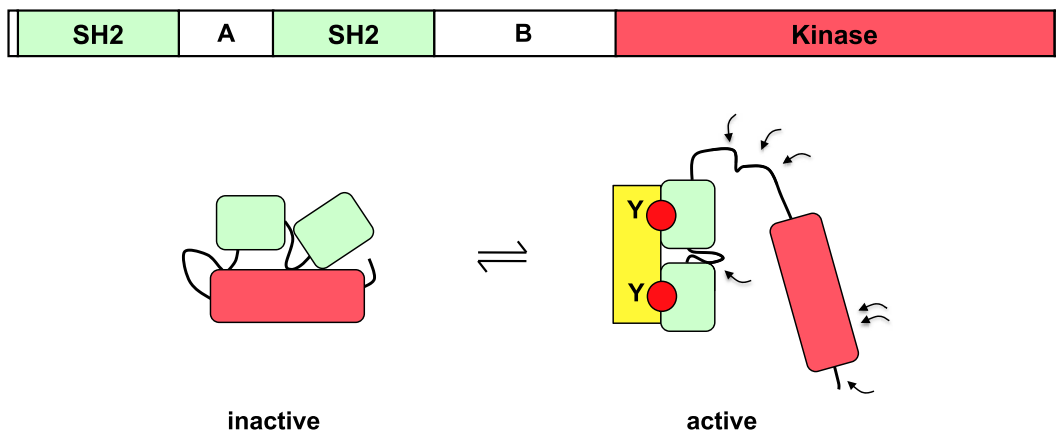


**Figure 1.4: Schematic view of the SYK protein domain structure.** SYK is characterized by its N-terminally located tandem SH2 domains (SH2) and its C-terminally located tyrosine kinase domain (Kinase). Intramolecular interaction of both, the SH2-SH2 amino acid linker A region (A) and the SH2-kinase linker B region (B) stabilize SYK in a conformationally inactive state. Upon interaction with double phosphorylated (red) ITAM based tyrosine (Y) residues, SYK enters a conformationally open state. Tyrosine phosphorylation (arrows) within the kinase domain, the linker regions A and B as well as the C-terminus offer a platform for positive and negative regulatory actions.

form [9]. Autophosphorylation or SRC kinase mediated phosphorylation of the activation loop tyrosine residues (Tyr525/526) establish full kinase activity [203]. Sustained SYK activity is hence thought to be promoted in an ITAM independent fashion [184] through autophosphorylation of linker tyrosine residues [63]. Phosphorylation of a C-terminally located tyrosine residue has also been discussed [99]. These phosphorylation sites constitute a platform for recruiting binding partners such as BLNK [99], VAV1 [45], PI3K(p85) [131], PLC $\gamma$ 2 [71], or PLC $\gamma$ 1 [107]. Within this model, both protein binding and phosphorylation contribute to stabilize SYK in its open, catalytically active form. Notably, in contrast to ZAP-70, SYK is neither dependent on SRC kinases to convey tyrosine phosphorylation of ITAMs [155] nor to phosphorylate its kinase domain [63]. This gives SYK the choice of establishing its own positive feedback loop for sustained signaling in a SRC kinase independent matter. Negative regulation of SYK has been described to occur by promoting re-entrance into the autoinhibitory conformation through dephosphorylation of linker and activation loop tyrosine residues [102]. One possible tyrosine phosphatase which takes over SYK dephosphorylation is SHP-1 [148]. Another mechanism for SYK negative regulation occurs through the Casitas B-lineage lymphoma (CBL) ubiquitin ligase [118]. Upon BCR stimulation, CBL binds to phosphorylated Tyr323 in the linker B region of SYK. Hence, SYK ubiquitinylation is induced, marking the kinase for proteasomal degradation [118]. Further, phosphorylation of linker A Tyr130 induces SYK detachment from BCR ITAMs, promoting SYK downregulation [91, 207].

Besides its role in regular cell signaling, SYK has been implicated in the pathogenesis of both hematopoietic and non hematopoietic diseases [128]. Aberrant SYK activity in lymphocytes has been mainly linked to cancer of B cells either in a developmental stage, such as pre B cell acute lymphoblastic leukemia or in a mature stage, such as B cell lineage chronic lymphocytic leukemia or B cell lymphoma [128]. Its role in disease development most likely derives from the fact, that SYK as signaling molecule downstream of the preBCR or BCR is essential for conveying cell proliferation, differentiation as well as anti-apoptotic signals [128]. When carried out in a deregulated fashion, both actions can contribute to cell transformation. The role of SYK in B cell malignancies has been substantiated by successes in clinical trials applying the SYK small molecule inhibitor R788 [58]. Notably, data have been emerging, which hint at an additional role for SYK in the development of T cell lymphoma. Streubel et al. [178] identified the translocational event t(5;9)(q33;q22) for a subgroup of patients diagnosed with PTCL-NOS. The translocation results in the expression of the fusion kinase ITK-SYK. Additionally, Feldman et al. [55] presented data which demonstrated SYK overexpression even in translocation negative cases of PTCL. These observations thus raised the hypothesis that SYK deregulation is a common mechanism involved in the process of lymphoma development, not only in B cells but also in T cells. Interestingly, besides the predominant role of SYK in BCR

signaling (Subsection 1.2.2), a selective role for SYK in pre-TCR or TCR signaling, such as in the early DN3 thymocyte stages [135], or in mature CD4<sup>+</sup> effector T cells [97], has been published. Due to the fact that SYK does have the capacity to act not only in a B cell but also in a T cell environment, aberrant SYK expression might well be associated with T cell transforming processes. Subsequently, Section 1.3 will focus on a subset of malignancies derived from mature T cells, namely PTCL-NOS, and will outline both the fundamentals and the remaining questions on this disease category.

## 1.3 Peripheral T Cell Lymphoma Not Otherwise Specified

### 1.3.1 Definition, Incidence, and Etiology

According to the latest World Health Organization's classification of tumors of hematopoietic and lymphoid tissues, PTCLs are a highly diverse, seldomly occurring and aggressive group of T cell and natural killer (NK) cell neoplasms [199]. They represent less than 15% of all non-Hodgkin lymphomas (NHL) worldwide [199]. In contrast to T cell lymphoblastic leukemias/lymphomas, which originate from T cell precursors or thymocytes, PTCLs derive from mature post-thymic T cells [57]. They are classified by their primary site of disease presentation into cutaneous, disseminated, extranodal or nodal cases. The primary nodal cases can be further divided into the sub-entities of angioimmunoblastic T cell lymphoma (AITL), anaplastic large-cell lymphoma (ALCL), positive or negative for the involvement of the anaplastic lymphoma kinase (ALK<sup>+</sup>/ALK<sup>-</sup>), and PTCL-NOS [57]. At 26%, PTCL-NOS account for the largest, yet most undefined and heterogeneous group of PTCLs with a geographically higher prevalence in North America than in Asia or Europe [193]. Although some morphological subgroups, such as the lymphoepithelioid, the T-zone, and the follicular variant have been described [44], PTCL-NOS is still regarded as an exclusion category due to its inhomogeneous histological features and limited molecular understanding.

Concerning the etiology, to date, no immunological defects, hereditary components or viral infections have been proven to affect the occurrence of PTCL-NOS. On a cellular level, the commonly observed histological involvement of inflammatory components in PTCL-NOS might hint towards a supportive role of chemokines and other inflammatory factors in the development of PTCL-NOS [163]. Chronic antigen receptor stimulation has also been discussed in the pathology of PTCLs. However, no experimental proof has been offered so far which could substantiate either of these aspects as an etiological component in PTCL-NOS pathology [163].

### 1.3.2 Clinical Presentation and Therapeutic Approaches

From a clinical point of view, PTCL-NOS presents itself as a highly aggressive disease with a poor prognosis, mainly affecting adult males in their fifth to seventh decade of life [44]. Although PTCL-NOS are described to have a primary nodal presentation, they are frequently characterized by the involvement of extranodal sites including liver, spleen, skin, the gastrointestinal tract, peripheral blood as well as the bone marrow. According to the Ann Arbor staging system, the majority of PTCL-NOS are diagnosed late in the disease course at stage III-IV, where dissemination of tumorous cells already has occurred [44].

Currently, conventional treatment options for PTCL-NOS are based on regimens approved for aggressive B cell lymphomas. These consist of anthracycline-based or cyclophosphamide/ doxorubicine/ vincristine/ prednisone (CHOP)-based combination chemotherapy [57]. However, these approaches were little effective with early and high relapse rates and a 5-year overall survival of 32% after first line treatment [57]. As a reasonable approach for relapsed and refractory disease autologous or allogeneic stem cell transplantation (ASCT) as a combinatorial regimen with high dose chemotherapy is being suggested [146]. The causes involved in the striking therapeutic response differences between aggressive T cell and B cell lymphomas are currently unsolved and still speculative. However, recent studies provide data showing that especially T cell and NK cell lymphomas activate drug resistance pathways, for instance, through the expression of the P-glycoprotein [79]. Another component accounting for bad treatment responses in these types of lymphomas might stem from an increased expression of BCL-2 and BCL-XL, both belonging to the class of anti-apoptotic proteins [144]. Thus, due to the unsatisfactory treatment response, alternative strategies are highly warranted and currently being investigated on their efficacy in PTCL therapy. Classes of new therapeutical agents include monoclonal antibodies against surface proteins such as CD52, CD4, CD2 or VEGF, fusion toxins, nucleoside analogons, metabolite analogons such as antifolates, immune modulatory agents, proteasome inhibitors and histone deacetylase inhibitors [79]. High hopes are further being placed in the class of signaling inhibitors, e.g. small molecules directed against signaling components. Potential targets are the receptor tyrosine kinase platelet-derived growth factor receptor (PDGFR) alpha, SYK, mammalian target of rapamycin (mTOR) or anti-apoptotic proteins, such BCL-2 family members [79, 201]. Individual agents are reviewed in Howman et al. [79]. The Food and Drug Administration (FDA) approved of Pralatrexate as antifolate for treating relapsed or refractory PTCL in 2009 [134]. Phase II clinical trails investigating the therapeutic effect of the SYK inhibitor R788 have been completed and await their evaluation also for treating relapse or refractory PTCL [57]. As for the other agents and small molecules, clinical trials and preclinical investigations are ongoing, or being initiated either for the single component or for a

combinatorial regimen approach. Overall, the future of PTCL therapy is seen to rest in combinatorial approaches of standard regimens and novel agents.

### 1.3.3 Phenotypic Characterization

Substantial efforts are made to identify phenotypical characteristics in order to provide the basis for dissecting sub-entities amongst the heterogenous group of PTCL-NOS. By determining the cellular and molecular variations of individual PTCL-NOS subtypes, the eventual goal is to understand the clinical implications for diagnosis, therapeutical guidelines, and prognosis. Within this Subsection, key phenotypical features of PTCL-NOS in terms of their morphology, surface expression, as well as recent studies aiming at classifying PTCL-NOS via gene expression profiling, shall be summarized.

Due to their heterogeneity, PTCL-NOS display a high variability also in terms of their cell morphology. Irregular T cells may differ in size and shape, possibly embedded in eosinophils, plasma cells, histiocytes, epithelioid cells or in a general reactive cellular background. Affected mature T cells are derived from the  $\alpha\beta$  T cell lineage, usually harboring a clonally arranged T cell receptor with TCR $\beta$  surface expression [44]. The majority of nodal cases show single expression of the T helper cell marker CD4 [154]. Far less frequently described are CD8 single positive and CD4/CD8 double positive or double negative scenarios [154]. CD52 is expressed in all neoplastic cells [66], CD30 positivity is seen in one third of all PTCL-NOS cases [43]. Additionally, a frequent loss is observed of CD7, seldomly of CD5, CD3, and/or CD2 [44]. Notably, affected T cells show a high proliferative index as measured by Ki-67 expression [163]. Epstein-Barr Virus (EBV) positivity, expression of the cytokine receptor CCR4, or the cytotoxic marker CD8 have also been associated with a dismal effect on patient overall survival [44].

Within the molecular approach to characterize PTCL-NOS subgroups, initial gene expression study showed that separation was possible according to the expression level of NF $\kappa$ B pathway genes [122]. Interestingly, low expression was associated with worse patient survival. A following approach suggested that PTCL-NOS be classified into three groups, as based on the expression of genes either correlated to tumor promotion (U1), T cell activation and apoptosis (U2), or mainly genes involved in the Interferon gamma (IFN $\gamma$ )/Janus kinase (JAK)/signal transducer and activator of transcription (STAT) signaling pathway (U3) [13]. Further studies led to the molecularly important insight that malignant cells resemble activated T cells belonging either to the CD4<sup>+</sup> or CD8<sup>+</sup> phenotype [139]. Additionally, the authors have demonstrated deregulation of genes involved in tumorigenic processes. These included deregulation of proliferation, apoptosis, cell cycle, chemoresistance, and of pathways engaged during cell dissemination, such as matrix remodeling and cell adhesion [139]. A recent study with increased sample numbers of PTCL-NOS cases identified a subgroup of PTCL-NOS with an expression pattern

reminiscent of a cytotoxic T cell phenotype, which correlated to dismal patient survival [83]. These results are in line with data generated by immunohistochemical analysis [10], and reflect the CD8<sup>+</sup> classification approach by Piccaluga et al. [139].

Overall, gene expression profiling helped to molecularly characterize PTCL-NOS cases and opened possibilities of subgroup definition. However, validation by large scale studies with increased PTCL-NOS cohorts is warranted and the diagnostic impact of the presented classification strategies still needs further investigation.

### 1.3.4 Genetic Characterization

Classical cytogenetics such as karyotyping or fluorescence in situ hybridization (FISH) analysis in accordance with comparative genomic hybridization, and single-nucleotide polymorphism (SNP) analysis have demonstrated that PTCL-NOS genomes display a high complexity concerning their genomic alterations [43]. Largely, the oncogenicity of these variations is not understood [57]. Genomic changes include aneuploidy, gains and losses of chromosomal material, as well as chromosomal translocations. An overview of documented aberrations is given by de Leval et al. [43].

To date, three chromosomal translocations have been described among PTCL-NOS for which both affected gene loci were identified and the recurrence of the translocation was shown [178, 54, 7]. Streubel et al. [178] described the translocational event t(5;9)(q33;q22), which was present in 17% (5/30) of analyzed PTCL-NOS cases. The translocation affects the SYK as well as the ITK gene locus, and results in the generation of a novel fusion kinase, termed ITK-SYK. Histopathologically, all translocation positive cases were classified as the follicular variant, potentially identifying t(5;9)(q33;q22) as a PTCL-NOS subtype specific genetic marker [178]. Notably, Feldman et al. [55] showed overexpression of activated SYK in translocation negative cases of nodal PTCL. Thus, SYK deregulation might be a common mechanism involved in PTCL pathology. The second two translocations described for PTCL-NOS involve the TCR $\alpha$  gene locus (TCRA) [54, 7]. Feldman et al. [54] described 3% (2/64) of PTCL-NOS cases carrying cytotoxic features with skin and bone marrow involvement to harbor the translocation t(6;14)(p25;q11.2). Molecular analysis demonstrated repositioning of the multiple myeloma oncogene-1/interferon regulatory factor-4 (IRF4) to the TCRA gene locus. This event is hypothesized to lead to IRF4 deregulation. Similar to (5;9)(q33;q22) positive cases, IRF4 translocation might also function as characteristic for a new subgroup definition. Lastly, Almire et al. [7] looked at two translocation t(14;19)(q11;q13) positive PTCL-NOS cases previously described by Martin-Subero et al. [121] and identified the poliovirus receptor-related 2 (PVRL2) gene to be translocated to the TCRA gene locus [7]. Both patient samples showed overexpression of PVRL2 [7]. It still needs to be investigated whether T cell transformation correlates to the genetic event.

## 1.4 Translocation $t(5;9)(q33;q22)$ and the Fusion Kinase ITK-SYK

As summarized in the previous Subsection 1.3.4, few recurrent translocations have been described for PTCL entities belonging to the category: not otherwise specified. Streubel et al. [178] published a reciprocal event to affect the chromosomal regions 5q33 and 9q22, respectively harboring the ITK and the SYK gene locus. Applying rapid amplification of cDNA ends (RACE), reverse transcriptase polymerase chain reaction (RT-PCR), and sequence analysis the authors had shown, that the translocational event results in the generation of two fusion transcripts of which solely the ITK-SYK transcript was substantiated to be functional [178]. Sequencing identified the in frame fusion to link the genomic region holding exon 8-14 of the SYK gene locus onto exon 5 of the ITK gene locus. In this situation, expression of the newly generated fusion transcript is regulated by the endogenous ITK promoter. On the protein level the translocation results in the fusion of the N-terminal region of the ITK protein (amino acid 1-165), containing the PH and the TEC homology (TH) domain, to the SYK kinase domain (amino acid 371-631). A residual SYK derived linker B fragment (amino acid 306-370) is preserved during this process, and connects the major protein domain structures of both kinases [178]. In total ITK-SYK consists of 495 amino acids with an estimated protein size of 55kDa. Figure 1.5 depicts the translocational consequences on the protein level.

Concurrent to this work at hand *in vitro* investigations by Rigby et al. [151] and Hussain et al. [82] provided initial insights on ITK-SYK functionality. Both groups of authors demonstrated that ITK-SYK has retained its catalytic properties as a kinase and seemingly conveys its activity in a constitutive manner. First kinase targets such

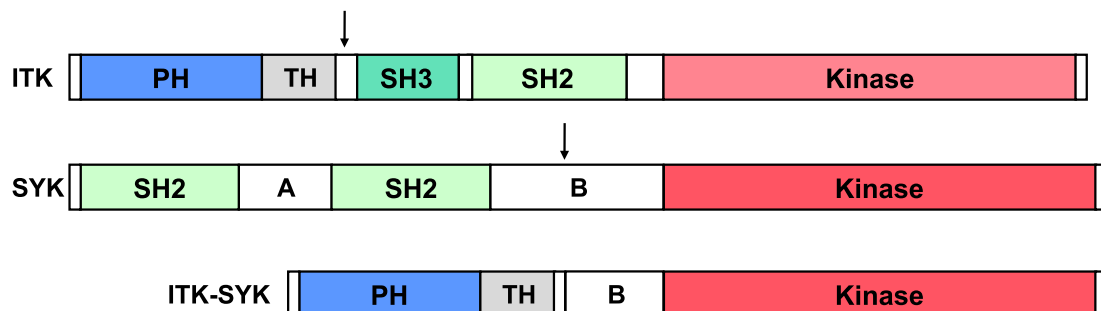


**Figure 1.5: Schematic view of ITK, SYK, and the fusion kinase ITK-SYK.** Translocation  $t(5;9)(q33;q22)$  results in the generation of the fusion kinase ITK-SYK, retaining the PH and TH domain from ITK, fused to the enzymatic SYK kinase domain. A residual SYK derived linker B amino acid stretch is further preserved. Arrows indicate the translocation breakpoints projected onto the protein level.

as SLP-76 and BLNK [82], as well as p42/p44 [151] have been identified. In terms of ITK-SYK conveying its full kinase activity, *in vitro* experiments additionally showed PI3K dependency [82, 151] and the necessity for correct membrane localization via the PH domain [151]. Ribgy et al. [151] complemented these data with first *in vitro* studies on the potential oncogenicity of ITK-SYK. The authors demonstrated contact inhibited cell growth in ITK-SYK expressing NIH3T3 cells, indicating that ITK-SYK is able to cause cell transformation [151].

# Chapter 2

## Research Objective

Chromosomal translocations as a specific form of genomic aberration, have long been associated with cancer development of the hematopoietic system [156, 42]. Two major scenarios have been described of how translocation events contribute to cellular transformation. On the one hand, gene deregulation may occur by placing the coding sequence of one gene under the control of another gene locus. On the other hand, chromosomal translocation may result in the generation of a new gene product by fusing the coding regions of two different gene loci [157]. Belonging to the latter category, Streubel et al. [178] identified a reciprocal translocation which was recurrent in a subgroup of patients diagnosed with PTCL-NOS. The translocation event  $t(5;9)(q33;q22)$  affects the ITK and SYK gene locus, and results in the functional expression of a new fusion tyrosine kinase called ITK-SYK. Currently, little is known about the molecular processes behind PTCL development, which especially holds true for the subgroup of PTCL-NOS, and adequate tools for its understanding are lacking.

On the basis of the isolated translocation, the research objective of the work at hand was to investigate the cellular consequences of ITK-SYK activity, and to clarify whether *de novo* expression of ITK-SYK may induce lymphomagenesis. The strategic approach of conditional gene targeting was employed. Therefore, the human ITK-SYK cDNA was introduced by homologous recombination into the murine, ubiquitously expressed ROSA26 locus [174]. The conditional approach was realized by the presence of a loxP site flanked STOP cassette in front of the ITK-SYK cDNA, preventing transcriptional readthrough in ROSA26<sup>loxSTOPlox-ITK-SYK</sup> mice. Only upon breeding with Cre-transgenic mice, deletion of the STOP cassette and cell type specific expression of the fusion kinase ITK-SYK would occur. Due to the translocation's origin, the primary focus was set on investigating effects of the fusion kinase on T cell biology. *In vivo* analysis were supported by *in vitro* experiments in retrovirally infected JurkatE T cells. However, due to the essential role SYK plays in B cell development [186, 33] and signaling [37] the opportunity of the conditional targeting approach was facilitated in order to study the

potential effect of ITK-SYK activity on B cell properties.

Thus, the scientific intent was to establish a mouse model which offers insights into ITK-SYK mediated pathogenesis, and which eventually might be useful for pre-clinical studies on PTCL treatability.

# Chapter 3

## Materials

### 3.1 Reagents

If not stated otherwise, all chemicals were purchased from Sigma-Aldrich. Additional reagent and kit information is provided in the respective methods section.

### 3.2 Employed Antibodies

#### 3.2.1 Westernblot Analysis

Identification	Company
$\alpha$ -phospho-PLC $\gamma$ 1 (Tyr783; rabbit polyclonal IgG)	Cell Signaling
$\alpha$ -phospho-tyrosine (P-Tyr-100; mouse monoclonal IgG)	Cell Signaling
$\alpha$ -Emt (2F12, mouse monoclonal IgG)	Santa Cruz Biotechnology
$\alpha$ -beta-actin (20-33, rabbit polyclonal IgG)	Sigma-Aldrich
$\alpha$ -mouse IgG HRP-linked (horse polyclonal IgG)	Cell Signaling
$\alpha$ -rabbit IgG HRP-linked (goat polyclonal IgG)	Cell Signaling

#### 3.2.2 Stimulation Experiments

Identification	Company
functional grade purified $\alpha$ -mouse CD3e (145-2C11)	eBioscience
functional grade purified $\alpha$ -mouse CD28 (37.51)	eBioscience
functional grade purified $\alpha$ -human CD3e (145-2C4)	BD Pharmingen
functional grade purified $\alpha$ -human CD28 (CD28.2)	BD Pharmingen
AffiniPure goat $\alpha$ -mouse IgG crosslinking antibody	Jackson Immuno Research

### 3.2.3 Flowcytometry: Extracellular Staining Panel

Applied antibodies were conjugated to one of the following fluorochromes: phycoerythrin (PE), phycoerythrin cyanin 5 (PE-Cy5) or allophycocyanin (APC). Exception, the  $\alpha$ -mouse CD16/32 antibody used for  $F_c$  receptor saturation was purified and unconjugated.

Identification	Company
$\alpha$ -mouse B220 (RA3_6B2)	eBioscience
$\alpha$ -mouse CD3 (1452C11)	eBioscience
$\alpha$ -mouse CD4 (Gk1.5)	eBioscience
$\alpha$ -mouse CD5 (53-7.3)	eBioscience
$\alpha$ -mouse CD8 (53-6.7)	eBioscience
$\alpha$ -mouse CD11b (M1/70)	BD Pharmingen
$\alpha$ -mouse CD16/32 (93), purified	eBioscience
$\alpha$ -mouse CD21/35 (7G6)	eBioscience
$\alpha$ -mouse CD23 (B3B4)	eBioscience
$\alpha$ -mouse CD44 (IM7)	eBioscience
$\alpha$ -mouse CD62L (MEK-14)	eBioscience
$\alpha$ -human CD69 (FN50)	eBioscience
$\alpha$ -mouse CD86 (GL1)	eBioscience
$\alpha$ -mouse IgM (II/41)	eBioscience
$\alpha$ -mouse IgD (11-26)	eBioscience
$\alpha$ -mouse TCRbeta (H57-597)	eBioscience
$\alpha$ -mouse TCRV $\beta$ 2 (B20.6)	BD Pharmingen
$\alpha$ -mouse TCRV $\beta$ 3 (KJ25)	BD Pharmingen
$\alpha$ -mouse TCRV $\beta$ 4 (CTVB4)	BD Pharmingen
$\alpha$ -mouse TCRV $\beta$ 5.1/5.2 (MR9-4)	BD Pharmingen
$\alpha$ -mouse TCRV $\beta$ 6 (RR4-7)	BD Pharmingen
$\alpha$ -mouse TCRV $\beta$ 7 (TR310)	BD Pharmingen
$\alpha$ -mouse TCRV $\beta$ 8.1/8.2 (MR5-2)	BD Pharmingen
$\alpha$ -mouse TCRV $\beta$ 8.3 (CT-8C1)	BD Pharmingen
$\alpha$ -mouse TCRV $\beta$ 10b (CTVB10b)	BD Pharmingen
$\alpha$ -mouse TCRV $\beta$ 11 (CTVB11)	BD Pharmingen
$\alpha$ -mouse TCRV $\beta$ 12b (CTVB12b)	BD Pharmingen

### 3.2.4 Flowcytometry: Intracellular Staining Panel

Antibodies used in phosflow analysis were either conjugated to phycoerythrin (PE) or Alexa Fluor<sup>®</sup>647 (AF647).

Identification	Company
$\alpha$ -human AKT (pS473)(M89-61)	BD Pharmingen
$\alpha$ -human ERK1/2 (pT202/pY204)(20A)	BD Pharmingen
$\alpha$ -human LAT (pY171)(I58-1169)	BD Pharmingen
$\alpha$ -human PLC $\gamma$ 1 (pY783)(27/PL)	BD Pharmingen
$\alpha$ -human p38 (pT180/pY182)(36/p38)	BD Pharmingen
$\alpha$ -human SLP-76 (pY128)(J141-668.36.58)	BD Pharmingen

### 3.2.5 Immunohistochemistry

Identification	Company
$\alpha$ -mouse CD3 (SP7)	Lab Vision
$\alpha$ -mouse B220 (RA3.6B2)	BD Pharmingen
$\alpha$ -mouse Ki-67 (SP6)	Lab Vision
$\alpha$ -mouse cleaved Caspase 3 (ASP 175)	Cell Signaling

## 3.3 Employed Primer

Primer were either synthesized at GATC Biotech or MWG Biotech. Previously unpublished primer sequences were designed using Gene Construction Kit<sup>®</sup> software and Net primer freeware (<http://www.premierbiosoft.com>).

### 3.3.1 ITK-SYK cDNA and Mutant Generation

Identification	Sequence 5'-3'
is_xhoI_fwd	CTCGAGAACAACCTTTATCCTCCTGGAA
itk_rev_overlap	GGCAGGGGAGGACCTGTTGTCTTCAGGAGTAG
syk_fwd_overlap	GAAGACAACAGGTCCTCCCCTGCCAAGGGA
is_ecoRI_rev	GAATTCAGGTGCGGGAGCGGTTAGTTC
is_xhoI_fwd	CTCGAGAACAACCTTTATCCTCCTGGAA
is_ecoRI_rev	GAATTCAGGTGCGGGAGCGGTTAGTTC
is_fwd_ascI	GGCGCGCCCCACCATGAACAACCTTTATCCTCCTGG
is_rev_ascI	GGCGCGCCAGGTGCGGGAGCGGTTAGTTC
is_kd_fwd	GTGAAAACCGTGGCTGTGAGAATACTGAAAAACGAGGCC

Identification	Sequence 5/-3/
is_kd_rev	GGCCTCGTTTTTCAGTATTCTCACAGCCACGGTTTTTCAC
is_ph_fwd	CCCTCGAACTTTAAAGTCTGCTTCTTTGTGTTAACC
is_ph_rev	GGTTAACACAAAGAAGCAGACTTTAAAGTTCGAGGG

### 3.3.2 Southern Probe Amplifikation

Identification	Sequence 5/-3/
probe_fwd	GATCAAAACACTAATGAACTT
probe_rev	TTAATTAAAACGAATATTTGGAAT

### 3.3.3 Genotyping

Identification	Sequence 5/-3/
geno_is_fwd	GATGGATGGGAAGTGGAGGTG
geno_is_rev	GGACCAAGTTCTGCCATCTC
Cre_fwd	ACCAGCCAGCTATCAACTCG
Cre_rev	TTACATTGGTCCAGCCACC
Cre7	TCAGCTACACCAGAGACGG
CD19c	AACCATTCAACACCCTTCC
CD19d	CCAGACTAGATACAGACCAG

### 3.3.4 Genescan Analysis

When indicated primer were 5/-labeled with 6-carboxyfluorescein (FAM). Primer sequences have been previously published for the TCR $\beta$  [4, 64] and the TCR $\gamma$  [89] locus.

Identification	Sequence 5/-3/
TCR $\beta$ -V $\beta$ 1	AAATGAGACGGTGCCCAGTCGTT
TCR $\beta$ -V $\beta$ 2	TCCTGGGGACAAAGAGGTCAAATC
TCR $\beta$ -V $\beta$ 3	GAAAAACGATTCTCTGCTGAGTGTCC
TCR $\beta$ -V $\beta$ 4	AGCTATCAAAAACCTTATGGACAATCAG
TCR $\beta$ -V $\beta$ 5	CAGCAGATTCTCAGTCCAACAGTTT
TCR $\beta$ -V $\beta$ 6	AAGGCGATCTATCTGAAGGCTATGA
TCR $\beta$ -V $\beta$ 7	AGCTGATTTATATCTCATACGATGTTG
TCR $\beta$ -V $\beta$ 8	TATATGTACTGGTATCGGCAGGACA
TCR $\beta$ -V $\beta$ 9	TTCCAATCCAGTCGGCCTAACAAT
TCR $\beta$ -V $\beta$ 10	GCGCTTCTCACCTCAGTCTTCAG

<b>Identification</b>	<b>Sequence 5'-3'</b>
TCR $\beta$ -V $\beta$ 11	TTCTCAGCTCAGATGCCCAATCAG
TCR $\beta$ -V $\beta$ 12	AGCTGAGATGCTAAATTCATCCTTC
TCR $\beta$ -V $\beta$ 13	CTGCTGTGAGGCCCTAAAGGAACTAA
TCR $\beta$ -V $\beta$ 14	AGAGTCGGTGGTGCAACTGAACCT
TCR $\beta$ -V $\beta$ 15	CCCATCAGTCATCCCAACTTATCC
TCR $\beta$ -V $\beta$ 16	GATTTTAGGACAGCAGATGGAGTTTC
TCR $\beta$ -V $\beta$ 17	TCGAAATGAAGAAATTATGGAACAAAC
TCR $\beta$ -V $\beta$ 18	CCGGCCAAACCTAACATTCTCAAC
TCR $\beta$ -V $\beta$ 19	CTACAAGAAACCGGGAGAAGAACTC
TCR $\beta$ -V $\beta$ 20	CTGGTATCAACAAAAGCAGAGCAAA
TCR $\beta$ -D $\beta$ 1	GAGGAGCAGCTTATCTGGTGGTTT
TCR $\beta$ -D $\beta$ 2	GTAGGCACCTGTGGGGAAGAAACT
TCR $\beta$ -J $\beta$ 1 (FAM)	CACAACCCCTCCAGTCAGAAATG
TCR $\beta$ -J $\beta$ 2 (FAM)	TGAGAGCTGTCTCCTACTATCGATT
TCR $\gamma$ -V $\gamma$ 4	AGTGTTTCAGAAGCCCGATGCA
TCR $\gamma$ -J $\gamma$ 1 (FAM)	AGAGGGAATTACTATGAGCT

# Chapter 4

## Methods

### 4.1 Work with Nucleic Acids

#### 4.1.1 Determination of Nucleic Acid Concentration

The amount of nucleic acid, as ultraviolet light adsorbing molecule [52], was determined on a NanoDrop<sup>®</sup> ND-100 Spectrometer (Peqlab Biotechnologie). An optical density unit of 1 measured at 260nm ( $OD_{260}$ ) equals  $40\mu\text{g}/\text{ml}$  of single-stranded (ss) RNA and  $50\mu\text{g}/\text{ml}$  of double-stranded (ds) DNA dissolved in water. The amount of adsorbed light is proportional to the amount of nucleic acid in solution, with ratio readings  $OD_{260}/OD_{280}$  being used as an estimate for sample purity. Pure RNA and DNA preparations result in ratios of 1.9–2.1 and 1.8–2.0, respectively. Significant protein or phenol contaminations will lead to reduced ratios.

#### 4.1.2 Agarose Gelectrophoresis

Agarose gelectrophoresis was performed to separate or purify negatively charged nucleic acid according to its size and conformation by migration through an agarose gel matrix (1-2% agarose (w/v) (BD Biosciences) in TAE buffer (0.4M Tris base, 1.1% (v/v) acetic acid, 0.5M EDTA). Migration was achieved by applying an electric field (90-150V)[159]. Ethidium bromide ( $0.5\mu\text{g}/\text{ml}$ , Eurobio), as DNA-intercalating fluorescent dye [62], was used for DNA visualization after excitation with ultraviolet light of 320nm wavelength on a GelDOC 2000 (Bio-Rad Laboratories). For gel loading, samples were resuspended in  $10\times$  DNA loading dye (50% glycerol (v/v), 0.05% bromophenol blue (w/v) (Roth), 1mM EDTA (pH 8.0)). DNA size was determined by comparing the fragment height to an appropriate DNA standard (100bp or 1kb DNA ladder, Peqlab). Gelectrophoresis supply was purchased from Bio-Rad Laboratories.

### 4.1.3 Polymerase Chain Reaction

The polymerase chain reaction (PCR) is used to amplify specific nucleotide sequences. It consists of three main phases: DNA double strand denaturation, oligonucleotide hybridization of one or several forward (fwd) as well as reverse (rev) primers, and DNA sequence amplification by a thermostable DNA polymerase. These steps are performed in repeated cycles at varying temperatures for maximal but sequence-specific product amplification [132]. For this work, PCR had been performed as part of several applications, such as RT-PCR (Subsection 4.1.4), DNA amplification prior to molecular cloning approaches (Subsection 4.1.6), site-directed mutagenesis (Subsection 4.3.1), southern probe generation (Subsection 4.1.7), and mouse genotyping (Subsection 4.5.4). A variation, the so-called touch-down PCR had been performed for genescan analysis (Subsection 4.1.5). For this specific PCR approach, initial reaction cycles share high annealing temperatures to maximize sequence-true primer binding for stringent product generation. As the reaction progresses, the annealing temperature of subsequent reaction cycles decrements to increase specific product amplification.

If not stated otherwise, the amplification reaction consisted of 0.2mM dNTP each (Bioline), 0.2 $\mu$ M primer each, 50ng template, 0.04U/ $\mu$ l of Illustra<sup>TM</sup> Taq DNA Polymerase (GE Healthcare) in reaction buffer (GE Healthcare). When applying the Phusion Hot Start High Fidelity DNA Polymerase (Finnzymes), the reaction set-up was composed of 0.2mM dNTP each (Bioline), 0.5 $\mu$ M primer each, 10ng of DNA, 0.02U/ $\mu$ l of polymerase in HF reaction buffer (Finnzymes). Reaction volumes were either 25 $\mu$ l or 50 $\mu$ l. PCR cycling conditions and primer sequences used for the individual application are stated in the respective chapters. All reactions were carried out on a PCR thermocycler (Biorad).

### 4.1.4 Reverse Transcriptase-Polymerase Chain Reaction

The technique of reverse transcriptase (RT)-PCR was firstly applied to enzymatically generate complementary DNA (cDNA) from RNA by reverse transcription, and secondly to amplify the cDNA region of interest by PCR. As starting material, total RNA was isolated from either  $1 \times 10^6$  JurkatE T cells or  $1 \times 10^6$  SuDHL6 cells by using the TRIzol<sup>®</sup> Reagent (Invitrogen). First strand cDNA synthesis was achieved by applying the SuperScript<sup>TM</sup> II RT system (Invitrogen) according to the manufacturer's instructions with a 20 $\mu$ l reaction consisting of 1 $\mu$ g total RNA, 0.5mM dNTPs each, 250ng random primers, 5mM DTT, and 10U/ $\mu$ l of SuperScript<sup>TM</sup> II RT. Random hexamer nucleotides were chosen as primers, consisting of a mixture of every possible six base-long single strand combination of nucleotides to ensure primer annealing and complete cDNA synthesis throughout the target RNA. Newly generated cDNA was used as a template for sequence specific amplification with the Phusion Hot Start High Fidelity DNA Polymerase

(Finnzymes) prior to molecular cloning as described (Subsection 4.1.6).

### 4.1.5 Genescan Analysis

PCR-based and computer-assisted fragment length analysis (genescan) was performed to assess TCR locus rearrangements in murine primary T cells as described [93, 191]. This method allows adequate resolution of similar sized PCR products by applying fluorescently labeled primers to visualize DNA fragments, and a polymer matrix to separate them according to their size by capillary gelelectrophoresis. 6-carboxyfluorescein (6-FAM<sup>TM</sup>) was chosen as 5-prime (5′)-labeling fluorochrome of the reverse primers, with an emission at 494nm wavelength after argon laser excitation. Emitted light is directly proportional to the amount of nucleic acid present in the reaction volume. The resulting data were graphically displayed in an electropherogram showing fluorescence intensity in relative fluorescent units (RFU) as a function of the fragment size.

Genomic DNA was extracted by using the GenElute<sup>TM</sup> Mammalian Genomic DNA Miniprep Kit (Sigma-Aldrich) from total splenic cell suspensions of diseased ITK-SYK<sup>CD4-Cre</sup>, ITK-SYK<sup>CD19-Cre</sup>, and control mice (CD4-Cre and CD19-Cre mice, respectively). The DNA was assayed for clonal gene rearrangements at the TCR $\beta$  and the TCR $\gamma$  locus. V-D-J and incomplete D-J rearrangements of the TCR $\beta$  locus were analyzed via five individual PCR reactions with the following primer combinations: V $\beta$ (1-20)-J $\beta$ 1, V $\beta$ (1-20)-J $\beta$ 2, D $\beta$ 1-J $\beta$ 1, D $\beta$ 2-J $\beta$ 2, and D $\beta$ 1-J $\beta$ 2. Primer sets consisted of a mixture of 20 family-specific upstream primers located within the V $\beta$  gene segments or consensus primers immediately located 5′ of the D $\beta$ 1/D $\beta$ 2 rearrangement and 5′-FAM-labeled consensus primers immediately located 3-prime (3′) of the J $\beta$ 1/J $\beta$ 2 rearrangement as described [64]. The TCR $\gamma$  locus was analyzed for V-J rearrangements by a single PCR reaction using a V $\gamma$ 4 and a 5′-FAM-labeled J $\gamma$ 1 consensus primer as described [89].

Primer sequences for amplification within the TCR $\beta$  and TCR $\gamma$  locus are listed in Subsection 3.3.4. The 25 $\mu$ l PCR reaction contained 100ng genomic DNA, 0.05U/ $\mu$ l Amplitaq Gold DNA-Polymerase, 2.8mM MgCl<sub>2</sub>, 0.2mM dNTP each (Bioline) and 0.2 $\mu$ M primer each in GeneAmp PCR Buffer I. PCR cycling conditions for amplifying incomplete D-J rearrangements of the TCR $\beta$  locus were 95°C for 5min, 37 cycles of 94°C for 1min, 63°C for 40s, 72°C for 1min, and an end-elongation step at 72°C for 5min. The PCR reaction for the TCR $\gamma$  locus used the same cycling conditions, with the exception of a lower annealing temperature (57°C). For the multiplex-PCR reactions V $\beta$ (1-20)-J $\beta$ 1 and V $\beta$ (1-20)-J $\beta$ 2 a touchdown-PCR approach was chosen with the following conditions: 95°C for 5min, 16 cycles of 94°C for 1min, 72°C for 40s (reduced by 0.7°C every cycle), 72°C for 1min, followed by 30 cycles of 94°C for 1min, 63°C for 40s, 72°C for 5min, and an end-elongation step at 72°C for 5min. PCR products were size-separated by capillary POP-7<sup>TM</sup> polymer electrophoresis and visualized via automated scanning with the

3700 Genetic Analyzer. Gene Scan<sup>TM</sup> 500HD ROX was used as internal standard. If not stated otherwise, all reagents for genescan analysis as well as the 3700 Genetic Analyzer were purchased from Applied Biosystems. Fragment size distribution was determined using GeneMapper<sup>®</sup> software, also obtained from Applied Biosystems. Genescan analysis was performed together with Julian Holch (medical student in the lab) in cooperation with Birgit Geist who supplied technical assistance (Institute of Pathology, Technische Universität München).

### 4.1.6 Molecular Cloning

Molecular cloning was performed for the generation of retroviral expression vectors and the generation of the pROSA26<sup>loxSTOPlox-ITK-SYK</sup> targeting vector. Standard molecular biology techniques were applied [159]. In brief, the cDNA of interest (insert DNA), flanked by specific restriction endonuclease (RE) recognition sites, was first introduced into the pCR<sup>®</sup>II-TOPO<sup>®</sup> vector by applying the TOPO TA Cloning<sup>®</sup> Kit (Invitrogen). PCR products amplified by DNA polymerases with proof reading activity, such as the Phusion Hot Start High Fidelity DNA Polymerase (Finnzymes), were pretreated with 0.05U/ $\mu$ l of the Illustra<sup>TM</sup> Taq DNA Polymerase (GE Healthcare), 0.2mM dNTP each (Bioline) in the supplied reaction buffer (GE Healthcare) at 72°C for 20min. This reaction generates a single 3'-adenine overhang required for insert ligation into TOPO TA<sup>®</sup> cloning vectors. One Shot<sup>®</sup> Top10 chemically competent *E.coli* (Invitrogen) were used for all TOPO TA Cloning<sup>®</sup> approaches.

Subsequently, a preparative digest was performed. To this end, 2 $\mu$ g of sequence verified pCR<sup>®</sup>II-TOPO<sup>®</sup> vector carrying the insert DNA and 2 $\mu$ g of the respective vector backbone (pMigR1 or pROSA26 targeting vector) were incubated with 1U/ $\mu$ l of the intended REs o/n at 37°C. Fragment size confirmation and DNA purification was achieved by agarose gelelectrophoresis (Subsection 4.1.2). Recovery of the linearized backbone and the insert DNA from the gel matrix was realized by using the QIAquick<sup>®</sup> Gel Extraction Kit (Qiagen). Purified vector backbone and insert DNA were then fused in an enzymatic reaction by the T4 Ligase, applying the Rapid DNA Ligation kit (Invitrogen) according to the manufacturer's instructions. In the presence of ATP, the T4 Ligase catalyzes the formation of phosphodiester bonds between complementary double-stranded DNAs with 3'-hydroxyl and 5'-phosphate ends. Molar ratios of 3:1, 5:1 and 10:1 of insert:vector backbone were used for the ligation reaction set-ups with 0.05U/ $\mu$ l T4 Ligase. Successfully ligated plasmids were propagated by transformation of Subcloning Efficiency<sup>TM</sup> DH5alpha<sup>TM</sup> chemically competent *E.coli* (Invitrogen) according to the manufacturer's protocol.

In the case of a bidirectional cloning strategy, which uses only one RE for plasmid linearization, dephosphorylation of the vector backbone prior to the ligation step was per-

formed. This was done by adding 0.025U/ $\mu$ l Calf Intestinal Alkaline Phosphatase (CIAP) (Invitrogen), followed by an incubation step at 37°C for 1h, and heat-inactivation at 72°C for 10min. CIAP catalyzes the hydrolysis of 5'-phosphate groups from the linearized DNA hence preventing recircularization of the linearized vector backbone. CIAP was subsequently removed by applying the QIAquick PCR Purification Kit (Qiagen) before setting up the final ligation reaction. Bidirectional cloning has been used for the generation of the pROSA26<sup>loxSTOPlox-ITK-SYK</sup> targeting vector.

In all molecular cloning approaches chemically competent bacteria were transformed by heat shock, and cultivated o/n at 37°C, 225rpm shaking, according to the manufacturer's instructions. Ampicillin-containing Luria-Bertani medium (1% bacto-tryptone (w/v) (BD Biosciences), 0.5% bacto-yeast extract (w/v) (BD Biosciences), 1% NaCl (w/v), 50 $\mu$ g/ml ampicillin (adjusted to pH7.0) (Roth) was used for selective bacterial propagation. Only bacteria which carry recombinant vectors expressing the ampicillin resistance gene beta-lactamase will grow under these culture conditions [179].

#### 4.1.7 Southernblot Analysis

Southernblot analysis was performed to screen electroporated E14K embryonic stem cells (ESCs) for homologous recombination within the ROSA26 locus. First described by Edwin Southern [175], this method consists of the membrane transfer (blot) of electrophoretically separated DNA fragments, and the fragment identification (detection) via probe hybridization.

Therefore, individually expanded ESCs were harvested from a 10cm cell culture plate, washed in PBS, resuspended in TNE lysis buffer (10mM Tris/HCl (pH7.6), 1mM EDTA (pH8.0), 100mM NaCl, 0.3mg/ml Proteinase K, 0.7mg/ml Pronase E, 0.7% SDS (w/v)), and incubated over night (o/n) at 37°C and 600rpm while shaking. Genomic DNA was isolated via phenol/chloroform precipitation [159]. DNA purity and concentration were determined as described (Subsection 4.1.1). 20 $\mu$ g of genomic stem cell DNA was digested with 1.6U/ $\mu$ l *XbaI* (New England Biolabs) o/n at 37°C and subjected to slow agarose gelelectrophoresis (1% agarose (w/v), TAE buffer, 30V, o/n) as described (Subsection 4.1.2). Gel preparation prior to membrane transfer included depurination in 0.25M HCl, denaturation in buffer I (1.5M NaCl, 0.5M NaOH), and gel neutralization in buffer II (1M Tris base, 1.5M NaCl) (pH7.4). O/n transfer of single stranded DNA molecules onto a positively charged nylon membrane (HYBOND-N<sup>+</sup>nylon membrane, GE Healthcare) was based on capillary force. DNA membrane immobilization was mediated by shortwave ultraviolet energy exposure (254nm, 120J) in a CL-1000 Ultraviolet Crosslinker (UVP).

Specific DNA fragment identification was achieved by membrane hybridization with a radioactively labeled probe located at the 5'-end of the ROSA26 locus. The probe detects a 4.6kb fragment for the wildtype and an 8.9kb fragment for the recombinant allele.

For that purpose, 40ng of ROSA26 probe was labeled by incorporation of [ $\alpha$ -P32]-dCTP (Hartman Analytic GmbH) via random priming using the Ready-To-Go<sup>TM</sup> DNA labeling beads (GE Healthcare). Subsequently, the radioactively labeled probe was purified by Micro Spin<sup>TM</sup> S-200 HR columns (GE Healthcare) according to the manufacturer's instructions. Pre-hybridization (1h, 65°C) and final radioactive hybridization of the membrane (o/n, 65°C) were done in Church buffer (1mM EDTA, 0.25M sodium phosphate buffer (pH7.2), 7% SDS (w/v), 1% BSA (w/v)). This procedure was followed by washing steps in buffer III (2× SSC, 0.1% SDS (w/v)) and buffer IV (0.2× SSC, 0.1% SDS (w/v)). Intended counts were below 50 IPS (incidents per second) as measured by a contamination monitor (LB122, Berthold Technologies). For signal detection the hybridized membrane was exposed to a phosphor storage screen (GE Healthcare) o/n, which is able to chemically trap radioactive energy. Upon red laser excitation in a PhosphorImager<sup>TM</sup> (Molecular Dynamics) the radioactive energy is released as emitted light, being proportional to the amount of radioactively labeled genomic DNA present on the membrane. Data were analyzed by using ImageQuant<sup>TM</sup> software.

Primer sequences (probe\_fwd/probe\_rev) used for probe amplification were kindly provided by M. Schmidt-Supprian (Max Planck Institute for Biochemistry, Molecular Immunology & Signal Transduction, Munich), and are listed in Subsection 3.3.2. Cycling conditions for generating a 607bp product were as follows: 98°C for 30s, 35 cycles of 98°C for 10s, 53.5°C for 30s, 72°C for 15s, and an end-elongation step at 72°C for 10min. The Phusion Hot Start High Fidelity DNA Polymerase (Finnzymes) was used for amplification with a standard reaction set-up as described in Subsection 4.1.3.

## 4.2 Work with Proteins

### 4.2.1 Westernblot Analysis

For whole cell protein analysis  $5 \times 10^6$  retrovirally infected JurkatE T cells or  $1 \times 10^7$  primary lymphocytes were lysed in ice-cold CHAPS buffer (10mM Tris (pH7.5), 1mM MgCl<sub>2</sub>, 1mM EGTA, 10% glycerol (v/v), 0.5% CHAPS (w/v)), supplemented with phosphatase (50mM NaF, 0.1mM Na<sub>3</sub>VO<sub>4</sub>, 10mM  $\beta$ -glycerophosphate) and protease (Complete EDTA free Protease Inhibitor Cocktail Tablets, Roche Diagnostics) inhibitors. Protein concentrations were spectrophotometrically determined. This is based on a coomassie brilliant blue G-250 dye/protein interaction, which causes a shift in the adsorption maximum from 465nm to 595nm wavelength [21]. Cell lysates were subsequently subjected to standard westernblot analysis [29]. To this end, proteins were denaturated in SDS sample buffer (62.5mM Tris/HCl (pH6.8), 2% SDS (w/v), 10% glycerol (v/v), 5% 2-mercaptoethanol (v/v), 0.02% bromphenol blue (w/v)) and incubated at 95°C for 5min

before loading. Polyacrylamid gel electrophoresis with a discontinuous buffer system was applied to separate proteins according to their molecular weight and SDS negativity [104]. A standard gel run was performed in a SDS-PAGE running buffer (25mM Tris (pH 8.3), 2M glycine, 1% SDS (w/v)) at 130-145V. Hence, the resolved proteins were transferred electrophoretically onto a PVDF (Amersham Hybond<sup>TM</sup>-P, GE Healthcare) or nitrocellulose (Protan<sup>®</sup> Nitrocellulose, Whatman<sup>®</sup>) membrane via a semi-dry blotting approach in transfer buffer (50mM Tris (pH 8.5), 40mM glycine, 0.03% SDS (w/v), 20% methanol (v/v) added prior to use). Membranes were probed with antigen specific primary antibodies (dilution range 1:1000–1:2000). Antibody dilutions were prepared in 5% skim milk powder (w/v) or 5% BSA (w/v) in TBST (0.025% Tween-20 (v/v), 20mM Tris (pH7.4), 137mM NaCl). For chemiluminescence-based detection, HRP-conjugated secondary antibodies (dilution 1:2000) and detection systems Lumigen<sup>TM</sup> TMA-6, Solution A+B (GE Healthcare) or Detection Reagent 1+2/Peroxid Solution (Thermo Scientific, Pierce) were applied. The applied antibody panel is summarized in Subsection 3.2.1.

## 4.2.2 Lipid Raft Preparations

Lipid raft fractionation was based on sucrose gradient centrifugation and applied as described [206]. In brief,  $5 \times 10^7$  purified lymphocytes were stimulated or kept unstimulated and lysed in 1ml ice-cold Brij lysis buffer (1% Brij97 (v/v), 150mM NaCl, 20mM Tris (pH7.5), 2mM EDTA, 10mM NaF, 1mM Na<sub>3</sub>VO<sub>4</sub>, protease inhibitors (Complete Protease Inhibitor Cocktail tablets, Roche Diagnostics)), and prepared by dounce homogenization. Alternatively,  $1 \times 10^7$  JurkatE T cells were harvested 36h post retroviral infection, stimulated, or kept unstimulated and prepared equally. For stimulation settings see Subsection 4.4.5. Historically described as non-ionic, detergent-resistant, cholesterol and glycosphingolipid enriched areas within the membrane lipid bilayer [25], lipid rafts remain intact during the applied lysis procedure. After centrifugation (2000rpm, 10min, 4°C) post-nuclear supernatants were mixed with an equal volume of 85% (w/v) sucrose, overlaid with 2ml of 35% (w/v) and 1ml of 5% (w/v) sucrose and separated according to their density by ultracentrifugation (Beckman SW41 Rotor, 200 000g, 4°C, 16h). Sucrose solutions were prepared in MES-buffered saline (25mM MES (pH6.5), 150mM NaCl, 5mM EDTA). Eleven 400μl fractions were harvested from the top of the gradient. Due to low amounts, raft-associated protein was concentrated with 10% trichloroacetic acid precipitation [159]. Both raft-associated protein (enriched from fraction 1-4) and non-raft protein (fraction 9-11) were resuspended in SDS sample buffer, pooled, and subjected to westernblot analysis (Subsection 4.2.1). Nitrocellulose membrane (Protan<sup>®</sup> Nitrocellulose, Whatman<sup>®</sup>) was used for protein blotting. Successful raft separation was confirmed from the collected gradient fractions 1-4 via chemiluminescence-based dot-blot analysis, visualizing the lipid raft associated ganglioside GM1 by interaction with the HRP labeled cholera

toxin B subunit (Sigma-Aldrich) [192]. Detection systems were applied as described for westernblot analysis (Subsection 4.2.1). Lipid raft experiments were performed together with Dr. Uta Ferch (former member of the lab).

## 4.3 Work with Retroviruses

### 4.3.1 Retroviral Expression Vectors

Retroviral constructs were generated by cloning the ITK-SYK cDNA into the MSCV-based vector pMigR1 [137]. As a special feature, this vector carries the coding sequence for the enhanced green fluorescent protein (eGFP), preceded by an internal ribosomal entry site (IRES). eGFP expression therefore enables convenient cell tracking via green fluorescence. Prior to vector generation, the human ITK-SYK fusion cDNA was created in a multistep PCR. On the one hand, the N-terminal fragment of the ITK-SYK cDNA, which encodes the first 165 amino acids of ITK (NM\_005546, exon 1–5) was amplified from JurkatE T cell cDNA. On the other hand, the C-terminal fragment of ITK-SYK which encodes the last 330 amino acids of SYK (NM\_003177, exon 9–14) was amplified from SuDL6 B cell cDNA. In a subsequent reaction both fragments were annealed at the overlapping breakpoint sequence. Amplified full-length ITK-SYK cDNA was then used for molecular cloning as described (Subsection 4.1.6). The primer pair *is\_xhoI\_fwd/itk\_rev\_overlap* and the primer pair *syk\_fwd\_overlap/is\_ecoRI\_rev* were used respectively for amplifying the N-terminal ITK (520bp) and the C-terminal SYK (1027bp) fragment. Amplification conditions for both fragments were 98°C for 30s, 35 cycles of 98°C for 10s, 65.6°C for 20s, 72°C for 20s followed by an end-elongation step at 72°C for 10min.

Individual fragments were purified as described (Subsection 4.1.6) and annealed by the following reaction cycles: 98°C for 30s, 8 cycles of 98°C for 10s, 80°C for 30s, 72°C for 48s, and 98°C for 30s. Amplification of the full-length *XhoI/EcoRI*-flanked ITK-SYK cDNA (1514bp) was obtained by running 22 cycles of 98°C for 10s, 61°C for 30s, 72°C for 30s, and an end-elongation step of 72°C for 10min, with the flanking primer pair *is\_xhoI\_fwd/is\_ecoRI\_rev*. The Phusion Hot Start High Fidelity DNA Polymerase (Finnzymes) was used in all reactions. Reactions were set-up as described (Subsection 4.1.3). Primer sequences used for individual amplifications are summarized in Subsection 3.3.1. Sequencing of the cloned *TOPO<sup>XhoI-ITK-SYK-EcoRI</sup>* vector confirmed the correct fusion cDNA [178]. The sequence had been additionally verified by alignment with the ITK-SYK cDNA generated directly from patient-derived RNA (provided by Berthold Streubel, Department of Pathology, Medical University of Vienna, Austria). Hence, *XhoI/EcoRI*-flanked ITK-SYK cDNA was hence available for cloning into pMigR1 as described (Subsection 4.1.6).

Retroviral constructs expressing the aminoacid exchange mutants ITK-SYK (K262R) (ITK-SYK<sup>KD</sup>) and ITK-SYK (R29C) (ITK-SYK<sup>PHmut</sup>) were generated from the template MigR1<sup>ITK-SYK</sup> by applying the Quick Change<sup>®</sup> Site-Directed Mutagenesis Kit (Stratagene). The procedure was performed according to the manufacturer's instructions. This approach combines PCR amplification, using oligonucleotide primers carrying the mutation of interest, with a methylation selective DNA digest. The use of *DpnI* (Roche), a RE which specifically targets methylated DNA, enables propagation of the newly synthesized, non-methylated plasmid DNA in competent bacteria. In brief, 5ng of pMigR1<sup>ITK-SYK</sup> vector template was amplified by adding 0.05U/ $\mu$ l Pfu Turbo DNA polymerase (Stratagene), 0.2mM dNTP each (Bioline) and 125ng primer each in the supplied reaction buffer (Stratagene), with a total reaction volume of 50 $\mu$ l. The primer pairs is\_kd\_fwd/is\_kd\_rev and is\_ph\_fwd/is\_ph\_rev were chosen to generate pMigR1<sup>ITK-SYK-KD</sup> and pMigR1<sup>ITK-SYK-PHmut</sup>, respectively. The applied PCR conditions were 95°C for 30s, 12 cycles of 95°C for 30s, 55°C for 60s, 68°C for 8min followed by a 2min incubation on ice. For digest of the parental plasmid DNA, 0.2U/ $\mu$ l *DpnI* (Roche) were added, and incubated for 1h at 37°C. Transformation of XL1-Blue supercompetent cells (Stratagene) with the newly generated plasmid DNA was done according to the manufacturer's instructions. Primer sequences used for site-directed mutagenesis are summarized in Subsection 3.3.1.

### 4.3.2 Retroviral Transduction

Retroviral transduction is the process of transferring genetic material to host cells by retroviruses. Early steps of retroviral transduction include virus adsorption and interaction of viral proteins, such as the envelope protein with host cell surface receptors, eventually triggering virus/cell membrane fusion [35]. In the case of ecotropic viruses, the host cell membrane receptor is a cationic amino acid transporter, designated mCAT-1, which is expressed selectively on murine and rat cells [6, 195, 92]. Infection of human cells nevertheless becomes possible when choosing cell lines which have been genetically modified to express the murine ecotropic retroviral receptor on their cell surface, such as JurkatE T cells [76]. Thus, a naturally host-restricted MSCV-based virus can be applied to transduce a human cell line. Applying this system, retroviral particles were produced by transiently transfecting the PhoenixE packaging cell line with the indicated retroviral expression vectors (Subsection 4.3.1) via the CaPO<sub>4</sub> precipitate method [69]. PhoenixE in itself carry the viral genes gag, pol, and env needed for retroviral particle assembly [85].

In practice, 12h prior to transfection,  $2.5 \times 10^6$  PhoenixE cells were seeded per 10cm plate in transfection medium (TM) (DMEM, 10% FBS (v/v), 1% penicillin (pen)/streptomycin (step) (v/v)) to achieve a 50–70% cell confluence on the day of transfection. Pretreatment of PhoenixE consisted of a 30min incubation step in TM supplemented with 40 $\mu$ M chloroquine. Chloroquine enhances the transfection efficiency by in-

creasing the intralysosomal pH, thus reducing enzymatic degradation of internalized retroviral DNA [119]. In parallel,  $2\mu\text{g}$  of the respective retroviral expression vector was mixed with  $125\text{mM}$   $\text{CaCl}_2$  in HBS buffer ( $140\text{mM}$   $\text{NaCl}$ ,  $0.75\text{mM}$   $\text{Na}_2\text{HPO}_4$ ,  $25\text{mM}$  HEPES (pH6.93)), and incubated at RT for 15min. Formed DNA/ $\text{CaCl}_2$  precipitates were then added dropwise to chloroquine-pretreated PhoenixE cells followed by a change of medium after 6h of incubation. Virus-containing supernatant was collected 48h and 72h post transfection, filtered (Millex<sup>®</sup>-HV Filter,  $0.45\mu\text{m}$ ), and stored at  $4^\circ\text{C}$  until used. For retroviral transduction  $0.5\times 10^6$  JurkatE T cells/ml were resuspended in viral supernatant, supplemented with  $25\text{mM}$  HEPES and  $10\mu\text{M}$  polybrene (Millipore<sup>TM</sup>). Polybrene, as cationic polymer, enhances initial viral adsorption and improves transduction efficiency [39]. JurkatE T cells were then subjected to one round of spin infection by centrifugation ( $2400\text{rpm}$ ,  $32^\circ\text{C}$ , 90min), and cultured for 12h before changing the medium and seeding for further analysis. Transduction efficiency was determined flow cytometrically, and was based on the percentage of eGFP<sup>+</sup> viable JurkatE T cells in culture. PhoenixE cells and JurkatE T cells were kindly provided by Garry P. Nolan (Department of Microbiology and Immunology, Stanford University, USA) and kept under standard cell culture conditions as described (Subsection 4.4.1).

## 4.4 Work with Eukaryotic Cells

### 4.4.1 Basic Cell Culture

JurkatE T cells were cultured in RPMI-1640 medium supplemented with 10% FBS (v/v) (Hyclone Perbio), 1% L-glutamine (v/v), 1% pen/step (v/v) and 0.1% 2-mercaptoethanol (v/v) at a density of  $0.1\times 10^6$  cells/ml and splitted at a density of  $0.5\times 10^6$  cells/ml. PhoenixE packaging cells were maintained in DMEM, supplemented as described for JurkatE T cells, seeded at  $2\times 10^6$  cells per 10cm plate, and splitted at a ratio of 1:5 every second day by trypsinization (1% Trypsin/EDTA (v/v)). Primary lymphocytes were kept in RPMI-1640, supplemented with 5% FBS (v/v), 1% L-glutamine (v/v), 1% pen/step (v/v), and 0.1% 2-mercaptoethanol (v/v) until analyzed. All cells were cultivated under standard cell culture conditions at  $37^\circ\text{C}$ , 5%  $\text{CO}_2$ , and a relative humidity of 95%. Cells were counted by light microscopy under consideration of cell viability as assessed by trypan blue (Trypan Blue Stain 0.4%(w/v), Gibco<sup>®</sup>) exclusion. For conservation, cells were kept in either RPMI or DMEM, depending on the cell line, supplemented with 10% DMSO (v/v)/10% FBS (v/v) and stored in liquid nitrogen. Medium and supplements other than FBS were purchased from Gibco<sup>®</sup>, and tissue culture labware was purchased from TPP<sup>®</sup> Techno Plastic Products AG or BD Falcon<sup>TM</sup>. For functional studies, the SYK inhibitor R406 (provided by Rigel Pharmaceuticals, San Francisco, USA) was added

to the cell culture medium at a concentration of  $2\mu\text{M}$  where indicated.

#### 4.4.2 Embryonic Stem Cell Culture

E14K embryonic stem cells (ESCs), derived from the mouse strain 129P2/OlaHsd [169], were cultured in ESC medium (DMEM supplemented with 15% FBS (v/v), 1% leukemia inhibitory factor (LIF) (v/v), 1% L-glutamine (v/v), 1% pen/strep (v/v), 0.1% 2-mercaptoethanol (v/v), and grown on a monolayer of murine embryonic fibroblasts (feeder cells). ESCs were passaged onto feeder cells every second day with a splitting ratio of 1:4–1:6, emphasizing to dissociate ESC colonies into single cells after trypsinization by thorough pipetting. ESC medium was changed daily. Monitoring of colony density and morphology was performed microscopically to control ESC quality. Cell culture on feeder monolayers as well as the addition of LIF to the ESC cell culture medium [198] were used as standard practice to prevent ESC differentiation processes, and to maintain their totipotency required for germline transmission [183].

Feeder cells were routinely cultured in FC medium (DMEM supplemented with 5% FBS (v/v), 1% pen/strep (v/v), 1% L-glutamine (v/v), 0.1% 2-mercaptoethanol (v/v), and passaged every second day with a splitting factor of 1:2. Cells were pretreated for 2h with mitomycin C containing FC medium (f.c.  $10\mu\text{g}/\text{ml}$ ) when seeded as monolayer for ESC propagation. Mitomycin C acts as an alkylating antibiotic and renders cells mitotically inactive by forming DNA crosslinks [182]. All cells were kept under standard cell culture conditions (Subsection 4.4.1). Supplements were approved for stem cell culture, and purchased from Biochrom AG. FBS was purchased from PAN-Biotech, and media was purchased from Gibco. Tissue culture labware was purchased from BD Falcon<sup>TM</sup>. LIF and feeder cells were kindly provided by the lab of Tim Sparwasser (Institute for Infection Immunology, Twincore Center, Hannover, Germany).

#### 4.4.3 Embryonic Stem Cell Electroporation and Selection

Electroporation was applied as a transformation technique to introduce the targeting vector pROSA26<sup>loxSTOPlax-ITK-SYK</sup> into murine E14K ESCs. This method utilizes pulsed electric current to induce transient permeabilizations within the phospholipid bilayer of eukaryotic cells [133], facilitating the transport of genetic material into the target cell. To this end, a surplus of  $50\mu\text{g}$  of pROSA26<sup>loxSTOPlax-ITK-SYK</sup> targeting vector was linearized per electroporation by incubation with  $0.4\text{U}/\mu\text{l}$  *SnaBI* (New England Biolabs) o/n at  $37^\circ\text{C}$ . Linearized DNA was purified by phenol/chloroform precipitation [159] and dissolved in PBS under sterile conditions. Per electroporation,  $5\times 10^6$  E14K ESCs were mixed with  $20\mu\text{g}$  of linearized targeting vector in  $800\mu\text{l}$  of ESC medium (Subsection 4.4.2), transferred to a Gene Pulser Cuvette (0.4cm electrode gap, Bio-Rad Laboratories) and electroporated

at  $250\mu\text{F}$ ,  $0.34\text{V}$  in a GenePulser<sup>TM</sup> electroporator (Bio-Rad Laboratories). Shocked cells were incubated for 3min at RT, followed by a 15min resting phase on ice, before being seeded on feeder cell monolayers as described (Subsection 4.4.2).

Stem cell selection was performed by Geneticin<sup>®</sup> (Invitrogen) treatment (f.c.  $200\mu\text{g}/\text{ml}$  in ESC medium) for ten days, with a change of selection medium every second day. Geneticin<sup>®</sup> is a gentamicin-related amino glycoside which interferes with 80S ribosome function in eukaryotic cells [14], ultimately leading to cell death [36]. Notably, ESCs carrying the neo cassette which originated from the pROSA26<sup>loxSTOPlax-ITK-SYK</sup> targeting vector, will express the bacterial neomycin resistance gene. It encodes for the amino glycoside 3'-phosphotransferase (APH) II [15]. These cells become Geneticin<sup>®</sup>-resistant and survive the ten day treatment. Subsequently, resistant ESC colonies were harvested under a stereomicroscope (MZ75, Leica Microsystems) and cultivated individually in 96-well plates according to stem cell culture conditions (Subsection 4.4.2). In total, four rounds of electroporation were performed, and eventually forty-two E14K clones with best morphology selected, propagated and analyzed for recombination at the ROSA26 locus by southernblot analysis (Subsection 4.1.7).

#### 4.4.4 Cell Purification

Enrichment of cell populations was either achieved by density gradient centrifugation or by cell type specific purification via magnetic beads. Prior to either procedure, individual organs were mashed, and harvested cells were subjected to red blood cell (RBC) lysis by resuspension in 1ml of RBC Lysis Buffer (eBioscience). This was followed by an incubation step at RT for 5min. Lastly, primary cells were washed in cell culture medium (Subsection 4.4.1) and further processed.

For protein analysis, primary T cells or B cells were purified from pooled spleen (SPL) and lymph node (LN) cell suspensions firstly by depletion of myeloid cells with  $\alpha\text{-CD11b}$  (M1/70; BD Pharmingen) and Dynabeads<sup>®</sup>M-450 sheep  $\alpha\text{-rat IgG}$ . Secondly, depletion of either B cells or T cells with either Dynabeads<sup>®</sup> mouse panT (Thy1.2) or mouse panB (B220) was performed. Bead-bound cells were separated by a magnetic field. Untouched cells of interest were collected from the flow-through by centrifugation (300g, 5min,  $4^\circ\text{C}$ ). All magnetic beads were purchased from Invitrogen. Primary total lymphocytes from organs such as liver (LIV), lung (LNG) and kidney (KID) were enriched by Percoll (Biochrom AG) density gradient centrifugation [138] prior to flow cytometric analysis (Subsection 4.4.7). Primary cells were resuspended in a 40% Percoll/PBS solution, carefully underlaid with an 80% Percoll/PBS solution, and subjected to centrifugation (2600rpm, 25min,  $20^\circ\text{C}$ , no brake). Mononuclear cells were collected from the 40/80 interface, washed in cell culture medium and prepared for further analysis.

### 4.4.5 Cell Stimulation

Cell stimulation of primary T cells and JurkatE T cells was based on antibody binding to the CD3 $\epsilon$  molecule of the TCR complex and the costimulatory molecule CD28, with or without crosslinking of the primary antibodies.

For lipid raft preparations,  $5 \times 10^7$  purified T cells were resuspended in resting medium (RM) (RPMI-1640, 0.2% BSA (w/v), 0.1% 2-mercaptoethanol (v/v)) and incubated for 1h at 37°C in a water bath. Functional grade purified  $\alpha$ -mouse CD3e (f.c. 5 $\mu$ g/ml, 145-2C11, eBioscience) and  $\alpha$ -mouse CD28 (f.c. 1 $\mu$ g/ml, 37.51, eBioscience) antibody were added. Subsequently, cells were incubated on ice for 20min, spun down (425g, 3 min, 4°C), resuspended in prewarmed AffiniPure rabbit  $\alpha$ -syrian hamster IgG (H+L) cross-linking antibody (f.c. 1 $\mu$ g/ml, Jackson ImmunoResearch), and incubated for 5min at 37°C in a water bath. Stimulation of  $1 \times 10^7$  retrovirally infected JurkatE T cells was carried out as outlined for primary T cells. In this regard, however, the functional grade purified  $\alpha$ -human CD3 (f.c. 5 $\mu$ g/ml, 145-2C4, BD Pharmingen),  $\alpha$ -human CD28 (f.c. 1 $\mu$ g/ml CD28.2, BD Pharmingen) antibody and the AffiniPure goat  $\alpha$ -mouse IgG (H+L) (f.c. 1 $\mu$ g/ml, Jackson ImmunoResearch) cross-linking antibody were used. Stimulation of JurkatE T cells was performed 36h after retroviral infection. Lipid raft preparation was performed as described (Subsection 4.2.2). For all stimulations, primary and cross-linking antibodies were diluted in RM. Mice older than 12 weeks were used for T cell preparations to obtain sufficient numbers of ITK-SYK expressing T lymphocytes.

For analyzing CD69 surface expression and IL-2 production, retrovirally infected JurkatE T cells were adjusted to a concentration of  $1 \times 10^6$  cells/ml in cell culture medium (Subsection 4.4.1) and kept under standard cell culture conditions for 12h prior to stimulation. The latter occurred with platebound  $\alpha$ -human CD3 (f.c. 10 $\mu$ g/ml, HIT3a, BD Pharmingen) and soluble  $\alpha$ -human CD28 antibody (f.c. 2 $\mu$ g/ml, CD28.2, BD Pharmingen), diluted in cell culture medium, respectively. CD3 immobilization was achieved by preincubating the wells of flat bottom plates with AffiniPure goat  $\alpha$ -mouse IgG (H+L) antibody (f.c. 10 $\mu$ g/ml in PBS, Jackson ImmunoResearch) o/n at 4°C. Supernatants were harvested 24h post stimulation and IL-2 concentrations were determined via ELISA (Subsection 4.4.6). CD69 surface expression was determined 24h and 48h post stimulation via flow cytometry (Subsection 4.4.7).

For phosflow analysis (Subsection 4.4.7), retrovirally infected JurkatE T cells were adjusted to a concentration of  $5 \times 10^6$  cells/ml in RPMI-1640 supplemented with 1% FBS (v/v) and 0.1% 2-mercaptoethanol, and subsequently rested on ice for 30min. Purified  $\alpha$ -human CD3 (f.c. 5 $\mu$ g/ml, HIT3a, BD Pharmingen) and  $\alpha$ -human CD28 antibody (f.c. 1 $\mu$ g/ml, CD28.2, BD Pharmingen) were added. Cells were incubated (rolling) at 4°C for 20min, spun down (425g, 3min, 4°C), and resuspended in prewarmed AffiniPure goat  $\alpha$ -mouse IgG (H+L) (f.c. 1 $\mu$ g/ml, Jackson ImmunoResearch) cross-linking antibody, fol-

lowed by a 5min incubation step at 37°C in a water bath. Primary antibodies and the cross-linking antibody were diluted in RPMI-1640 supplemented with 1% FBS (v/v) and 0.1% 2-mercaptoethanol. For all individual approaches, stimulations were terminated by adding ice-cold PBS. Cells were further processed depending on the method applied.

#### 4.4.6 Enzyme-linked Immunosorbent Assay

The immunological technique of enzyme-linked immunosorbent assay (ELISA) employs the principle of specific antigen/antibody interaction combined with chemiluminescent detection systems. IL-2 concentrations in cell supernatants from retrovirally-infected JurkatE T cells, kept unstimulated or stimulated (Subsection 4.4.5), were determined via the OptEIA Human IL-2 ELISA Set (BD Pharmingen), according to the manufacturer's instructions. In brief, IL-2 was captured via plate bound antigen specific antibody ( $\alpha$ -human IL-2, dilution ratio 1:250) and detected by a soluble biotinylated  $\alpha$ -IL-2 specific antibody (detection antibody:  $\alpha$ -human IL-2, dilution ratio 1:250). Biotin/streptavidin interaction, as strong non-covalent biological interactions [32], was utilized to target enzymatic HRP activity to the site of specific antigen/antibody interaction. HRP-mediated conversion of 3', 3', 5', 5'-tetramethylbenzidine (TMB) under the presence of hydrogen peroxide, yielded a blue colored oxidized form of TMB. Substrate turnover was terminated by the addition of 2N H<sub>2</sub>SO<sub>4</sub>. The resulting color change to yellow was spectrophotometrically detected at a wavelength of 450nm and correlated to IL-2 concentrations present in the cell supernatant.

#### 4.4.7 Flow Cytometry

Immunophenotyping of cell populations was done by flow cytometry. This method allows cell distinction according to its cell size, granularity, cell surface marker expression, and various intracellular targets using fluorescently labeled antibodies. Light scatter and fluorescence signals emitted after laser excitation are detected, amplified, and converted into electrical signals, which are then processed on the computer [116].

Primary cell suspensions from thymus (THY), SPL, LN, bone marrow (BM) and peripheral blood were subjected to RBC lysis (Subsection 4.4.4). Cells were directly used for flow cytometric staining, whereas cell suspensions from LIV, KID or LNG were additionally purified by Percoll gradient centrifugation (Subsection 4.4.4) prior to cell staining. For extracellular staining,  $0.7 \times 10^6$  cells were resuspended in FACS buffer (FB) (PBS, 3% FBS), spun down (400g, 5min, 4°C) and pre-incubated with purified  $\alpha$ -mouse CD16/32 antibody (dilution ratio 1:200 in FB, eBioscience) for blocking accessible F<sub>c</sub> receptor binding sites. Subsequent extracellular staining was performed in a total volume of 100 $\mu$ l FB for 20min at 4°C, with a final washing step in FB before analysis. Cell activation of retro-

virally infected JurkatE T cell was assessed by surface staining with the  $\alpha$ -human CD69 antibody (FN50) (dilution ratio 1:50 in FB). Fluorescently labeled antibodies against murine epitopes were used at a 1:200 or 1:400 dilution ratio in FB. Subsection 3.2.3 gives an overview of antibodies applied for extracellular staining. Data were acquired either on a FACSCalibur<sup>TM</sup> or a FACSCantoII<sup>TM</sup> flow cytometer.

Activation of retrovirally infected JukatE T cells was analyzed via intracellular staining with phospho-specific antibodies (phosflow). For that purpose, cells were treated with 2% PFA for fixation followed by membrane permeabilization with 70% ice-cold methanol as described [165]. Viability distinction was realized by staining with an amine-reactive dye (violet Live/Dead, Invitrogen). Subsection 3.2.4 summarizes the phospho-specific fluorescently labeled antibodies applied (dilution ratio 1:10 in FB). Data acquisition was carried out on a LSRII flow cytometer. Fluorescently labeled antibodies were purchased from either BD Biosciences or eBioscience. All flow cytometers were purchased from BD Biosciences. FlowJo software (Tree Star, Inc.) was used for data analysis. Phosflow analysis was performed together with Marc Schweneker (former member of the lab) and Julian Holch (medical student in the lab).

## 4.5 Work with Mice

### 4.5.1 Mouse Husbandry

All animals were housed under standardized, specific pathogen free conditions in individually ventilated cages (Thoren MaxiMiser<sup>®</sup> caging systems or TechniPlast IVC). Studies were conducted in compliance to federal and institutional guidelines. Animal protocols were approved by the government of Upper Bavaria.

### 4.5.2 Generation of ROSA26<sup>loxSTOPlox-ITK-SYK</sup> Mice

Conditional gene targeting at the ROSA26 locus was chosen to generate mice with ubiquitous expression of a loxSTOPlox-ITK-SYK-eGFP fusion transcript. The newly generated mouse strain is termed ROSA26<sup>loxSTOPlox-ITK-SYK</sup>. Due to the loxP-site flanked STOP cassette positioned upstream of the ITK-SYK and eGFP coding sequences, expression of both proteins is blocked and only realized upon breeding to Cre-transgenic mouse strains (Subsection 4.5.3).

Starting point for creating the ROSA26<sup>loxSTOPlox-ITK-SYK</sup> mouse strain was the generation of the fusion ITK-SYK cDNA via overlap PCR as described (Subsection 4.3.1). A final amplification step with the primer pair *is\_fwd\_ascI*/*is\_rev\_ascI* produced an *AscI*-flanked ITK-SYK cDNA (1523bp) product. Notably, the forward primer contained a Kosaq consensus sequence (CCACC) [96] directly positioned upstream of the ITK-SYK

cDNA start codon for optimal translational initiation. The PCR conditions were 98°C for 30s, 35 cycles at 98°C for 10s, 65.6°C for 30s, 72°C for 48s with an end-elongation step at 72°C for 10min. The Phusion Hot Start High Fidelity DNA Polymerase (Finnzymes) was used for amplification with a standard reaction set-up as described (Subsection 4.1.3). Primer sequences are outlined in Subsection 3.3.1.

The ITK-SYK amplicate was introduced into the pCR<sup>®</sup>II-TOPO<sup>®</sup> vector, sequence verified, and upon *AscI*-digestion was cloned into the core pROSA26 targeting vector [160]. The vector was kindly provided by Marc Schmidt-Supprian (Max Planck Institute for Biochemistry, Molecular Immunology & Signal Transduction, Munich, Germany). Correct orientation of the ITK-SYK insert was determined by RE digest and subsequent vector sequencing. Hence, the *SnaBI*-linearized pROSA26<sup>loxSTOPlox-ITK-SYK</sup> targeting vector was introduced into E14K ESCs by electroporation. Geneticin<sup>®</sup> treatment was used for positive stem cell selection as described (Subsection 4.4.3). Geneticin-resistant clones were screened by southernblot analysis for recombination at the ROSA26 locus (Subsection 4.1.7). ESC clones with best morphology and growth characteristics were injected into C57BL/6/J blastocysts and subsequently transferred to pseudopregnant foster mice as described [183]. Two independent clones gave rise to chimeric offspring, which after breeding with C57BL/6 mice eventually generated ROSA26<sup>loxSTOPlox-ITK-SYK</sup> heterozygous mice. Germline transmission of the targeted ROSA26 allele was verified by PCR of tail DNA from agouti coat colored F1 offspring mice (Subsection 4.5.4). Blastocyst microinjection was carried out by Susanne Weiss in collaboration with Tim Sparwasser (Institute for Infection Immunology, Twincore Center, Hannover, Germany).

### 4.5.3 Mouse Breeding Approaches

In order to achieve cell type specific expression of ITK-SYK, ROSA26<sup>loxSTOPlox-ITK-SYK</sup> mice were bred to individual Cre-transgenic mouse strains. Within these mice the Cre recombinase expression is put under the control of a lineage specific promoter. Thus, for T cell specific expression of the fusion kinase, ROSA26<sup>loxSTOPlox-ITK-SYK</sup> mice were crossed with CD4-Cre [108] mice. For B cell specific expression crossing with CD19-Cre mice [150] took place. The resulting mouse strains are referred to as ITK-SYK<sup>CD4-Cre</sup> and ITK-SYK<sup>CD19-Cre</sup>, respectively. All mice were of mixed C57BL/6 and 129P2/OlaHsd genetic background. If not stated otherwise, littermates were used in all experiments.

### 4.5.4 Genotyping

Mouse progeny were identified through amplification of strain-specific sequences at the recombinant locus. For that purpose, genomic DNA was extracted from tail pieces applying the Wizard SV Genomic DNA Purification System (Promega). The targeted ROSA26

locus was identified with the primer pair `geno_is_fwd/geno_is_rev`, yielding a 569bp fragment for the recombinant locus. The PCR conditions were 95°C for 5sec, 30 cycles of 95°C for 30s, 58°C for 30s, 72°C for 34s, and an end-elongation step at 72°C for 10min. The Cre allele from CD4-Cre mice [108] was identified with the primer pair `Cre_fwd/Cre_rev`, yielding a 200bp fragment for the recombinant locus. The PCR conditions were 95°C for 2s, 15 cycles of 95°C for 30s, 64°C for 30s, 72°C for 30s followed by 20 cycles of 95°C for 30s, 58°C for 30s, 72°C for 30s, as well as an end-elongation step at 72°C for 10min. The Cre allele originating from CD19-Cre mice [150] was amplified by using the primers `Cre7/CD19c/CD19d`. The PCR conditions were 95°C for 2s, 30 cycles of 95°C for 45s, 57°C for 45s, 72°C for 50s, and an end-elongation step at 72°C for 10min. A 492bp fragment was amplified for the wildtype and a 715bp fragment for the recombinant locus, respectively.

PCR reaction set-ups were performed as described (Subsection 4.1.3). All genotyping reactions were carried out with the Illustra Taq DNA Polymerase (GE Healthcare). Product separation was achieved by agarose gelelectrophoresis (Subsection 4.1.2). Primer sequences are summarized in Subsection 3.3.3.

### 4.5.5 Transplantation

Transplantation experiments have been performed to analyze the oncogenic potential of ITK-SYK expressing primary T cells *in vivo*. For that purpose, 6 week old Hsd:Athymic Nude-Foxn1<sup>nu</sup> mice [56, 136] were intravenously injected with  $1.5 \times 10^7$  splenocytes isolated from diseased ITK-SYK<sup>CD4-Cre</sup> mice. Splenocytes were subjected to RBC lysis and resuspended in 200 $\mu$ l sterile PBS (Gibco) prior to injection. Recipients were daily monitored for signs of disease such as weight loss, hunched posture and extended abdomen. Blood samples were regularly analyzed by flow cytometry (Subsection 4.4.7) at the indicated timepoints. Blood sampling was performed as described [68]. Hsd:Athymic Nude-Foxn1<sup>nu</sup> mice were purchased from Harlan Netherlands B.V.

### 4.5.6 Histology

Histological analysis had been done in collaboration with Dr. Leticia Quintanilla-Fend (Institute for Pathology, University of Tuebingen, Germany) and performed as previously described [100]. In brief, organs were fixed in 4% formaldehyde and embedded in paraffin. Sections (3–5 $\mu$ m) were cut and cell nuclei were visualized by haematoxylin staining, followed by counterstaining with eosin for cellular detail (H&E staining). To specify and characterize cell types involved in mouse pathology, immunohistochemistry was performed on an automated immunostainer (Ventana Medical System Inc., Tuscan, Ariz.) according to the company's protocols. The applied primary antibody panel is summarized in Sub-

section 3.2.5. For all systems applied (Basic DAB/iVIEW DAB detection kit (Ventana Medical System, Inc., Tucson, AZ), and ABC-Kit (Vector, Burlingame, Canada)), epitope detection was indirect via HRP-linked secondary antibodies.

## 4.6 Statistical Analysis

Where indicated, results were analyzed for statistical significance with the unpaired two-tailed Student's *t* test. Differences between groups were considered as significant at *p*-values <0.05. Statistical analysis has been performed with Prism Version 4.0a Graph-Pad Software, Inc.

# Chapter 5

## Results

### 5.1 ITK-SYK Expression Leads to T Cell Activation

#### *In Vitro*

The chromosomal translocation t(5;9)(q33;q22) was originally described in a subgroup of patients with PTCL-NOS. The translocation results in the generation of a novel transcript which encodes for the non receptor tyrosine fusion kinase ITK-SYK [178].

To gain first insights into ITK-SYK functionality and its potential role in aberrant signaling, a set of retroviral transduction experiments were performed. Jurkat T cells, which are commonly used to study T cell receptor signaling [1], were chosen as a cellular system. Specifically, JurkatE T cells express the ecotropic murine viral receptor [76] which allows the infection with MSCV-based retroviruses. To generate retroviral expression vectors, ITK-SYK cDNA was cloned into the pMigR1 vector. It contains an internal ribosomal entry site (IRES) as well as the coding sequence for the enhanced green fluorescent protein (eGFP) [137]. The expression of eGFP permitted convenient tracking of retrovirally infected cells by flow cytometry. ITK-SYK functionality was further studied by generating retroviral vectors expressing ITK-SYK protein mutants. To investigate the importance of ITK-SYK kinase activity, an amino acid exchange of lysine to arginine at position 262 (K262R) was introduced by site directed mutagenesis (nucleotide exchange: AAA $\Rightarrow$ AGA). This exchange rendered a kinase dead mutant of ITK-SYK (ITK-SYK<sup>KD</sup>) by destroying the ATP binding site in the catalytic center of the SYK derived kinase domain [181]. To analyze the necessity of ITK-SYK membrane recruitment, a PH domain mutant (ITK-SYK<sup>PHmut</sup>) was generated by an amino acid exchange of arginine to cysteine at position 29 (R29C) (nucleotide exchange: CGC $\Rightarrow$ TGC). This mutation was described for the wildtype ITK molecule to abrogate membrane recruitment by destroying its lipid binding pocket [28]. Figure 5.1 schematically depicts the fusion tyrosine kinase ITK-SYK and its mutated protein versions.

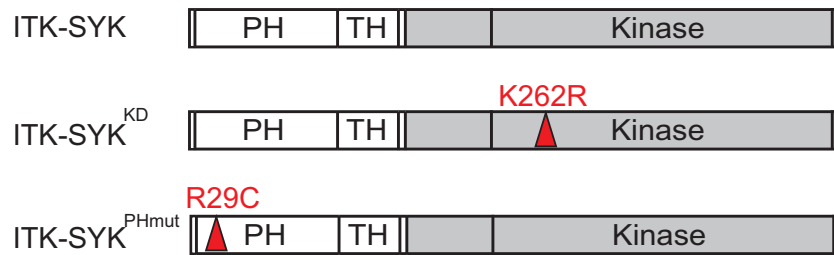


**Figure 5.1: Schematic view of the fusion kinase ITK-SYK and its mutants.** Red triangles indicate sites of an amino acid exchange introduced to generate the kinase dead version (ITK-SYK<sup>KD</sup>, K262R) and the PH domain mutated version (ITK-SYK<sup>PHmut</sup>, R29C) of ITK-SYK. Protein domains are indicated. PH, Pleckstrin homology domain; TH, Tec homology domain; SH2, SRC homology 2 and SH3, SRC homology 3 domain; Kinase, tyrosine kinase domain.

The following *in vitro* experiments were intended to analyze early ITK-SYK mediated signaling events. They included the analysis of protein recruitment into lipid rafts, which have been described as important signal initiation and transduction platforms upon receptor engagement [113], as well as the analysis of activating protein phosphorylation by westernblotting and intracellular flow cytometry.

To address the aspect of membrane recruitment, lipid raft as well as non raft fractions were isolated by sucrose gradient centrifugation from retrovirally infected JurkatE T cells, expressing wildtype ITK-SYK, ITK-SYK<sup>KD</sup> or ITK-SYK<sup>PHmut</sup>. They were subjected to westernblot analysis with antibodies directed against ITK, total phospho-tyrosine or phosphorylated PLC $\gamma$ 1 (pY783). As a negative control, JurkatE T cells were infected with retrovirus expressing only the eGFP fusion protein (GFP). These cells are subsequently referred to as control JurkatE T cells. As a positive control to study TCR dependent signaling events upon receptor engagement, control JurkatE T cells were stimulated with the agonistic CD3 and CD28 antibodies. As seen in Figure 5.2 A, westernblotting against ITK showed strong recruitment of the fusion kinase ITK-SYK into the lipid raft fraction of ITK-SYK expressing JurkatE T cells. ITK-SYK expression resulted in tyrosine phosphorylation of raft-associated proteins. Amongst those events, tyrosine phosphorylation of PLC $\gamma$ 1 was detected, which is known to be a key step in promoting signal transduction downstream of the TCR [23]. Notably, the observed phosphorylation events as well as the recruitment of endogenous ITK into the lipid raft fraction after ITK-SYK expression were both comparable to a TCR stimulatory setting ( $\alpha$ -CD3,  $\alpha$ -CD28) applied to control JurkatE T cells. As for the protein domain mutants, ITK-SYK<sup>KD</sup> was still recruited into the raft fractions to an equal extent as observed for the wildtype fusion kinase, whereas membrane recruitment was completely blocked in ITK-SYK<sup>PHmut</sup>, as expected. Interestingly, expression of neither ITK-SYK<sup>KD</sup> nor ITK-SYK<sup>PHmut</sup> induced tyrosine phospho-

rylation of raft-associated proteins above baseline, although expressed to similar amounts as seen for the non raft fractions after westernblotting against ITK.

Intracellular flow cytometry was further applied to determine activating protein phosphorylation upon ITK-SYK expression. Therefore, retrovirally infected JurkatE T cells expressing ITK-SYK or eGFP only were stained with phosphospecific antibodies directed against key proximal as well as downstream positioned signaling molecules involved in TCR signaling. Levels of phosphorylation in live, transduced (eGFP<sup>+</sup>) JurkatE T cells, expressing ITK-SYK (tinted histogram) or eGFP only (untinted histogram) are depicted in Figure 5.2 B. Histogram overlay analysis showed activating phosphorylation of the TCR proximal adapter proteins SLP-76 (pY128), LAT (pY171), and of the signal transducer PLC $\gamma$ 1 (pY783) upon ITK-SYK expression. Increased phosphorylation of the protein kinase AKT (pS473), as well as the MAP kinases p38 (pT180/pY182) and ERK1/2 (pT202/pY204) were additionally detected. As already observed for lipid raft recruited proteins, the extent of protein phosphorylation after ITK-SYK expression was similar to the one seen in control JurkatE T cells stimulated with CD3 and CD28 antibodies (Figure 5.2 C).

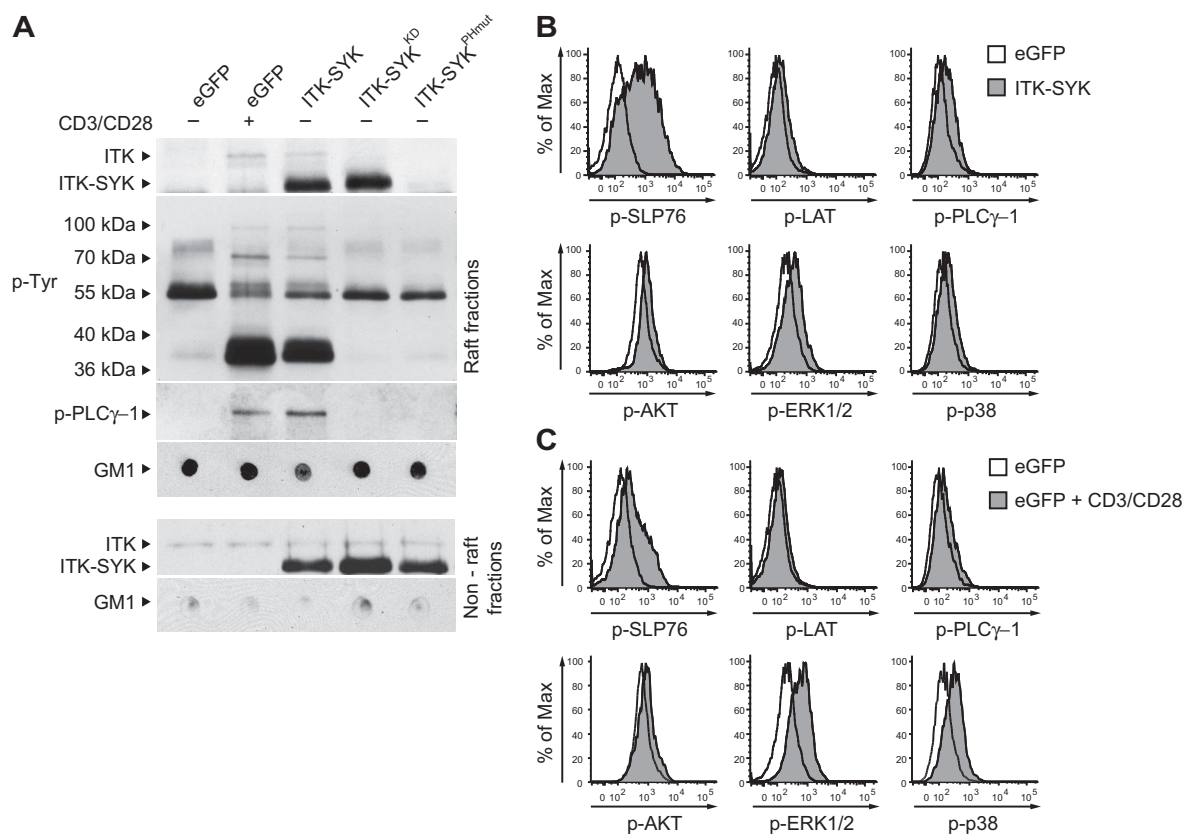


**Figure 5.2: ITK-SYK induces signaling events similar to a TCR signal *in vitro*.** (A) Constitutive ITK-SYK signaling in T cell lipid rafts. JurkatE T cells were infected with retroviruses carrying ITK-SYK, ITK-SYK<sup>KD</sup>, ITK-SYK<sup>PHmut</sup> together with an eGFP or eGFP only as a control. Lipid raft fractions from unstimulated or  $\alpha$ -CD3 (5 $\mu$ g/ml)/ $\alpha$ -CD28 (1 $\mu$ g/ml)-stimulated cells were prepared and subjected to western blot analysis with antibodies against ITK (top), total phosphotyrosine (p-Tyr), or phosphorylated PLC $\gamma$ 1 (p-PLC $\gamma$ 1). Dot blot analysis of the lipid raft marker GM1 confirmed successful raft preparation and equal loading. Data shown are representative of at least two independent experiments. (B) Phosflow analysis of ITK-SYK mediated signaling. JurkatE T cells were infected with ITK-SYK together with eGFP (ITK-SYK) or eGFP only (eGFP) expressing retrovirus and intracellularly stained with activation-specific  $\alpha$ -phospho antibodies directed against the indicated signaling molecules. Signaling was analyzed within the infected viable eGFP<sup>+</sup> population as determined by amine-reactive dye exclusion. Data shown are representative of four independent experiments. (C) Phosflow analysis of stimulated JurkatE T cells. JurkatE T cells were infected with eGFP only expressing retroviruses (GFP). Cells were left unstimulated or stimulated for 5min with  $\alpha$ -CD3 (5 $\mu$ g/ml)/ $\alpha$ -CD28 (1 $\mu$ g/ml) antibody and analyzed as in (B). Results are representative of three independent experiments.

To investigate the consequences of ITK-SYK related activation on a cellular level, surface expression of the early activation marker CD69 and production of the autocrine cytokine IL-2 were assessed, since both events respond to TCR engagement [74, 30]. For that purpose, retrovirally infected JurkatE T cells expressing the wildtype ITK-SYK, ITK-SYK<sup>KD</sup> or ITK-SYK<sup>PHmut</sup> were analyzed by flow cytometry to determine CD69 expression. Control JurkatE T cells, expressing eGFP only were used as a negative control. CD3/CD28-stimulated control JurkatE T cells were used as a positive control for TCR dependent cell activation. Contour blot analysis of gated viable cells showed a clear surface expression of CD69 in retrovirally transduced cells expressing ITK-SYK, which was neither observed in JurkatE T cells expressing ITK-SYK<sup>KD</sup> or ITK-SYK<sup>PHmut</sup> (Figure 5.3 A). In agreement with the performed lipid raft experiments, cell activation was comparable to CD3/CD28-stimulated JurkatE T cells, which expressed CD69 on the cell surface. Both control JurkatE T cells and non infected cells did not show CD69 expression as expected. In correlation to the observed cellular activation, ITK-SYK expression also led to a strong IL-2 production. This is not observed in JurkatE T cells expressing the ITK-SYK<sup>KD</sup> or ITK-SYK<sup>PHmut</sup> mutant (Figure 5.3 B). Amounts of IL-2 measured in the cell supernatant by ELISA were increased fivefold compared to control JurkatE T cells subjected to optimal TCR stimulation with CD3/CD28 antibodies. As an additional approach to substantiate the dependency of ITK-SYK on its kinase activity, retrovirally transduced JurkatE T cells expressing ITK-SYK were treated with the small molecule inhibitor R406. It has been shown to R406 blocks wildtype SYK kinase activity *in vitro*, while its orally available compound R788 does so *in vivo* [24]. Both CD69 expression and IL-2 production was abrogated in the presence of R406 (Figure 5.3 A, B).

From these *in vitro* experiments it can be concluded that ITK-SYK is a lipid raft-associated tyrosine kinase, which initiates signaling responses similar to those seen after TCR engagement. Protein domain mutant analyses showed that ITK-SYK induced signaling is dependent on membrane recruitment and on the functional kinase activity of the fusion kinase. The later aspect was supported by the fact that ITK-SYK activity could be blocked upon SYK inhibitor treatment.

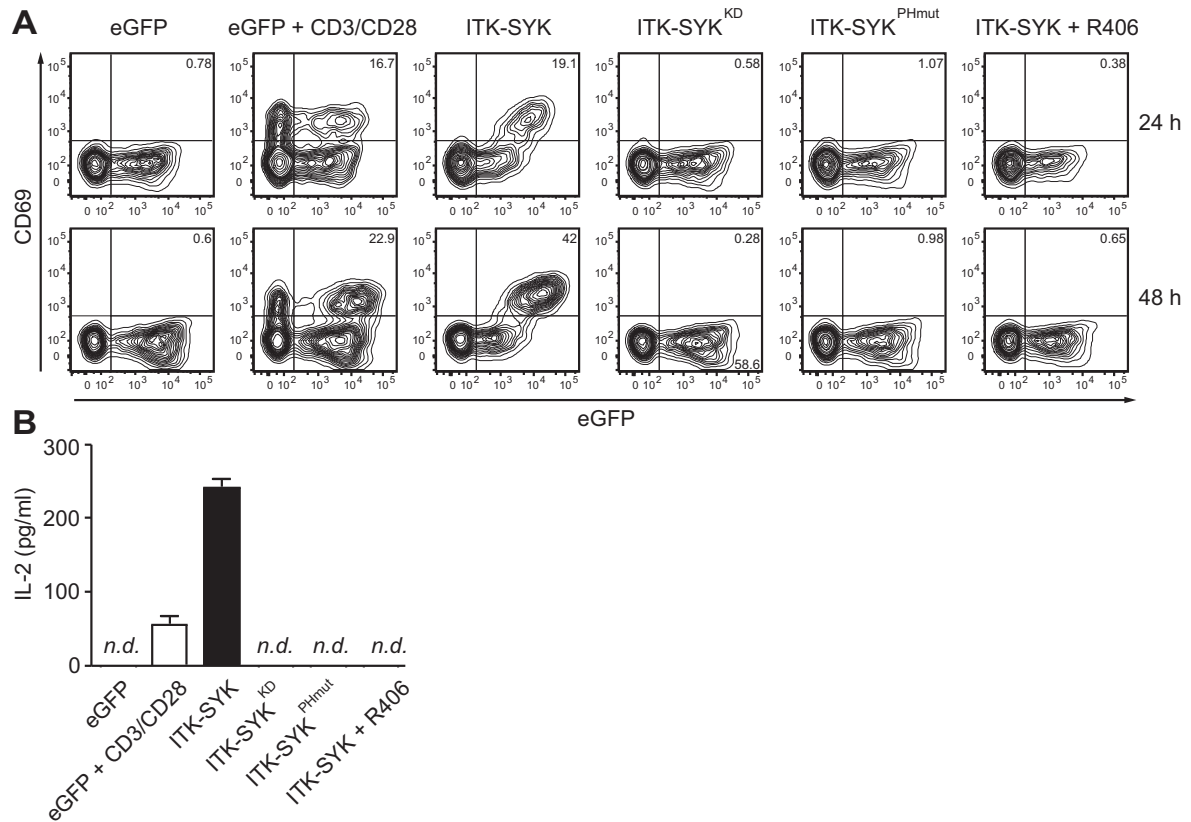


**Figure 5.3: ITK-SYK induces cellular outcomes similar to a TCR signal *in vitro*.** (A) ITK-SYK triggers kinase and PH domain dependent T cell activation. JurkatE T cells were infected with retroviruses carrying ITK-SYK, ITK-SYK<sup>KD</sup>, ITK-SYK<sup>PHmut</sup> together with an eGFP or eGFP only as a control. Cells were left either unstimulated, stimulated with 10 $\mu$ g/ml  $\alpha$ -CD3 and 2 $\mu$ g/ml  $\alpha$ -CD28, or treated with 2 $\mu$ M R406 as indicated and analyzed by flow cytometry. The percentage of infected eGFP<sup>+</sup> CD69-expressing cells from unstimulated, stimulated, or R406-treated cells is indicated. Data shown are representative of five independent experiments. (B) ITK-SYK induces kinase and PH domain dependent IL-2 production. JurkatE T cells were infected and treated as in (A). IL-2 concentrations in the cell supernatants were determined by ELISA. Shown are the mean $\pm$ standard deviation (SD) from triplicate samples. Data shown are representative of four independent experiments.

## 5.2 Mouse Model for Conditional ITK-SYK Expression

### 5.2.1 Targeting the ROSA26 Locus

Data gathered from *in vitro* retroviral transduction experiments suggested a possible scenario where ITK-SYK is capable of mimicking aspects of a TCR signal, seemingly doing so without the need for an antigen to be present. Constitutive receptor signaling might therefore cause cell transformation and eventual T cell lymphoma development.

To study long-term consequences of ITK-SYK expression *in vivo*, a genetically modified mouse model was generated. Conditional targeting of the ROSA26 locus was chosen to achieve cell type specific expression of the fusion kinase ITK-SYK by applying the Cre/loxP system [72]. The ROSA26 locus has been well characterized and utilized for knock-in approaches. It is positioned on chromosome 6, consists of three exons, and shows ubiquitous promoter activity with moderate expression levels [174, 176]. Importantly, homozygous recombination at the ROSA26 locus does not result in any phenotypical defects [202] and efficient gene targeting is provided due to high recombination frequencies present at the chosen locus [174, 59]. For vector generation, the ITK-SYK fusion cDNA was cloned into a previously described pROSA26 targeting vector upon *AscI* digestion [160]. To ensure optimal translation initiation a consensus CCACC sequence was placed directly in front of the ITK-SYK start codon [96]. Within the targeting vector, the ITK-SYK cDNA was positioned downstream of an adenovirus splice acceptor site (SA), followed by a loxP site flanked neomycin resistance stop cassette (NEO-STOP), and upstream of an FRT site flanked IRES-eGFP cassette (IRESeGFP), followed by a polyadenylation sequence (pA). Annealing of the so-called short and long arm of homology, which consisted of identical sequences surrounding the site of integration, enabled recombination within intron 1 at the wildtype (WT) ROSA26 locus. Figure 5.4 A schematically depicts features of the targeting vector as well as the applied targeting strategy. Locus specific recombination in targeted embryonic stem cells was assessed by southernblot analysis. Size-separated *XbaI*-digested genomic DNA was exposed to a 5'-located probe, resulting in the detection of a 4.6kb fragment for the WT, and an 8.9kb fragment for the targeted allele. Successful targeting of the ROSA26 locus is representatively shown for one embryonic stem cell clone (Figure 5.4 B). Altogether, 28% of all screened clones carried the targeted allele. Germline transmitting chimeras were obtained from two independent clones, and breeding to C57BL/6 mice resulted in the generation of the ROSA26<sup>loxSTOPlox-ITK-SYK</sup> mouse strain. It carried the ITK-SYK cDNA within the recombined (Rec) ROSA26 locus heterozygously. In these mice transcriptional readthrough from the Rec locus is still interrupted by the presence of the NEO-STOP cassette. Only upon breeding with promoter-specific Cre transgenic mice,

the loxP site flanked NEO-STOP cassette is excised from intron 1. The splice acceptor (SA), which is positioned upstream of the ITK-SYK sequence, hence allows correct splicing onto the endogenous exon 1 of the ROSA26 locus and production of an exon 1-ITK-SYK-IRES-eGFP bi-cistronic mRNA becomes possible. Since no open reading frame is defined for an exon 1 containing transcript from the WT ROSA26 locus, translation is initiated at the start codon provided by the ITK-SYK cDNA. The internal ribosomal entry site enables additional translation of the eGFP protein from the bi-cistronic transcript. Green fluorescence thus allowed detection of cells expressing the ITK-SYK cDNA and could be used for cell tracking throughout mouse analysis.

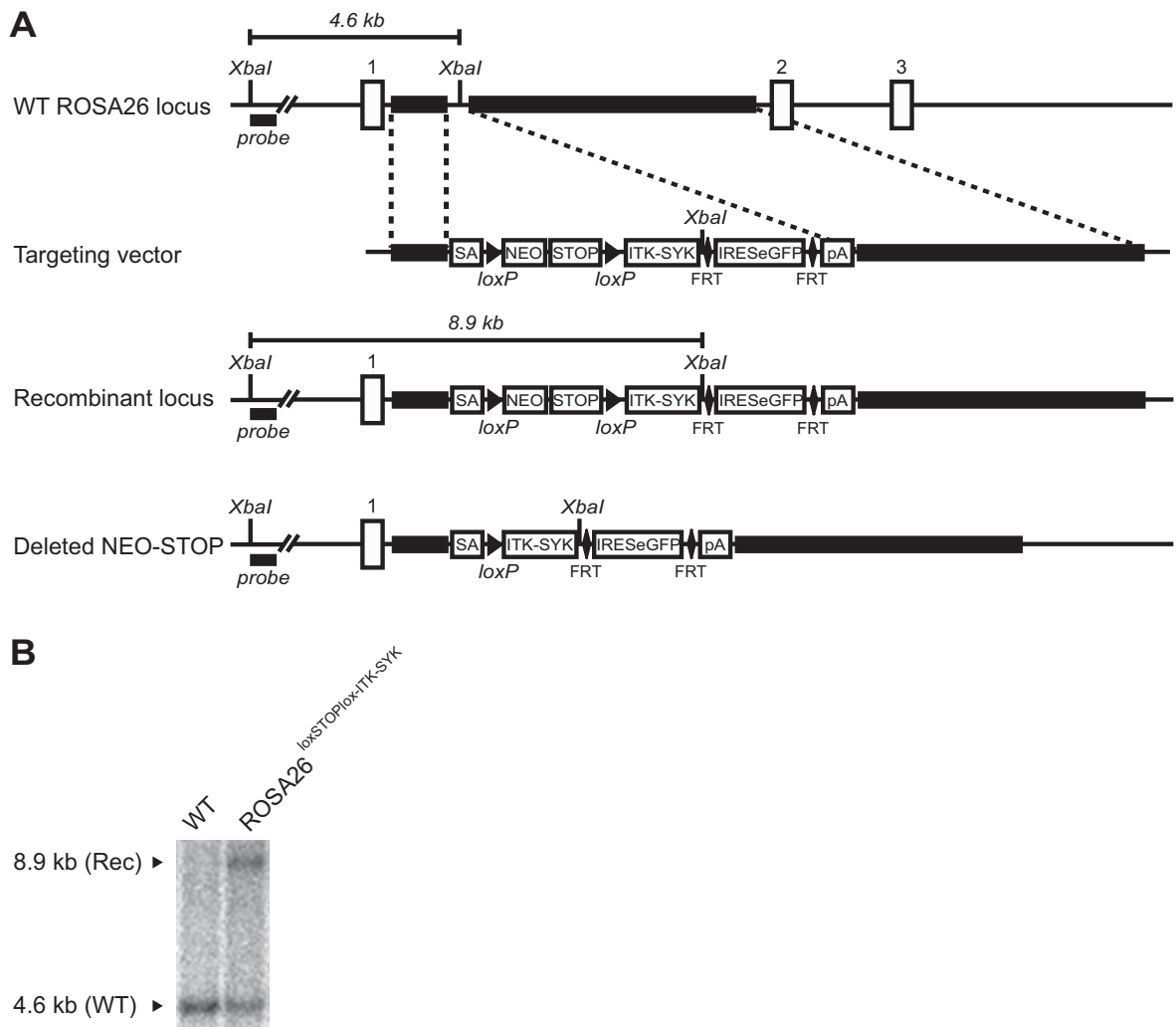


**Figure 5.4: Successful targeting of the ROSA26 locus.** (A) Schematic representation of the gene targeting strategy. A targeting vector that carries the human ITK-SYK cDNA together with an IRES eGFP sequence preceded by a loxP site flanked NEO-STOP cassette was constructed and used to generate ROSA26<sup>loxSTOPlox-ITK-SYK</sup> mice as described (Subsection 4.5.2). The wildtype (WT), recombinant (Rec) ROSA26 locus and the ITK-SYK expressing locus upon Cre mediated deletion of the NEO-STOP cassette are indicated. Black bars highlight regions for homologous recombination in intron 1. SA, splice acceptor site; pA, polyadenylation signal sequence; 1-3, ROSA26 exon 1-3; probe, flanking probe for southernblot analysis. (B) Southernblot analysis. Genomic DNA from a WT and a successfully targeted ROSA26<sup>loxSTOPlox-ITK-SYK</sup> embryonic stem cell clone was digested with *XbaI* and southernblotted with the 5'-flanking probe as indicated in (A). A total number of n=42 ESCs were screened for recombination events. Sizes of the WT and Rec fragments are indicated.

## 5.2.2 Cell Type Specific Expression of ITK-SYK

The availability of the conditional  $\text{ROSA26}^{\text{loxSTOPlox-ITK-SYK}}$  mouse strain enabled the study of ITK-SYK in a cell type specific manner. Two parallel breeding approaches were pursued. To generate mice expressing ITK-SYK in a T cell restricted manner,  $\text{ROSA26}^{\text{loxSTOPlox-ITK-SYK}}$  mice were crossed with CD4-Cre transgenic mice [108] (Figure 5.5 A). To additionally study the effects of ITK-SYK expression on B lymphocytes,  $\text{ROSA26}^{\text{loxSTOPlox-ITK-SYK}}$  mice were crossed with CD19-Cre transgenic mice [150] (Figure 5.5 B). The resulting offspring were referred to as  $\text{ITK-SYK}^{\text{CD4-Cre}}$  and  $\text{ITK-SYK}^{\text{CD19-Cre}}$  mice, respectively. As outlined in Subsection 5.2.1, Cre-mediated excision of the loxP site flanked NEO-STOP cassette, is expected to permit the expression of the fusion kinase ITK-SYK as well as the fluorescent protein eGFP from a bi-cistronic mRNA. Thus, functionality of the resulting mouse strains was tested by flow cytometry and westernblot analysis of splenocytes isolated from 5 week old  $\text{ITK-SYK}^{\text{CD4-Cre}}$  and  $\text{ITK-SYK}^{\text{CD19-Cre}}$  mice. Flow cytometric analysis in both strains showed that over 80% of T cells isolated from  $\text{ITK-SYK}^{\text{CD4-Cre}}$  mice or B cells isolated from  $\text{ITK-SYK}^{\text{CD19-Cre}}$  mice have functionally deleted the NEO-STOP cassette from the recombined ROSA26 allele, as determined by eGFP positivity (Figure 5.6 A). Westernblot analysis with an ITK specific antibody further confirmed cell type specific expression of the fusion kinase ITK-SYK from the respective mouse strain (Figure 5.6 B). ITK-SYK was detected at a size of 54kDa, as expected. Since only one targeted ROSA26 allele is present in

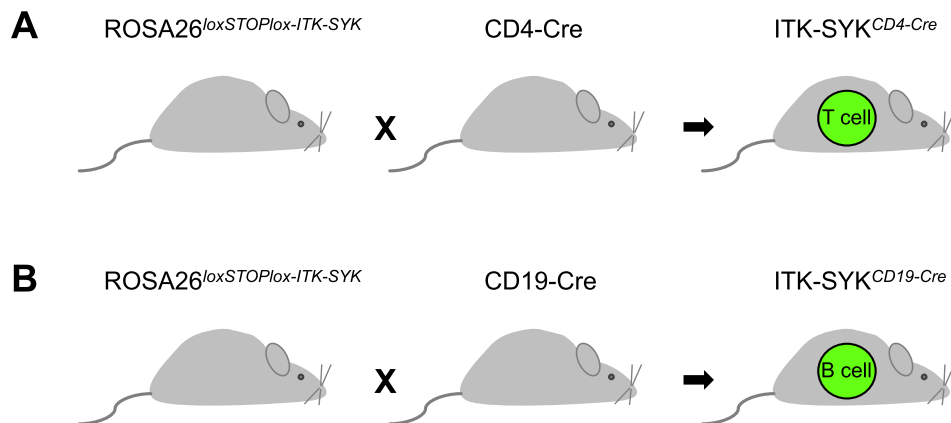


**Figure 5.5: Breeding scheme.** (A)  $\text{ROSA26}^{\text{loxSTOPlox-ITK-SYK}}$  mice were crossed with CD4-Cre transgenic mice for T cell specific expression of ITK-SYK, generating the  $\text{ITK-SYK}^{\text{CD4-Cre}}$  strain. (B) For B cell specific expression  $\text{ROSA26}^{\text{loxSTOPlox-ITK-SYK}}$  mice were crossed to CD19-Cre transgenic mice, resulting in the  $\text{ITK-SYK}^{\text{CD19-Cre}}$  strain. For both breeding approaches eGFP expression indicates successful Cre-mediated deletion of the loxP site flanked NEO-STOP cassette and expression of the ITK-SYK cDNA.

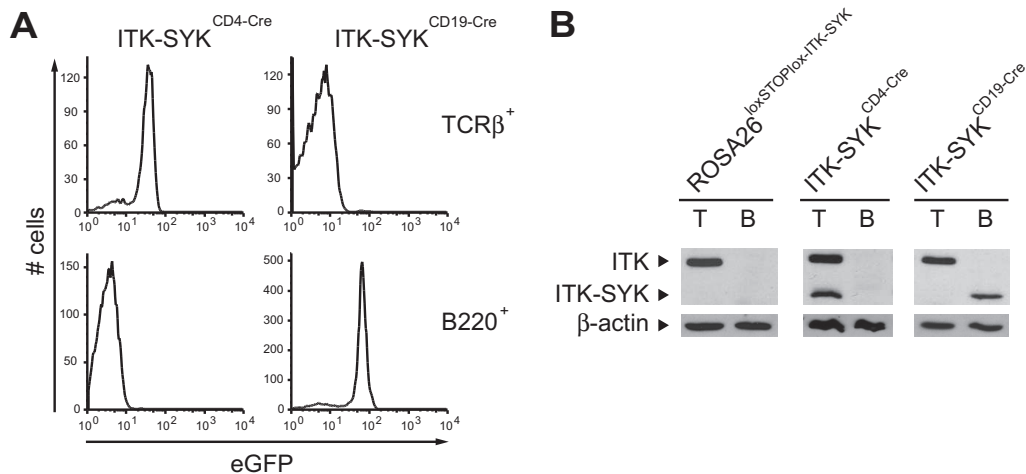


**Figure 5.6: Conditional Expression of ITK-SYK in T or B cells *in vivo*.** (A) ROSA26<sup>loxSTOPlox-ITK-SYK</sup> mice were crossed to CD4-Cre or CD19-Cre transgenic mice for T cell or B cell specific ITK-SYK expression, respectively. Peripheral lymphocyte suspensions from spleens of 5 week old ITK-SYK<sup>CD4-Cre</sup>, or ITK-SYK<sup>CD19-Cre</sup> mice were stained against TCR $\beta$  or B220. eGFP fluorescence indicative of ITK-SYK expression in the TCR $\beta$ <sup>+</sup> T cells or B220<sup>+</sup> B cells of the respective animals was analyzed using flow cytometry. Data shown are representative of over forty mice per genotype analyzed. (B) Mature T or B cell populations from 5 week old ROSA26<sup>loxSTOPlox-ITK-SYK</sup>, ITK-SYK<sup>CD4-Cre</sup> or ITK-SYK<sup>CD19-Cre</sup> mice were sorted with magnetic beads and subjected to westernblot analysis with an  $\alpha$ -ITK antibody. Bands of wildtype ITK (72kDa) and recombinant ITK-SYK (54kDa) are indicated. Westernblotting for  $\beta$ -actin (42kDa) demonstrated equal protein loading. Data shown are representative of five independent experiments.

both mouse strains - resulting from a heterozygous breeding approach - ITK-SYK was expressed to a lesser extent than seen for the T cell specific endogenous ITK protein. Favorably for later strain comparison, both T cells isolated from ITK-SYK<sup>CD4-Cre</sup> and B cells isolated from ITK-SYK<sup>CD19-Cre</sup> mice showed equal expression levels of the fusion kinase (Figure 5.6 B). These initial results confirm the functionality of the generated ROSA26<sup>loxSTOPlox-ITK-SYK</sup> mouse strain.

### 5.2.3 ITK-SYK Can Imitate a TCR Signal *In Vivo*

Since the ITK-SYK producing translocation has been originally isolated from patients diagnosed with PTCL-NOS, the primary focus was on investigating ITK-SYK related effects on T cell development and activation. Those aspects were first analyzed by flow cytometry in 4-5 week old ITK-SYK<sup>CD4-Cre</sup> mice. Within these mice the Cre recombinase expression is put under the control of the CD4 promoter. Therefore, excision of the NEO-STOP cassette and subsequent ITK-SYK expression was expected to begin at the

double positive (DP) CD4<sup>+</sup>CD8<sup>+</sup> thymocyte stage and to continue throughout the CD4<sup>+</sup> T cell lineage [108]. In agreement with that, recombination of the NEO-STOP cassette, as indicated by eGFP fluorescence, was detected within the DP thymocyte compartment in ITK-SYK<sup>CD4-Cre</sup> mice. Full fluorescence levels were reached within the further matured CD4<sup>+</sup> or CD8<sup>+</sup> single positive (SP) population (Figure 5.7 A). Over 90% of the SP CD4<sup>+</sup> and 75% of the SP CD8<sup>+</sup> cells were eGFP<sup>+</sup>, indicative of ITK-SYK expression. Concerning thymic development, ITK-SYK expression resulted in a striking reduction of DP thymocytes as seen by a decrease in both frequency and total cell number (Figure 5.7 B, C). The amount of CD4<sup>+</sup> SP and CD8<sup>+</sup> SP thymocytes was also severely diminished (Figure 5.7 C). Regarding peripheral lymphoid populations, a profound loss of mature T cells in lymph node and spleen was observed, as shown by both a reduction in frequency (Figure 5.8 A) and a reduction of total cell numbers (Figure 5.8 B). Amongst the T cells, both CD4<sup>+</sup> and CD8<sup>+</sup> cells were equally affected as is shown by diminished frequencies in lymph node and spleen (Figure 5.8 C). Total B cell numbers, however, remained unaltered in ITK-SYK<sup>CD4-Cre</sup> mice (Figure 5.8 B).

Flow cytometric analysis further revealed that the majority of mature T cells present in the periphery expressed ITK-SYK, as detected by eGFP expression (Figure 5.6 A, Figure 5.8 D). They also displayed an activated phenotype as indicated by a cell size increase, high expression of the activation marker CD44 [41], and low expression of the naive T cell marker CD62L [170] (Figure 5.9 A). This pattern was accompanied by a reduced surface expression of the TCR $\beta$  chain, being an additional characteristic of activated T cells [189]. The described phenotype was seen for both the CD4<sup>+</sup> and the CD8<sup>+</sup> T cell population. Loss of CD62L was observed to a lesser extent for CD8<sup>+</sup> T cells compared to the CD4<sup>+</sup> T cell population (Figure 5.9 A). Being in line with an activated phenotype and previously performed *in vitro* experiments (Figure 5.2 A), peripheral T cells isolated from ITK-SYK<sup>CD4-Cre</sup> mice showed constitutive lipid raft recruitment of the TCR signal transducer p-PLC $\gamma$ 1 (Figure 5.9 B). The degree of phosphorylation was similar to wildtype T cells isolated from CD4-Cre control mice stimulated via  $\alpha$ -CD3e and  $\alpha$ -CD28 antibodies (Figure 5.9 B).

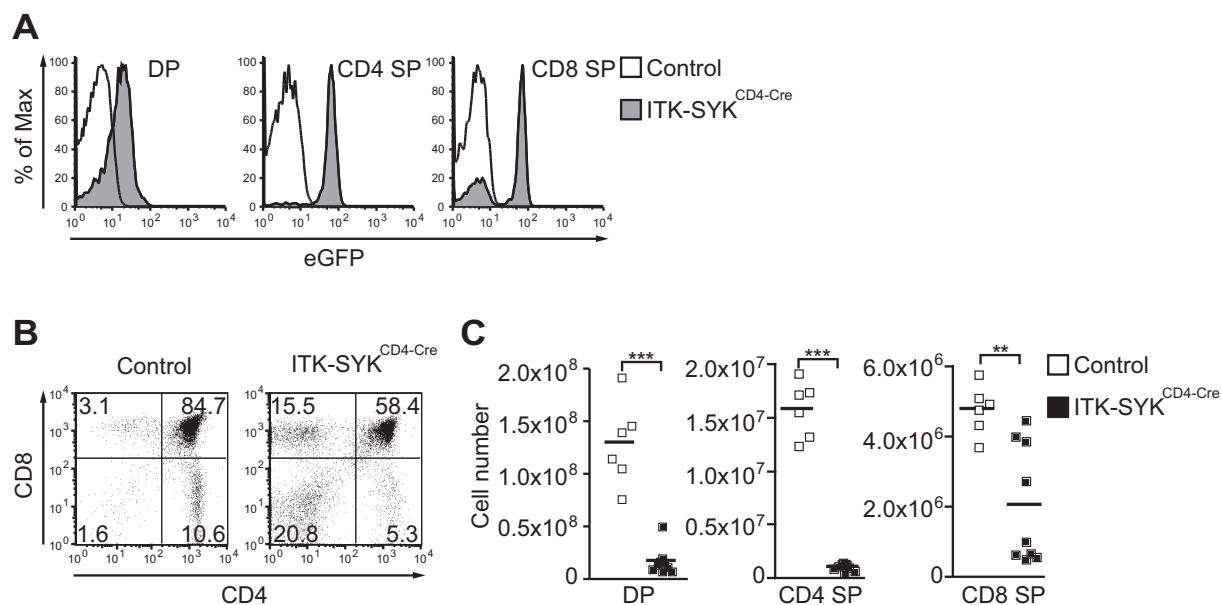


**Figure 5.7: ITK-SYK induces loss of thymocytes in ITK-SYK<sup>CD4-Cre</sup> mice.** (A) Thymocytes were stained against CD4 and CD8, and analyzed by flow cytometry. eGFP fluorescence indicative of ITK-SYK expression was measured in the CD4<sup>+</sup>/CD8<sup>+</sup> double positive (DP) and in the CD4<sup>+</sup> or CD8<sup>+</sup> single positive (SP) populations of 4-5 week old ITK-SYK<sup>CD4-Cre</sup> and CD4-Cre control mice. (B and C) ITK-SYK induces DP thymocyte deletion. (B) Thymocytes were stained as in (A) and analyzed for the expression of CD4 or CD8. The frequencies of individual thymocyte subsets are indicated. Data shown in (A) and (B) are representative of five independent experiments with at least ten mice analyzed per genotype. (C) The total DP, CD4 SP, or CD8 SP thymocyte cell numbers from ITK-SYK<sup>CD4-Cre</sup> (n=9) or CD4-Cre control (n=6) mice are shown. Each symbol represents an individual mouse. Statistical significance was analyzed using the unpaired two-tailed Student's *t* test. Statistically significant (\*\*\*) $p < 0.0001$ ; (\*\*) $p = 0.0027$ ). Horizontal bars indicate the means.

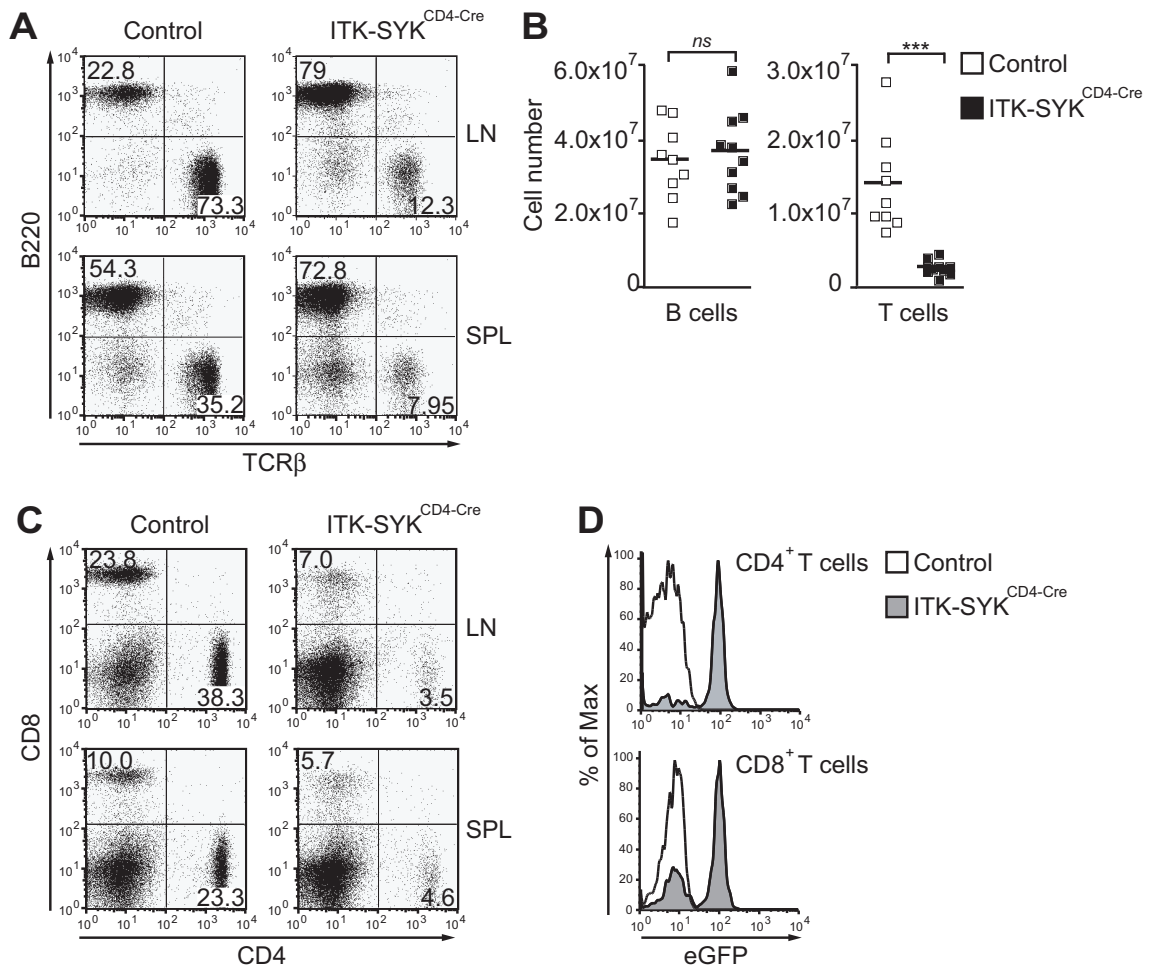


**Figure 5.8: ITK-SYK induces loss of peripheral T cells in ITK-SYK<sup>CD4-Cre</sup> mice.** (A, C) Single cell suspensions from lymph nodes (LN) or spleens (SPL) from 4-5 week old ITK-SYK<sup>CD4-Cre</sup> or CD4-Cre control mice were either stained against TCR $\beta$  and B220 (A) or CD4 and CD8 (C), and analyzed by flow cytometry. The frequencies of individual TCR $\beta$ <sup>+</sup>, B220<sup>+</sup>, CD4<sup>+</sup>, and CD8<sup>+</sup> subsets in LN and SPL are indicated. (B) Total splenic B cell or T cell numbers from ITK-SYK<sup>CD4-Cre</sup> (n=10) or CD4-Cre control (n=9) mice are indicated. Each symbol in (B) represents an individual mouse. D) eGFP fluorescence indicative of ITK-SYK expression was determined in peripheral CD4<sup>+</sup> or CD8<sup>+</sup> T cells of ITK-SYK<sup>CD4-Cre</sup> and CD4-Cre control mice. Data from spleen are shown. Statistical significance was analyzed using the unpaired two-tailed Student's *t* test. \*\*\*, statistically significant ( $p < 0.0001$ ); ns, not statistically significant ( $p \geq 0.05$ ). Horizontal bars indicate the means. Data shown in (A), (C) and (D) are representative of five independent experiments with at least ten mice analyzed per genotype.

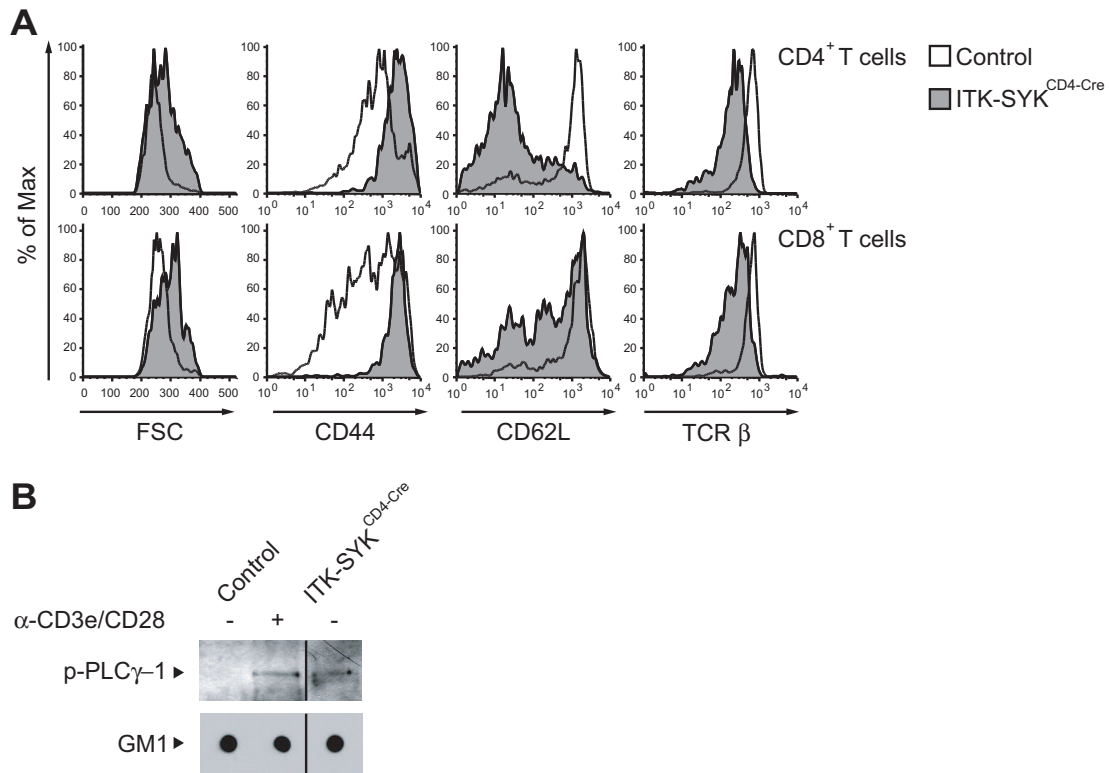


**Figure 5.9: ITK-SYK expressing T cells exhibit an activated phenotype *in vivo*.** (A) Peripheral lymphocytes from 4-5 week old ITK-SYK<sup>CD4-Cre</sup> or CD4-Cre control mice were stained against CD4, CD8, CD44, CD62L, and TCRβ. Forward scattering (FCS) as a parameter for cell size and expression of CD44, CD62L, and TCRβ were analyzed in the CD4<sup>+</sup> and CD8<sup>+</sup> T cell compartment using flow cytometry. Data shown are representative of five independent experiments with at least ten mice analyzed per genotype. (B) ITK-SYK induces PLCγ1 phosphorylation in primary T cells *in vivo*. Splenic T cells were isolated from CD4-Cre control or ITK-SYK<sup>CD4-Cre</sup> mice that were over 12 weeks old. Cells were left unstimulated and control cells were additionally stimulated with 5μg/ml of α-CD3e and 1μg/ml of α-CD28. Lipid raft fractions were prepared and subjected to westernblot analysis with an antibody directed against p-PLCγ1. Dot blots for GM1 show successful raft preparation and equal protein loading. Data are representative of three independent experiments. Black lines indicate that intervening lanes have been spliced out.

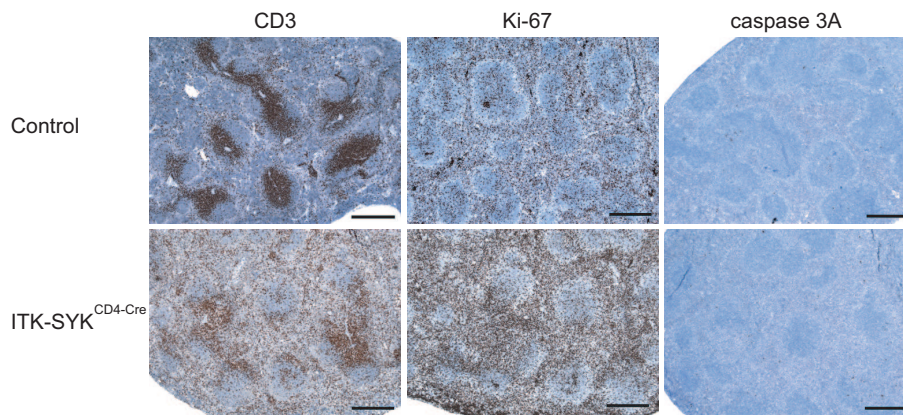


**Figure 5.10: ITK-SYK expressing T cells proliferate but do not undergo apoptosis *in vivo*.** Spleen sections of 4-5 week old ITK-SYK<sup>CD4-Cre</sup> or CD4-Cre control mice were used for immunohistochemistry with antibodies directed against CD3, Ki-67, or the cleaved active form of caspase 3 (caspase 3A). Data are representative of three ITK-SYK<sup>CD4-Cre</sup> and two CD4-Cre control mice analyzed. Bars, 1.2mm.

To further characterize the activated T cells and to address the possible effect of ITK-SYK expression on T cell proliferation and survival, immunohistochemical analyses were performed on spleen sections from ITK-SYK<sup>CD4-Cre</sup> and CD4-Cre control mice. Diffusely distributed CD3<sup>+</sup> T cells showed strong proliferative features as determined by staining against the proliferation marker Ki-67 [164] in comparison to control spleen samples (Figure 5.10). However, no increased apoptosis was detectable in spleens from ITK-SYK<sup>CD4-Cre</sup> mice when stained against the apoptotic marker molecule active caspase-3 [140].

Concludingly, data demonstrate that a T cell specific expression of ITK-SYK leads to a severe loss of thymic T cells in ITK-SYK<sup>CD4-Cre</sup> mice. Although strongly reduced in cell numbers, matured T cells emerging from the thymus are activated and in a proliferative state. These observations substantiate the postulation made from *in vitro* experiments that ITK-SYK mimics aspects of a strong TCR signal.

#### 5.2.4 ITK-SYK Does Not Affect BCR Signaling *In Vivo*

Due to the fact that SYK is an essential receptor proximal tyrosine kinase initiating BCR signaling [102], it was of additional interest to study the potential effect of the fusion kinase ITK-SYK on B cell development and activation. For that purpose, the previously mentioned ITK-SYK<sup>CD19-Cre</sup> mouse strain (Subsection 5.2.2) was analyzed at 5-7 weeks of age. Since within these mice Cre recombinase expression relies on CD19 promoter activity, deletion of the NEO-STOP cassette and consequent ITK-SYK expres-

sion was expected to begin in early B cell compartments and to continue throughout B cell development and maturation [161]. In consistency with that, successful recombination, as indicated by eGFP expression, was first detected in a low percentage B cells within the bone marrow (BM). However, peripheral splenic B cell compartments, such as follicular (FO) and marginal zone (MZ) B cells, and peritoneal B1 B cells showed high recombination frequencies of over 80% (Figure 5.11 A, Figure 5.6 A). Surprisingly, flow cytometric analysis revealed that ITK-SYK expression had no effect on B cell development in the bone marrow, as seen by normal distributions of pro/pre ( $B220^{low}IgM^{neg}$ ), immature/transitional ( $B220^{low-hi}IgM^{int-hi}$ ), and mature/recirculating ( $B220^{hi}IgM^{int}$ ) B cells in ITK-SYK<sup>CD19-Cre</sup> compared to CD19-Cre control mice (Figure 5.11 B). Similarly, no significant deviations were observed among the frequencies of peripheral splenic B cells from ITK-SYK<sup>CD19-Cre</sup> mice (Figure 5.11 C). These included follicular ( $CD21^{int}CD23^{hi}$ ), non-follicular ( $CD21^{low}CD23^{low}$ ), and marginal zone ( $CD21^{hi}CD23^{low}$ ) B cells (Figure 5.11 D). The same holds true for peritoneal B1 B cells ( $B220^{int}CD5^{int}$ ) (Figure 5.11 E). Not only B and T cell distribution but also total B and T cell numbers were unaffected as demonstrated for the spleen of ITK-SYK<sup>CD19-Cre</sup> and CD19-Cre control mice (Figure 5.11 C, F). To further investigate possible effects of ITK-SYK on B cell physiology, the activation status of peripheral B cells prepared from ITK-SYK<sup>CD19-Cre</sup> mice was assessed. Neither an increase in cell size nor an upregulation of the activation marker CD86 [20] were detected for ITK-SYK expressing B cells (Figure 5.12 A). Additionally, no difference in the overall tyrosine phosphorylation pattern was observed in purified splenic B cells isolated from ITK-SYK<sup>CD19-Cre</sup> in comparison to CD19-Cre control mice (Figure 5.12 B).

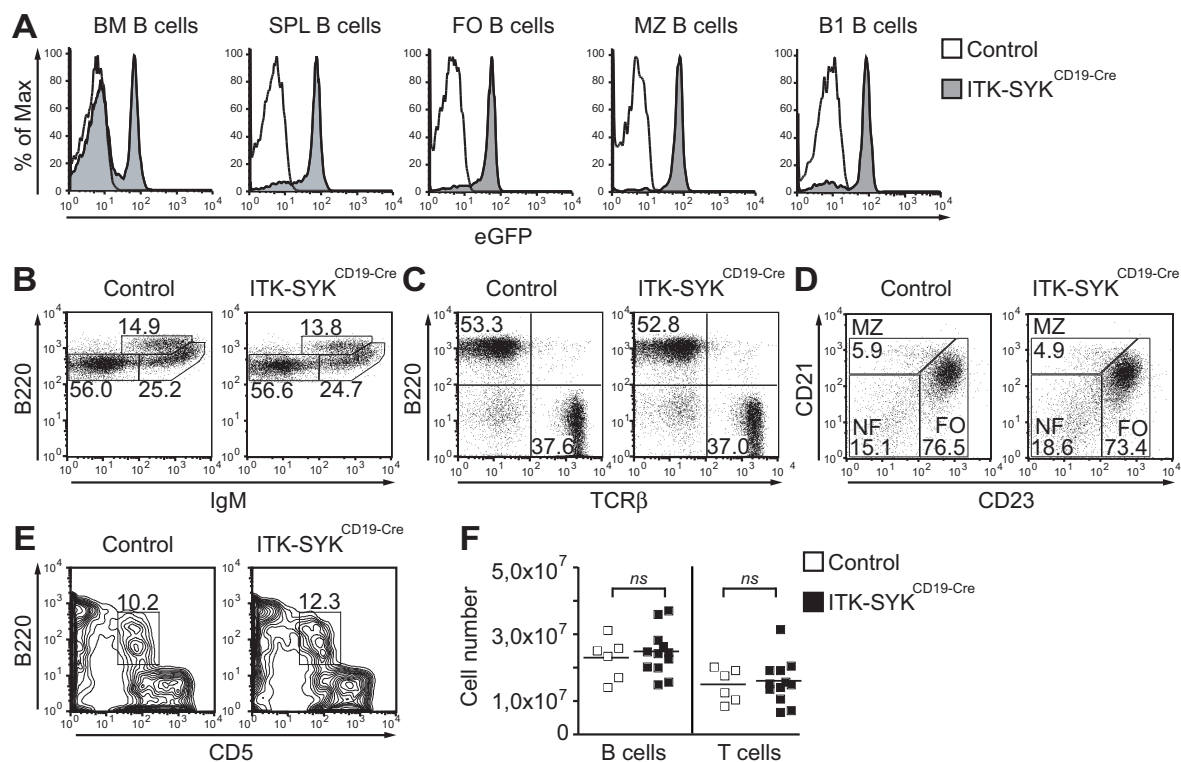


**Figure 5.11: B cell-intrinsic ITK-SYK expression does not affect B cell development.** (A) Single cell suspensions from the bone marrow (BM), spleen (SPL) or peritoneal cavity of ITK-SYK<sup>CD19-Cre</sup> or CD19-Cre control mice were stained against B220, CD21, CD23, and CD5. eGFP fluorescence indicative of ITK-SYK expression was determined in gated B220<sup>+</sup> cells from BM, SPL, follicular (FO), non-follicular (NF), marginal zone (MZ), or peritoneal B1 B cell compartments using flow cytometry. (B)-(E) Lymphocyte preparations from BM (B), SPL (C,D) or peritoneal cavity (E) of ITK-SYK<sup>CD19-Cre</sup> or CD19-Cre control mice were stained against the indicated surface markers and analyzed by flow cytometry. The percentages of individual B cell populations are indicated. B220<sup>+</sup> cells were gated for (B) and (D). FO, follicular B cells; MZ, marginal zone B cells. (F) Total splenic B or T cell numbers from ITK-SYK<sup>CD19-Cre</sup> (n=12) or CD19-Cre control (n=6) mice are shown. Each symbol represents an individual mouse. Statistical significance was analyzed using the unpaired two-tailed Student's *t* test. *ns*, not statistically significant differences ( $p \geq 0.05$ ). Horizontal bars indicate the means. Data shown in (A)-(E) are representative of four independent experiments with at least six 5-7 week old mice analyzed per genotype.

*In vitro* experiments performed in JurkatE T cells showed that PH domain-mediated membrane recruitment of ITK-SYK was necessary for ITK-SYK functionality (Figure 5.2 A, Figure 5.3 A, B). To analyze whether the observed differences in the T and B cell phenotype might be due to differences in ITK-SYK positioning at the cell membrane, lipid raft experiments were performed. Purified T cells from ITK-SYK<sup>CD4-Cre</sup> and purified B cells prepared from ITK-SYK<sup>CD19-Cre</sup> mice were subjected to western blotting with an ITK-specific antibody. T cells purified from ROSA26<sup>loxSTOPlax-ITK-SYK</sup> mice were used as a control. Experiments demonstrated that both ITK-SYK and endogenous ITK molecule were strongly recruited into the lipid rafts of T cells, a feature already observed in retrovirally infected JurkatE T cells expressing ITK-SYK (Figure 5.2 A). However, ITK-SYK could not be detected in the lipid raft fraction of B cells isolated from ITK-SYK<sup>CD19-Cre</sup> mice, although the fusion kinase was expressed in both T and B cells to similar amounts as seen for the non-raft fractions (Figure 5.12 C). Equal protein expression was also previously shown for splenic cytosolic lysates from both ITK-SYK<sup>CD4-Cre</sup> and ITK-SYK<sup>CD19-Cre</sup> mouse strains (Figure 5.6 B).

All in all, the analysis of ITK-SYK<sup>CD19-Cre</sup> mice showed that neither B cell development and maturation nor B cell activation were affected by a B cell specific expression of ITK-SYK. The missing membrane recruitment of ITK-SYK to the antigen receptor environment may be held accountable for the surprising differences being seen in the effect the fusion kinase has on T cells but not on B cells, despite strong similarities given between the TCR and BCR signal initiation and transduction mechanism [90].

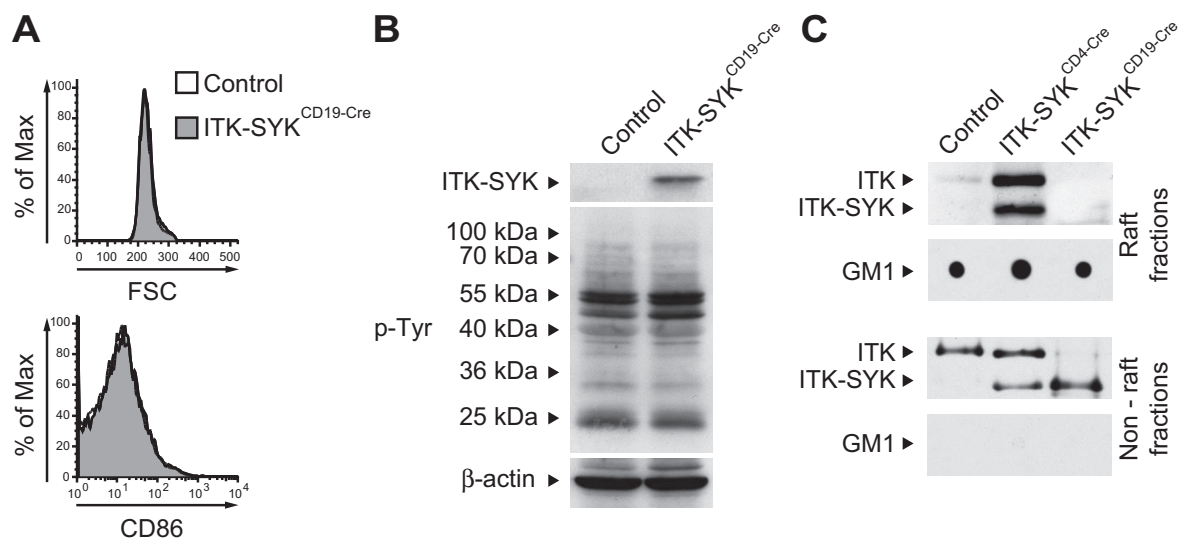


**Figure 5.12: Lacking B cell activation and T cell specific recruitment of ITK-SYK into lipid rafts.** (A) Forward scattering (FSC) and CD86 expression were analyzed on B220<sup>+</sup> splenic B cells from ITK-SYK<sup>CD19-Cre</sup> or CD19-Cre control mice by applying flow cytometry. Data shown are representative of four independent experiments with at least six 5-7 week old mice analyzed per genotype. (B) Cytoplasmic extracts of purified splenic B cells from 5 week old ITK-SYK<sup>CD19-Cre</sup> or CD19-Cre control mice were subjected to westernblot analysis with an antibody directed against ITK and total phospho-tyrosine residues (p-Tyr). Westernblotting against  $\beta$ -actin demonstrated equal protein loading. Data shown are representative of three independently performed experiments. (C) Lipid raft and non-raft fractions were prepared from purified splenic T cells of ITK-SYK<sup>CD4-Cre</sup> or ROSA26<sup>loxSTOPlox-ITK-SYK</sup> control mice or from purified splenic B cells of ITK-SYK<sup>CD19-Cre</sup> mice that were >12 weeks of age. The fractions were subsequently analyzed for the presence of ITK or ITK-SYK by westernblot analysis with an ITK specific antibody. Dot blots for GM1 depict successful raft preparation and equal protein loading. Data shown are representative of three independent experiments.

## 5.3 Peripheral T Cell Lymphoma in ITK-SYK Expressing Mice

### 5.3.1 ITK-SYK Expression in T Cells Results in a Fatal Lymphoproliferative Disease with Neoplastic Character

Analysis of 4-6 week old ITK-SYK<sup>CD4-Cre</sup> mice demonstrated that T cell development and activation are affected upon T cell specific expression of the fusion kinase ITK-SYK (Subsection 5.2.3). Thymocytes were lost at the DP and SP stage. Also, a severe loss of T cells in the peripheral lymphoid organs was observed. The remaining peripheral T cells however expressed ITK-SYK and displayed an activated phenotype with proliferative features.

To see whether continued ITK-SYK expression can be accounted for lymphoma development, longterm observations of a defined cohort of ITK-SYK<sup>CD4-Cre</sup> (n=19) and ITK-SYK<sup>CD19-Cre</sup> (n=8) mice were initiated. Regular blood sampling was performed to monitor the percentages of eGFP<sup>+</sup> T cells as well as eGFP<sup>+</sup> B cells of the respective mouse strain via flow cytometry. As seen in Figure 5.13 A, the frequency of eGFP<sup>+</sup> T cells increased steadily in ITK-SYK<sup>CD4-Cre</sup> up to 90%, whereas the mean frequency of eGFP<sup>+</sup> B cells remained fairly stable in ITK-SYK<sup>CD19-Cre</sup> animals at around 40%. Most distinctly, during the course of observation, mice of the ITK-SYK<sup>CD4-Cre</sup> genotype were lost by death or eventually had to be sacrificed due to increasing disease symptoms with an onset at about 12 weeks of age. The final disease stage was characterized by wasting and runting symptoms, lethargy, hunched postures, and distended abdomens. None of the ITK-SYK<sup>CD19-Cre</sup> mice, however, developed disease related symptoms within that time frame. Therefore, data obtained from blood sampling hinted towards the development of a lymphoproliferative disorder upon T cell specific expression of ITK-SYK with a fatal outcome for ITK-SYK<sup>CD4-Cre</sup> mice.

In order to substantiate these initial observations, survival curves from a larger cohort of ITK-SYK<sup>CD4-Cre</sup> and CD4-Cre control mice were generated. Indeed, all ITK-SYK<sup>CD4-Cre</sup> mice eventually succumbed to disease related symptoms within 27 weeks showing a median survival of 20.6 weeks of age (Figure 5.13 B). CD4-Cre control mice remained unaffected. Analysis of diseased ITK-SYK<sup>CD4-Cre</sup> mice revealed enlarged spleens with a mean 4.6 fold weight increase compared to spleens isolated from control mice (Figure 5.13 C). Flow cytometric analysis confirmed expansion of eGFP<sup>+</sup> T cells, completely replacing the remaining cell compartments (Figure 5.13 D).

Further characterization followed to determine whether the lymphoproliferative disease exhibited features of a neoplastic disorder. Thus, histological analysis in combination with studies concerning T cell clonality and transplantability were performed. As for the

histological analysis of diseased ITK-SYK<sup>CD4-Cre</sup> mice, a complete disruption of the normal spleen architecture by a diffuse infiltrate of medium to large-sized lymphoid cells was observed. T cells demonstrated irregular nuclei, prominent nucleoli and high mitotic rates, all features strongly supporting a situation of neoplastic cell growth (Figure 5.14 A). The proliferative nature of the T cells was verified by Ki-67 positivity. Flow cytometric analysis showed, that in 61% of all cases the CD4<sup>+</sup> T cell population (Type 1) was expanded, in 23% of all cases the CD8<sup>+</sup> T cell population (Type 2), and in 16% of all cases both the CD4<sup>+</sup> and the CD8<sup>+</sup> population were expanded (Type 3). The three disease subtypes observed in the spleens of ITK-SYK<sup>CD4-Cre</sup> mice are depicted in Figure 5.14 B. Notably, the presence of abnormally expanding T cells was not limited to the spleen. Massive T cell infiltration into the bone marrow (Figure 5.14 C) and into solid organs such as KID, LIV and LNG were observed (Figure 5.14 D). T cells invading and partially destroying the walls of blood vessels or epithelial cells were regularly detected throughout organ samples.

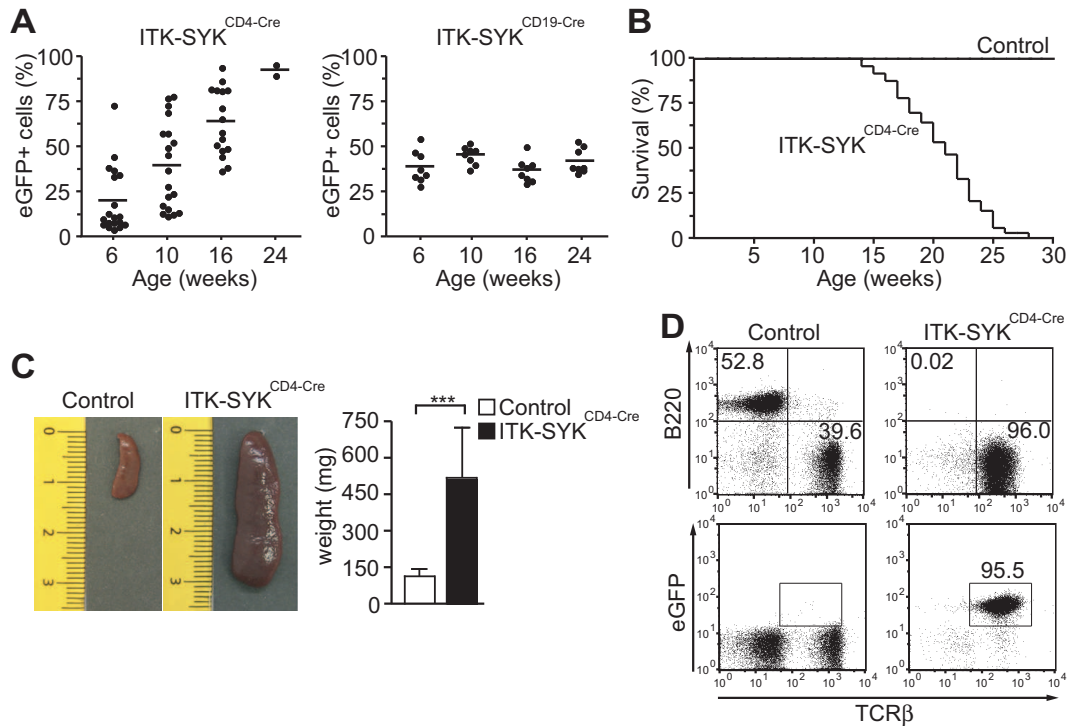


**Figure 5.13: Conditional expression of ITK-SYK in T cells induces a fatal lymphoproliferative disease.** (A) Peripheral blood samples from ITK-SYK<sup>CD4-Cre</sup> (starting with n=19) and ITK-SYK<sup>CD19-Cre</sup> mice (n=8) were obtained at the indicated time points. The frequencies of eGFP<sup>+</sup> lymphocytes in individual animals were determined by flow cytometry. The total number of ITK-SYK<sup>CD4-Cre</sup> mice declined over time as a result of disease related mortality. Horizontal bars indicate the means. (B) Kaplan-Meier curve of ITK-SYK<sup>CD4-Cre</sup> (n=73) and CD4-Cre control mice (n=15). (C) Macroscopic appearance of representative spleens from 20 week old ITK-SYK<sup>CD4-Cre</sup> and CD4-Cre control mice are shown (in centimeters). Spleen weights from diseased ITK-SYK<sup>CD4-Cre</sup> (n=11) and CD4-Cre control (n=6) mice are presented with mean values  $\pm$ SD. Statistical significance was analyzed using the unpaired two-tailed Student's *t* test, statistically significant (\*\*\*)  $p < 0.0001$ ). (D) Splenocytes from 20 week old ITK-SYK<sup>CD4-Cre</sup> and CD4-Cre control mice were stained with antibodies directed against TCR $\beta$  and B220. Frequencies of the individual populations are indicated. Data shown are representative of at least twenty mice analyzed per genotype.

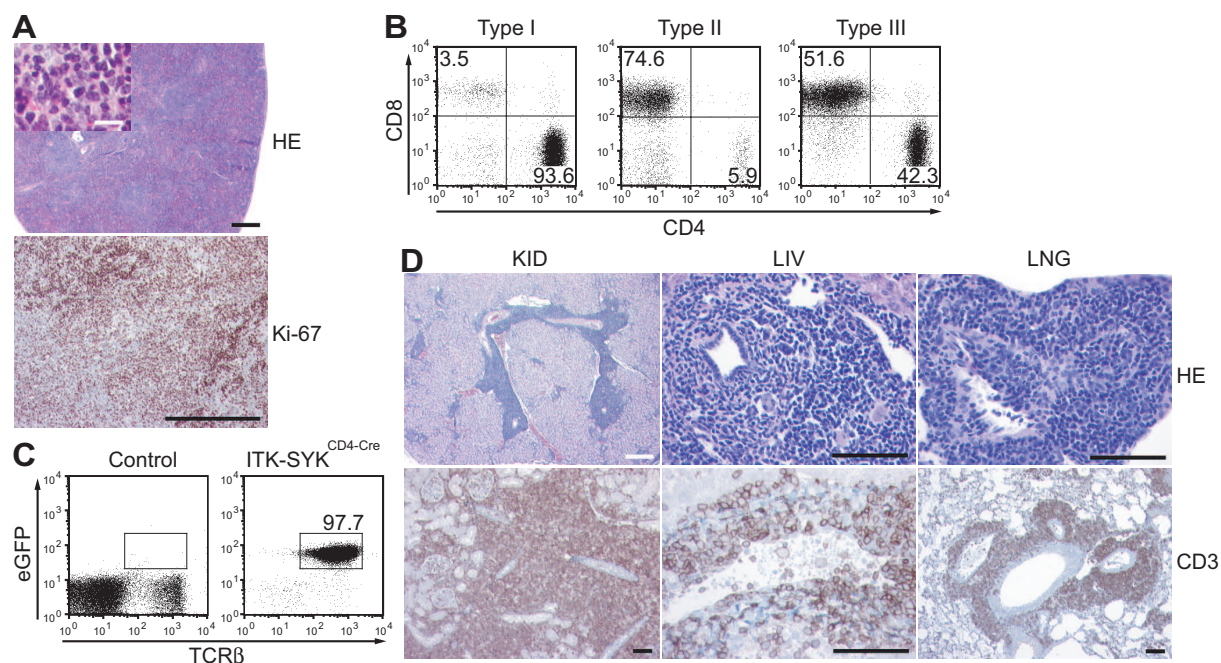


**Figure 5.14: Severe organ infiltration caused by abnormal T cell expansion in  $ITK-SYK^{CD4-Cre}$  mice.** (A) Disruption of the splenic architecture with highly proliferative cells in  $ITK-SYK^{CD4-Cre}$  mice was revealed by hematoxylin and eosin (H&E) staining and immunohistochemistry with anti-Ki-67 antibodies. Bars: black, 1mm; white,  $50\mu m$ . Data shown are representative of five diseased  $ITK-SYK^{CD4-Cre}$  mice analyzed. (B) Splenic cells from diseased  $ITK-SYK^{CD4-Cre}$  mice were stained against CD4 and CD8 and analyzed by flow cytometry. Representative examples of T cell expansion from forty analyzed mice are shown. (C) Bone marrow cell preparations from diseased  $ITK-SYK^{CD4-Cre}$  or CD4-Cre control mice were stained with antibodies against TCR $\beta$ . The frequency of eGFP<sup>+</sup> T cells in diseased mice is indicated. Data are representative of five independent experiments with fifteen mice analyzed per genotype. (D) Solid organ infiltration of abnormal CD3<sup>+</sup> T cells. Tissue sections from kidney (KID), liver (LIV), and lung (LNG) of affected  $ITK-SYK^{CD4-Cre}$  mice were stained with H&E. Anti-CD3 antibodies were used for immunohistochemical analysis. Bars: black,  $200\mu m$ ; white, 1mm. Data shown are representative of five diseased  $ITK-SYK^{CD4-Cre}$  and three control mice analyzed. Control mice were of CD4-Cre or  $ROSA26^{loxSTOPlox-ITK-SYK}$  genotype. Data in (A)-(D) are from  $ITK-SYK^{CD4-Cre}$  mice that were older than 12 weeks of age and displayed severe disease symptoms.

To investigate whether the expanded T cells were of clonal origin, splenocytes isolated from diseased ITK-SYK<sup>CD4-Cre</sup> and CD4-Cre control mice were stained against a defined panel of TCRV $\beta$  chains (Subsection 3.2.3). Flow cytometric analysis revealed that the T cell compartment of ITK-SYK<sup>CD4-Cre</sup> mice always showed an irregular distribution of individual T cell clones compared to control mice (Figure 5.15 A). Several TCRV $\beta$  chain variants were underrepresented or lost completely, whereas the percentage of one or few variants was increased (Figure 5.15 B). A preferential TCRV $\beta$  chain rearrangement in diseased ITK-SYK<sup>CD4-Cre</sup> mice was not observed. Notably, the expanded splenic TCRV $\beta$ -chain<sup>+</sup> T cells were again detected in other affected solid organs such as KID and LIV of the same diseased animal (Figure 5.15 C), indicating clonal cell expansion. To confirm clonality on the genomic level, genescan analysis was performed to amplify V-D-J joining regions within the rearranged TCR $\beta$  and TCR $\gamma$  locus. Analyses were performed in diseased ITK-SYK<sup>CD4-Cre</sup> and CD4-Cre control mice. Whereas all control T cell samples gave rise to a plethora of PCR products with a normal size distribution, the amplified PCR product profile from splenocytes isolated from diseased ITK-SYK<sup>CD4-Cre</sup> mice showed that few distinct amplification products came up. Exemplary, genescan analysis for the rearrangement of the D $\beta$ 2/J $\beta$ 2 junction in T cells of a control and diseased ITK-SYK<sup>CD4-Cre</sup> mouse are shown (Figure 5.15 D). Therefore, both flow cytometry and genescan analysis demonstrated a clonal expansion of ITK-SYK expressing T cells in diseased ITK-SYK<sup>CD4-Cre</sup> mice.

As a final approach to analyze the neoplastic nature of ITK-SYK expressing T cells, transplantation experiments were performed. To this end, total splenocytes isolated from ITK-SYK<sup>CD4-Cre</sup> mice were injected into the tail vein of immunocompromised Hsd:Athymic Nude-Foxn1<sup>nu</sup> mice. The frequencies of eGFP<sup>+</sup> cells from blood samples were monitored over time as was the health status of the transplanted recipient mice. Flow cytometric analysis showed that the frequency of transferred eGFP<sup>+</sup> cells increased steadily over time within individual recipients (Figure 5.16 A). Cells isolated from 90% of donor mice transplanted the disease. All successfully transplanted recipients eventually succumbed to disease symptoms such as weight loss, extended abdomen and hunched postures with a median survival of 15 weeks post transplantation. Organ preparations revealed splenomegaly (Figure 5.16 B) and flow cytometric analysis demonstrated a massive T cell expansion within the SPL and BM of these animals (Figure 5.16 C). H&E staining in combination with immunohistochemical detection of Ki-67 confirmed that recipient spleens were flooded by enlarged, proliferating cells. Cell infiltration into solid organs was further detected as exemplary depicted for LIV and LNG sections (Figure 5.16 D). The T cell nature of the infiltrates was verified by immunohistochemical staining against the surface marker CD3.

Ultimately, analysis of diseased ITK-SYK<sup>CD4-Cre</sup> mice showed that T cell specific

expression of the fusion kinase ITK-SYK leads to uncontrolled T cell expansion with a fatal outcome. The malignant phenotype of the disease was characterized by abnormal T cell morphology and clonal expansion of highly infiltrative T cells, which upon transplantation recreated the disease in recipient mice.

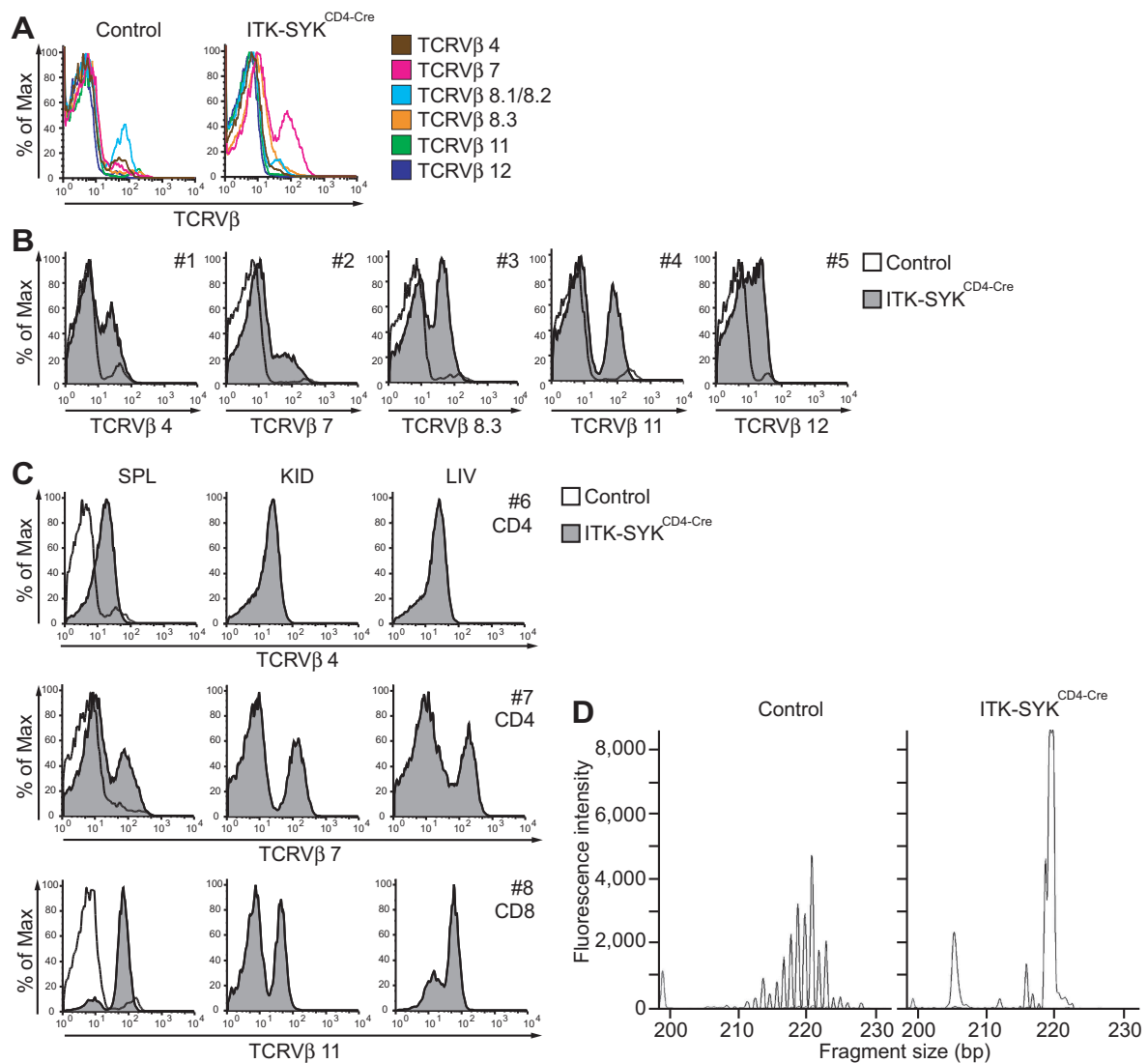


**Figure 5.15: Selective expansion of distinct T cell clones in affected *ITK-SYK<sup>CD4-Cre</sup>* mice.** (A) Splenocytes isolated from a *CD4-Cre* control and diseased *ITK-SYK<sup>CD4-Cre</sup>* mouse were stained with antibodies directed against CD4, CD8, and a panel of TCRV $\beta$  chain specific antibodies. The distribution of TCRV $\beta$  chain<sup>+</sup>CD4<sup>+</sup> T cells is shown by histogram overlay. (B) Splenocytes were stained as in (A). Frequencies of expanded CD4<sup>+</sup> cells expressing the indicated TCRV $\beta$  chains in the spleen of five diseased *ITK-SYK<sup>CD4-Cre</sup>* mice (#1-5, tinted histograms) are depicted. Control mice (untinted histograms) were of *CD4-Cre* or *ROSA26<sup>loxSTOPlox</sup>-ITK-SYK* genotype. A total amount of n=33 diseased *ITK-SYK<sup>CD4-Cre</sup>* mice was screened for skewed TCRV $\beta$  chain expression. (C) Single cell suspensions from spleen (SPL), kidney (KID), and liver (LIV) of three individual mice were stained as in (A). Frequencies of CD4<sup>+</sup> or CD8<sup>+</sup> cells expressing the indicated TCRV $\beta$  chains in SPL, KID and LIV of *CD4-Cre* control (untinted histograms) or diseased *ITK-SYK<sup>CD4-Cre</sup>* mice (#6-8, tinted histograms) are depicted. (D) Genescan analysis for TCR gene rearrangements. Representative fragment size distributions of fluorochrome-labeled PCR products of the D $\beta$ 2/J $\beta$ 2 junction of a *CD4-Cre* control and a diseased *ITK-SYK<sup>CD4-Cre</sup>* mouse are presented. Data shown are representative of three mice analyzed per genotype. Data in (A)-(D) are from *ITK-SYK<sup>CD4-Cre</sup>* mice that were older than 12 weeks of age and showed severe disease symptoms.

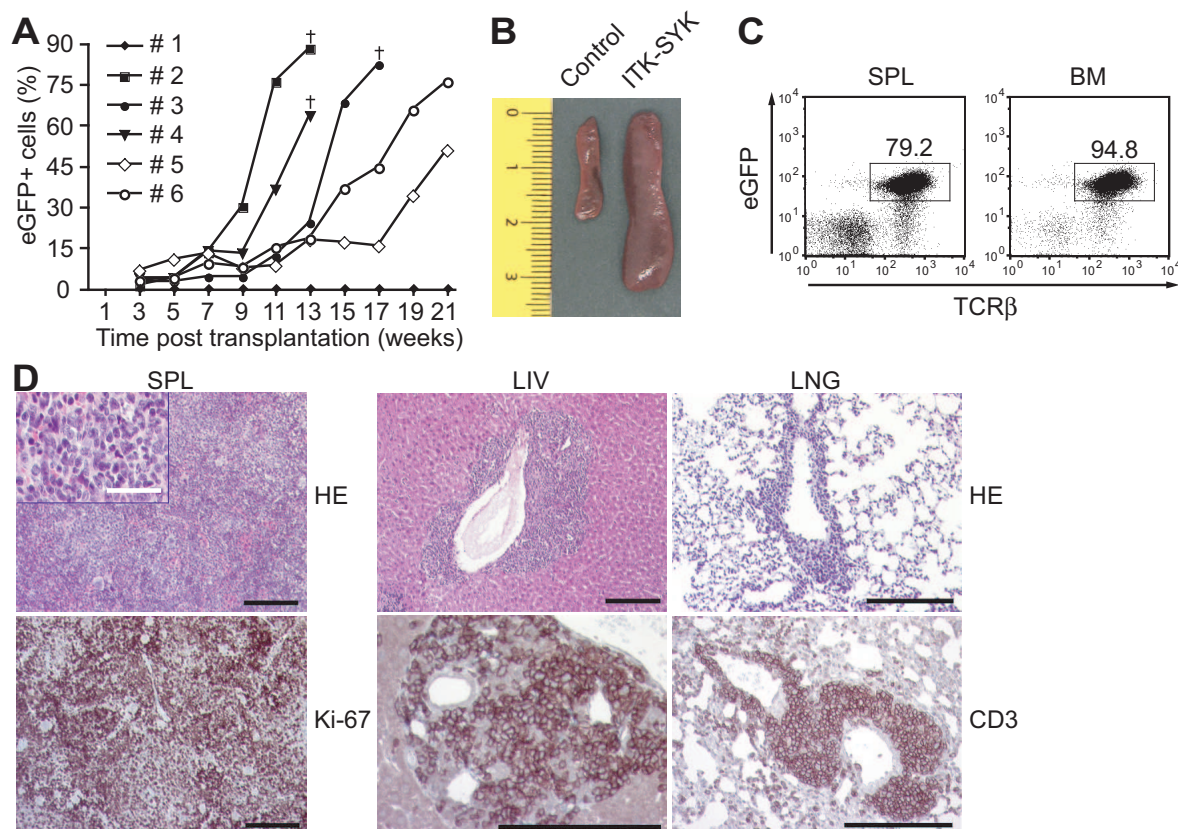


**Figure 5.16: Proliferation and infiltration of ITK-SYK expressing T cells upon transplantation.** (A) Splenic cells from diseased ITK-SYK<sup>CD4-Cre</sup> mice were intravenously injected into Hsd:Athymic Nude-Foxn1<sup>nu</sup> recipient mice for transplantation. The frequencies of eGFP<sup>+</sup> peripheral blood cells in the recipients were monitored over time by flow cytometry. Recipients that succumbed to the disease are indicated ( $\dagger$ ). Representative examples are shown. Nine out of ten donor mice transplanted the disease. Five independent transplantations were performed. (B) Spleens (SPL) from a Hsd:Athymic Nude-Foxn1<sup>nu</sup> control and a representative recipient mouse from (A) are shown (in centimeter). (C) Recipients were sacrificed upon signs of disease, and bone marrow (BM) and SPL suspensions were stained against TCR $\beta$ . Representative frequencies of eGFP<sup>+</sup> T cells in SPL and BM of ten diseased recipients are indicated. (D) Tissue sections from SPL, liver (LIV), and lung (LNG) were analyzed by H&E staining or by immunohistochemistry with  $\alpha$ -CD3 or  $\alpha$ -Ki-67 specific antibodies. Bars: black, 1mm; white, 125 $\mu$ m. Representative examples of four diseased recipients are shown.

### 5.3.2 Sporadic ITK-SYK Expression in Single T Cells is Able to Induce T Cell Lymphomas in ITK-SYK<sup>CD19-Cre</sup> mice

As described in Subsection 5.2.4, B cell specific expression of the fusion kinase ITK-SYK neither affected B cell development nor activation. Furthermore, ITK-SYK<sup>CD19-Cre</sup> mice displayed a normal survival pattern up to 35 weeks of age. However, continued flow cytometric monitoring of the percentage of eGFP<sup>+</sup> cells in peripheral blood from ITK-SYK<sup>CD19-Cre</sup> mice revealed an expanding eGFP<sup>+</sup> population which was positive for the T cell marker TCR $\beta$  (Figure 5.17 A). This eGFP<sup>+</sup> T cell population had developed next to the expected eGFP<sup>+</sup> B cell population. With increasing percentages of eGFP<sup>+</sup> T cells in the peripheral blood, ITK-SYK<sup>CD19-Cre</sup> mice became overtly ill, and eventually all mice died or had to be sacrificed for ethical reasons. ITK-SYK<sup>CD19-Cre</sup> mice displayed a median survival of 47.4 weeks of age (Figure 5.17 B). Notably, disease symptoms were reminiscent of ITK-SYK<sup>CD4-Cre</sup> mice and were composed of wasting and runting symptoms, lethargy, hunched postures, as well as extended abdomens. Extensive splenomegaly was observed upon mouse dissection with a mean 8.3 fold weight increase compared to CD19-Cre control mice (Figure 5.17 C). Flow cytometric analysis confirmed that the expanded splenic eGFP<sup>+</sup> population was of T cell origin, as shown by staining against TCR $\beta$  (Figure 5.17 D). H&E staining in combination with immunohistochemical detection of CD3 and B220 further supported a loss of the normal splenic organization with expansion of irregular T cells and replacement of the B cell compartment (Figure 5.17 E). T cells were activated as determined by upregulation of CD44 and loss of the naive T cell maker CD62L (Figure 5.18 A). Further characterization revealed that the expanding T cell population consisted of CD4<sup>+</sup> T cells in 75% of all diseased ITK-SYK<sup>CD19-Cre</sup> mice (Type I). The remaining cases showed an expansion of the CD8<sup>+</sup> T cell population (Type II) (Figure 5.18 B). Notably, no simultaneous expansion of both the CD4<sup>+</sup> and the CD8<sup>+</sup> T cell population was observed. Besides uncontrolled T cell growth within the SPL, T cells again invaded several other organs such as BM (Figure 5.18 C), LIV and LNG (Figure 5.18 D) as demonstrated by H&E staining and immunohistochemical detection of CD3. Staining against Ki-67 verified the proliferative nature of the infiltrating T cells (Figure 5.18 D).

To define whether the observed lymphoproliferative disease holds characteristics of a neoplastic disorder, T cell clonality was assessed in affected ITK-SYK<sup>CD19-Cre</sup> mice. Flow cytometric analysis revealed a selective expansion of distinct TCRV $\beta$ <sup>+</sup> T cell clones in diseased ITK-SYK<sup>CD19-Cre</sup> compared to CD19-Cre control mice (Figure 5.19 A). As a sign of T cell activation, downregulation of the respective TCRV $\beta$ <sup>+</sup> chain was detected in the gated T cell population from ITK-SYK<sup>CD19-Cre</sup> mice (Figure 5.19 A). The indicated clonal T cell expansion was supported on a genomic level by amplification of the TCRV $\beta$  and TCRV $\gamma$  locus via multiplex PCR. Genescan analysis showed that the expected PCR

product length distribution of T cells isolated from CD19-Cre control mice was entirely lost in T cells isolated from diseased ITK-SYK<sup>CD19-Cre</sup> mice (Figure 5.19 B). TCR locus rearrangements for one or more clones were predominantly observed, confirming a clonal T cell expansion in ITK-SYK<sup>CD19-Cre</sup> mice.

Concludingly, data show that ITK-SYK<sup>CD19-Cre</sup> mice all eventually developed a neoplastic disease of T cell origin. Although the onset was significantly delayed, the disease phenotype was reminiscent of ITK-SYK<sup>CD4-Cre</sup> mice. Thus, results imply a scenario where the unlikely event of CD19 promoter activity in a small number of T cells is sufficient to induce Cre-mediated deletion of the loxP site flanked NEO-STOP cassette. Sporadic ITK-SYK expression triggers T cell expansion and eventually leads to the development of PTCL also in ITK-SYK<sup>CD19-Cre</sup> mice.

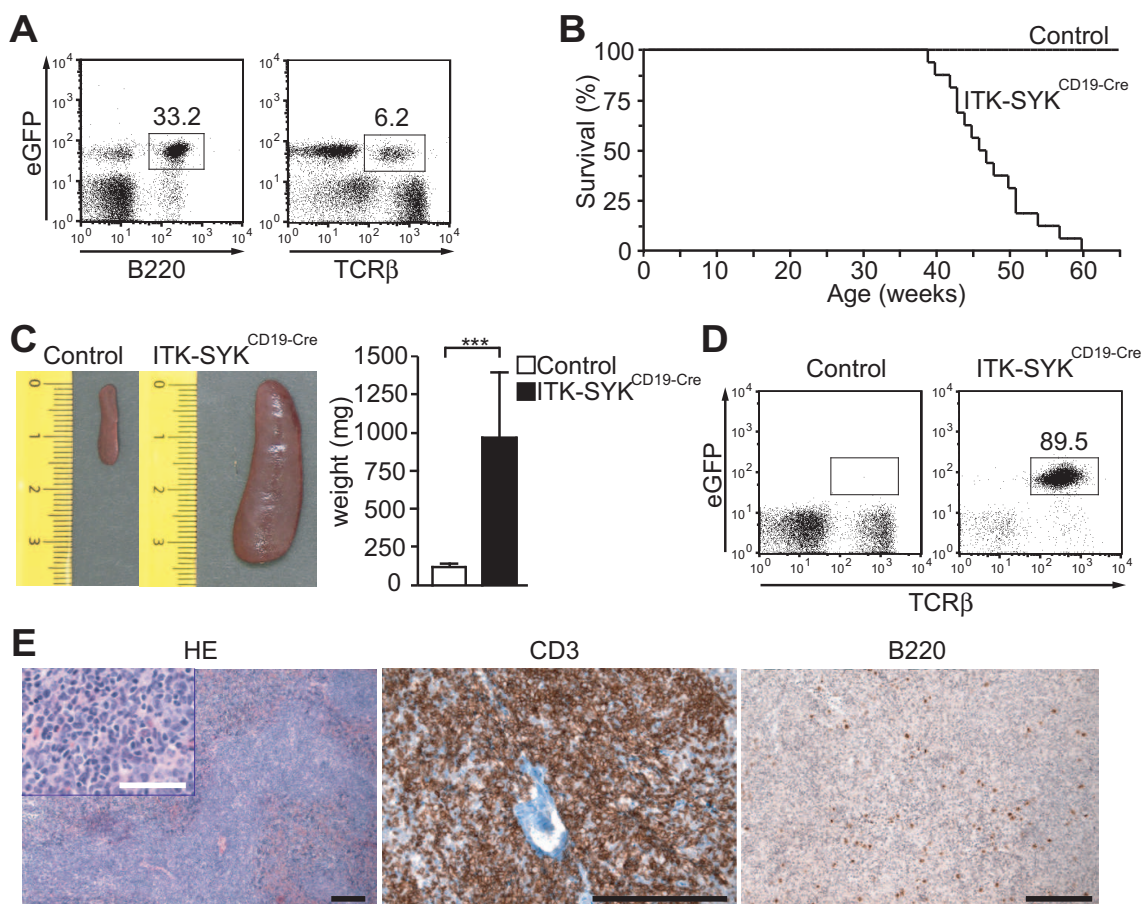


**Figure 5.17: ITK-SYK<sup>CD19-Cre</sup> mice develop a lymphoproliferative disease.** (A) Peripheral blood from a 25 week old ITK-SYK<sup>CD19-Cre</sup> mouse was stained against B220 and TCR $\beta$ . The eGFP<sup>+</sup>TCR $\beta$ <sup>+</sup> or eGFP<sup>+</sup>B220<sup>+</sup> population is indicated. (B) Kaplan-Meier curve of ITK-SYK<sup>CD19-Cre</sup> (n=18) and CD19-Cre control mice (n=10). (C) Splenomegaly in ITK-SYK<sup>CD19-Cre</sup> mice. Representative spleens from 50 week old CD19-Cre control and diseased ITK-SYK<sup>CD19-Cre</sup> mice are shown (in centimeter). Spleen (SPL) weights from diseased ITK-SYK<sup>CD19-Cre</sup> (n=15) and CD19-Cre control mice (n=8) are depicted with mean values $\pm$ SD. Statistical significance was analyzed using the unpaired two tailed Student's *t* test, statistically significant (\*\*\*) $p < 0.0001$ . (D) Splenocytes from 50 week old CD19-Cre control and ITK-SYK<sup>CD19-Cre</sup> mice were stained against TCR $\beta$ . The frequency of eGFP<sup>+</sup> T cells in a representative ITK-SYK<sup>CD19-Cre</sup> mouse is indicated. Data in (A), (C), and (D) are representative of six independent experiments with at least eight mice analyzed per genotype. (E) H&E staining and immunohistochemistry with  $\alpha$ -CD3 and  $\alpha$ -B220 antibodies were performed on SPL sections. Bars: black, 500 $\mu$ m; white, 125 $\mu$ m. Data representative of six diseased ITK-SYK<sup>CD19-Cre</sup> mice are shown.

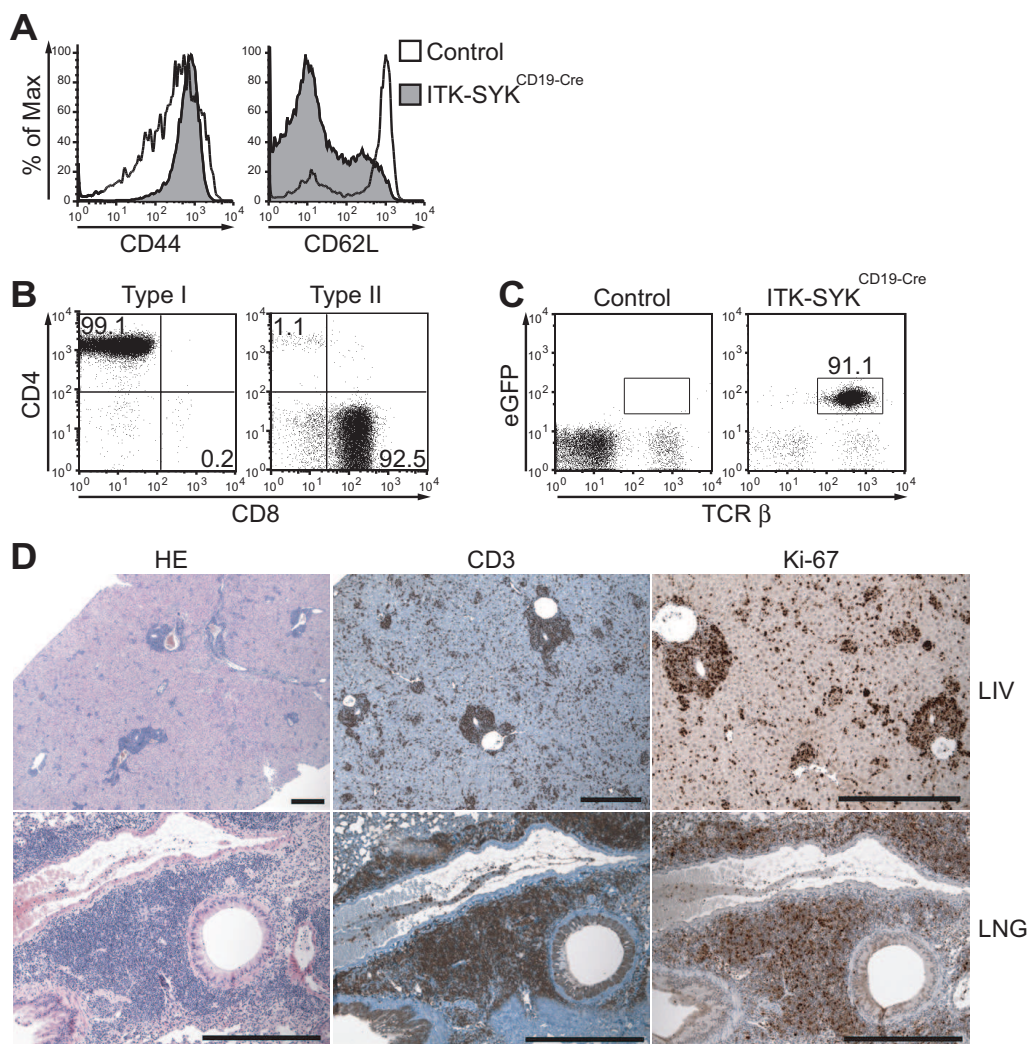


**Figure 5.18: ITK-SYK<sup>CD19-Cre</sup> mice display organ infiltration by activated T cells.** (A) Expanded T cells in ITK-SYK<sup>CD19-Cre</sup> mice display an activated phenotype. Splenocytes of 50 week old CD19-Cre control (untinted histograms) and diseased ITK-SYK<sup>CD19-Cre</sup> mice (tinted histograms) were stained against CD4, CD44 and CD62L. Surface expression of CD44 and CD62L were assessed by flow cytometry from gated CD4<sup>+</sup> T cells. (B) Splenocytes from diseased ITK-SYK<sup>CD19-Cre</sup> mice (n=16) were stained against CD4 and CD8. Examples of preferential CD4<sup>+</sup> T cell (Type I) or CD8<sup>+</sup> T cell (Type II) expansions are shown. (C) Bone marrow cell suspensions of 50 week old CD19-Cre control and diseased ITK-SYK<sup>CD19-Cre</sup> mice were stained against TCRβ. The frequency of eGFP<sup>+</sup> T cells in a representative diseased ITK-SYK<sup>CD19-Cre</sup> mouse is indicated. (D) Solid organ infiltration with abnormally proliferating T cells in ITK-SYK<sup>CD19-Cre</sup> mice. H&E staining and immunohistochemistry with anti-CD3 and anti-Ki-67 antibodies were performed on liver (LIV) and lung (LNG) sections. Bars, 1mm. Data representative of six diseased ITK-SYK<sup>CD19-Cre</sup> mice are shown. Data in (A) and (C) are representative of six independent experiments with at least ten mice analyzed per genotype.

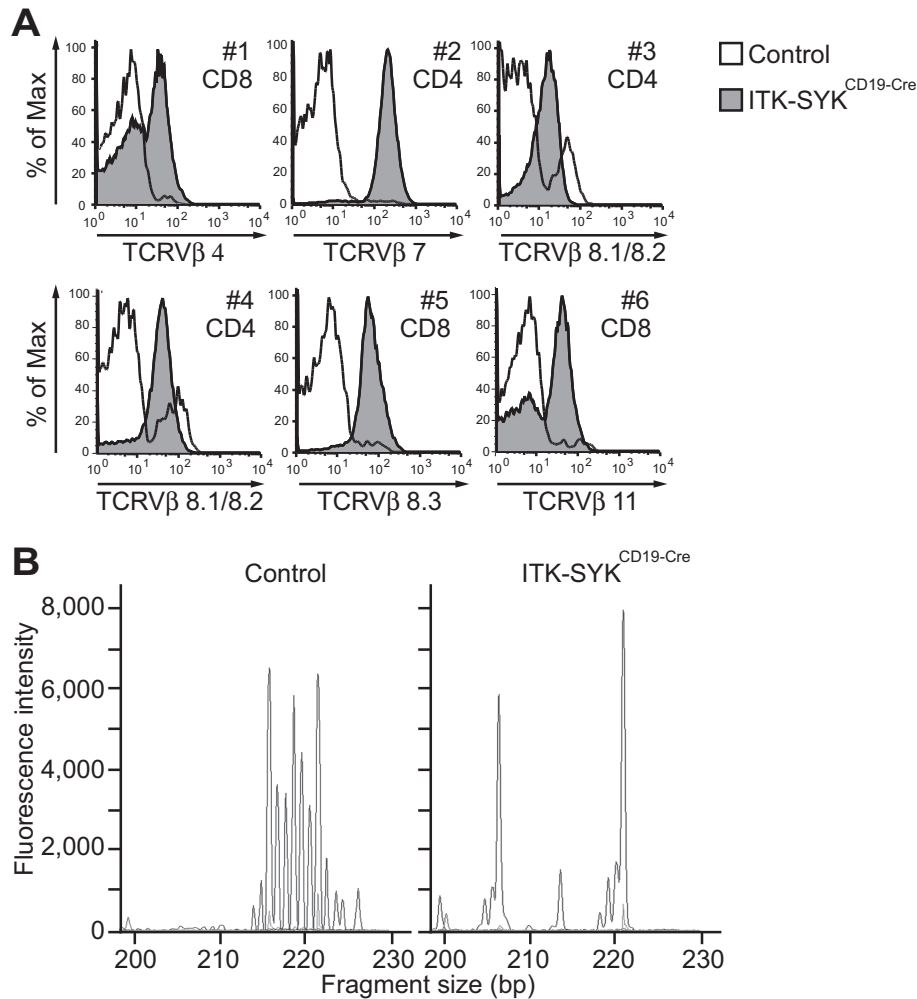


**Figure 5.19: Selective expansion of distinct T cell clones in ITK-SYK<sup>CD19-Cre</sup> mice.** (A) Single cell suspensions from spleens of CD19-Cre control (untinted histograms) and diseased ITK-SYK<sup>CD19-Cre</sup> mice (tinted histograms) were stained with antibodies directed against CD4, CD8, and a panel of TCRVβ chain specific antibodies (Subsection 3.2.3). Frequencies of expanded CD4<sup>+</sup> or CD8<sup>+</sup> T cells expressing the indicated TCR-Vβ chains from individual, diseased ITK-SYK<sup>CD19-Cre</sup> mice (#1-6) are shown. A total number of n=12 diseased ITK-SYK<sup>CD19-Cre</sup> mice was screened for skewed TCRVβ chain expression. (B) Genescan analysis for TCR gene rearrangements. Representative fragment size distributions of fluorochrome labeled PCR products of the Dβ2/Jβ2 junction of a CD19-Cre control mouse and a diseased ITK-SYK<sup>CD19-Cre</sup> mouse are depicted. Data shown are representative of five mice analyzed per genotype.

# Chapter 6

## Discussion

### 6.1 ITK-SYK: Investigating a Novel Fusion Protein

Aiming at understanding deregulated signaling pathways and their role in tumorigenic processes, a novel gene fusion found in a subgroup of patients diagnosed with PTCL-NOS was recognized. The chromosomal translocation  $t(5;9)(q22;q33)$  involves the ITK and SYK gene locus and leads to the production of an unprecedented fusion transcript, encoding for the tyrosine kinase ITK-SYK [178]. Despite its novelty, interest in the translocation was additionally given since it involved two kinases, which both are key players in AgR signaling [90].

Especially in the field of hematological disorders, it is well established that the identification of cytogenetic aberrations is a key step in the classification and eventual molecular understanding of a tumorigenic entity. Even if genomic aberrations concern merely a small fraction of patient samples, studies have shown that gene loci hit by chromosomal rearrangements are often affected by other mutations, leading to signal deregulation [157]. Thus, chromosomal aberrations might suggest a more general mechanism in tumor initiation, maintenance or progression. Affected molecules or downstream pathways might therefore constitute promising and rational targets for therapeutic intervention. The described process of identifying a translocation, understanding the molecular consequences, and using this knowledge to develop a treatment strategy, has been successfully applied for the tyrosine fusion kinase BCR-ABL. The fusion kinase is expressed as a result of the reciprocal translocation  $t(9;22)(q34;q11)$ , being present in 95% of all cases of chronic myeloid leukemia (CML) [125]. The translocation was the first recurrent genetic aberration to be associated with a human cancer [156, 42], and is now a prime example for the strategic approach to target aberrant tyrosine kinase activity by small molecule inhibitors [205]. In the case of CML, understanding cancer pathogenesis was clearly accelerated by the availability of mouse models [95]. *In vivo* systems help to validate *in vitro* observations, and at present are still a reasonable choice for evaluating therapeutic approaches during

preclinical investigations. Compiling studies within the complexity of a whole organism becomes especially relevant when dealing with a multistep process such as tumorigenesis.

As for PTCL-NOS, no genetically reproducible *in vivo* models were available prior to this work. With the knowledge on the recurrent translocation t(5;9)(q22;q33), the aim was to describe *in vitro* and *in vivo* effects of ITK-SYK expression, and to answer the question whether a causal link between the presence of ITK-SYK and the development of PTCL exists. Since the question called for a cell type specific investigation, conditional gene targeting employing the Cre/lox-P system was chosen. Implications from both analysis in Jurkat E T cells and the generated mouse strains ITK-SYK<sup>CD4-Cre</sup> and ITK-SYK<sup>CD19-Cre</sup> for ITK-SYK functionality and its disease correlation are outlined in the following.

## 6.2 *In Vitro* Implications of Aberrant ITK-SYK Signaling

Based on translocation t(5;9)(q33;q22) [178], the hypothesis was put forward that ITK-SYK induces T cell activation and that the related cellular changes eventually lead to T cell transformation. Initial *in vitro* investigations had indeed shown that ITK-SYK expression triggers events that are characteristic of activated T cells. On a molecular level this is reflected by recruitment of tyrosine phosphorylated proteins into lipid rafts of ITK-SYK expressing JurkatE T cells. Accumulation of signaling proteins into lipid rafts and raft clustering are important events in AgR signaling [168]. It is known that antigen mediated TCR ligation induces activation of the SRC kinase LCK, which upon ITAM phosphorylation recruits the SYK family member ZAP-70 to the receptor complex. Correctly positioned within the LAT/SLP-76 signalosome, phosphorylated PLC $\gamma$ 1 generates the second messengers DAG and IP3. Both molecules eventually induce T cell activation by engaging several signaling cascades [171]. The here presented experiments showed that phosphorylated PLC $\gamma$ 1 was constitutively associated with lipid rafts in ITK-SYK expressing JurkatE T cells. Next to phosphorylated PLC $\gamma$ 1, phosflow analysis demonstrated activating phosphorylation of the scaffold proteins SLP-76 and LAT. Additionally, phosphorylation of LCK was observed (Julian Holch, medical student in the lab, unpublished data). Thus, these data support a scenario where ITK-SYK expression results in the activation of TCR proximal signaling molecules. Furthermore, phosphorylation of AKT indicated that the PI3K signaling pathway is activated, which in T cells is regularly engaged by signaling from the costimulatory molecule CD28 [171]. Nonetheless, it has to be taken into consideration that Jurkat T cells intrinsically show irregular PI3K activity due to PTEN deficiency [1]. However, in all retroviral infection experiments, ITK-SYK expressing JurkatE T cells were compared to empty vector control JurkatE T cells. Therefore,

increased AKT phosphorylation indicative of PI3K activity can be attributed to ITK-SYK activity.

As distal signaling events, ITK-SYK induced activation of the MAPKs p38 and ERK1/2. In concurrence, other authors also described activating phosphorylation of SLP-76 [82], AKT [151], and ERK1/2 [151] in 292 T cells. Via inhibitor studies Julian Holch showed that not only the MAPK signaling pathways but also the NFkB, the Calcineurin, as well as the STAT5 signaling pathways are activated by the fusion kinase ITK-SYK (unpublished data). Activation of STAT-5 by ITK-SYK has also been demonstrated by Dierks et al. [48]. Inhibition of individual signaling components reduced or completely abrogated JurkatE T cell activation, as measured by CD69 expression and IL-2 secretion. Both CD69 surface expression and IL-2 production are early T cell activation markers [73, 172], and both effects were seen to be strongly induced upon ITK-SYK expression. Notably, ITK-SYK related activation events were similarly observed in JurkatE T cells stimulated via the TCR and the costimulatory CD28 molecule. Therefore, the results indicate that ITK-SYK acts as an intracellular mimic of a TCR signal. However, ITK-SYK signaling is not identical to the ligand-induced TCR signal. It was observed to differ in terms of phosphorylation kinetics and quantitative aspects like induction of maximal IL-2 production or CD69 expression. Moreover, while normal TCR signaling is self-limiting at the end of an immune response [171], ITK-SYK signaling appears to be chronic due to its independence on external TCR stimulation.

Besides the recruitment of phosphorylated proteins, ITK-SYK itself was found to be constitutively present in JurkatE T cell lipid rafts. Membrane recruitment could be an important factor required for ITK-SYK activation and for the fusion kinase to gain proximity to its substrates (Section 6.3). Indeed, mutational *in vitro* analysis showed that a defective PH domain abrogated ITK-SYK mediated T cell activation. The same outcome was observed for the ITK-SYK<sup>KD</sup> mutant. The importance of correct enzymatic activity was further supported by the fact that treatment of ITK-SYK expressing JurkatE T cells with the SYK inhibitor R406 blocked T cell activation, as was determined by lacking IL-2 secretion and CD69 expression. In line with this observation, Rigby et al. [151] demonstrated that ITK-SYK kinase activity and membrane localization are also required for ITK-SYK mediated transformation of the NIH3T3 immortalized fibroblast cell line *in vitro*. Hussain et al. [82] indirectly supported the importance of membrane recruitment by showing that ITK-SYK activation, and subsequent SLP-76 phosphorylation is dependent on PI3K activity. PI3K is the responsible kinase to generate PIP3, which is the ligand for PH domain mediated membrane recruitment of ITK [8]. Thus *in vitro* data show that ITK-SYK functionality depends on its enzymatic activity and on membrane recruitment. As indicated here, once correctly positioned, ITK-SYK may act on various signaling proteins. The upcoming chapter will take a closer look at the structural consequences of the

translocational event and in which manner these changes can be interpreted in regard to ITK-SYK actions downstream of the TCR.

### 6.3 Structural Aspects of ITK-SYK and its Potential Mode of Action

Considering the structural and regulatory aspects of the individual translocation partners ITK (Subsection 1.2.3) and SYK (Subsection 1.2.4), it becomes clear that the fusion kinase ITK-SYK has lost most of the regulatory elements contained in the original kinases. The discussed model for ITK regulation postulates that the kinase is kept in an enzymatically inactive state through intermolecular interactions between the SH3 and SH2 domains, as well as through intramolecular interactions between the PRR and the SH3 domain [8]. Additionally, an SH2 domain located *cis*-prolin has been suggested to promote ITK inactivity [120]. These protein modules are lost upon translocation along with the intrinsic tyrosine kinase domain. Merely, the PH and TH domain of ITK are retained. As for SYK, the translocational event preserves the tyrosine kinase domain but sheds both the linker A connected SH2 domains and nearly half of the linker B region (Figure 1.5). Thus, the normally performed conformational changes promoting SYK inactivation, such as linker A/B mediated tandem SH2 domain interaction with its kinase domain (Figure 1.4), appear unrealized within the fusion kinase ITK-SYK. Hence, it is well conceivable that merely based on its domain composition, ITK-SYK might obtain a conformationally susceptible state, promoting its enzymatic activity without the need for greater structural changes to occur. Along this line, mutational analyses in wildtype SYK have shown that by partial loss of the linker A region [3] or by complete loss of the tandem SH2 domains [155], SYK enters a state of enzymatic activity. These *in vitro* observations support the scenario of a constitutively active fusion kinase due to the loss of structural regulatory elements. The only negative regulatory option maintained within the fusion kinase originates from the residual linker B region, namely tyrosine residue Tyr183. This residue corresponds to Tyr323 in the wildtype SYK molecule. It has been shown that upon phosphorylation of Tyr323, binding of CBL family members to SYK occurs, mediating SYK ubiquitinylation, and its subsequent proteasomal degradation [118]. As to whether this mechanism is employed for ITK-SYK negative regulation is still a matter of discussion, however, first data from bone marrow transplantation experiments have indicated that this might be the case [48].

One prerequisite for signal initiation downstream of the TCR and BCR is for signaling molecules to obtain proximity to the receptor/coreceptor complex as well as to other lipid raft associated signaling components. From the perspective of the full length SYK molecule, membrane recruitment and conformational activation are achieved through tan-

dem SH2 domain binding to dp-ITAMs, which are located in the receptor associated CD3 chains in T cells or Ig $\alpha$  and Ig $\beta$  chains in B cells [90]. As preceedingly outlined, in the case of ITK-SYK the SH2 domains are lost. However, structurally this loss seems to be compensated by retaining the ITK derived PH domain. PH domains are known to facilitate membrane recruitment by phosphoinositide binding with different substrate specificities for either PIP2 or PIP3 [109]. PH domains are common binding modules not only used by the TEC family of protein tyrosine kinases but also by other signaling molecules, e.g., PLC $\gamma$ 1/2, AKT or its activating kinase PDK1 [109]. As for ITK, PH domain interaction with PIP3 is needed for ITK activation and its function in T cells [12, 28]. ITK membrane recruitment is abrogated in the amino acid exchange mutant ITK (R29C) by destroying the lipid binding pocket of the PH domain [28]. As stated in Section 6.2 membrane localization of the respective PH domain mutated version of ITK-SYK is abolished as are its T cell activating capacities. These data substantiate the importance of the PH domain and support its compensatory role for the lost SYK derived SH2 domains for ITK-SYK membrane recruitment. Next to phosphoinositide interaction, oligomerization capacities of the PH domain are discussed in the literature [87, 80, 142]. Considering that oligomerization is a common mechanism observed for oncogenic tyrosine fusion kinases to gain enzymatic independence [110, 124], it can be hypothesized that the PH domain not only conveys membrane localization but also ITK-SYK oligomerization. Notably, concerning dimerization, Kolanus et al. [94] demonstrated, that clustering of the SYK kinase domain is able to induce its enzymatic activity to a similar degree as seen upon dp-ITAM binding.

Besides the demonstrated importance of both an intact PH and functional kinase domain for ITK-SYK activity (Section 6.2) [151, 82], another structural aspect should be considered when hypothesizing on how the fusion kinase might operate. On the protein level, the translocational event seems to spare key tyrosine residues within the remaining SYK derived linker B region. Among those are tyrosine residue Tyr183, Tyr208, and Tyr212 in the fusion protein, corresponding to tyrosine Tyr323, Tyr348, and Tyr352 in the wildtype SYK molecule. Within SYK, these sites have been shown to be targeted by autophosphorylation [63] and constitute binding sites for the classical signaling molecules: VAV1 (Tyr348) [45], PI3K(p85) (Tyr323/352) [131], PLC $\gamma$ 2 (Tyr348/352) [71], and PLC $\gamma$ 1 (Tyr348/352) [107]. Notably, translocation t(9;12)(q22; p12), generating the TEL-SYK fusion kinase, affects the same breakpoint region within the SYK gene locus as in ITK-SYK [101, 178]. Future investigations will show whether q22 might present a genomic region prone to chromosomal breaks within the SYK gene locus. In terms of potential interaction partners, another important tyrosine residue is retained at the far C-terminus of ITK-SYK, Tyr490. This residue corresponds to Tyr630 in the wildtype SYK molecule. Upon BCR stimulation and subsequent Tyr630 autophosphorylation, SYK has been shown to interact with the B cell scaffold protein BLNK (SLP-65) [99]. This interac-

tion stabilizes SYK in a conformationally active form [99]. Due to the structural homology between BLNK and SLP-76 [197] it is conceivable that SLP-76 recognizes phosphorylated Tyr490, contributing to ITK-SYK stability or supporting ITK-SYK recruitment to the LAT/SLP-76 signalosome. Until now, no experimental proof for direct interaction between SLP-76 or BLNK with ITK-SYK is available. However, SLP-76 is phosphorylated upon ITK-SYK expression (Section 6.2) as is BLNK [82].

On the basis of the experimental data provided and the structural aspects outlined, the following model of ITK-SYK mediated T cell activation is presented (Figure 6.1). ITK-SYK molecules are recruited to the membrane by PH domain interaction with PIP3. Relocalization from the cytoplasm to the membrane and possible oligomerization could induce conformational changes promoting ITK-SYK activity, leading to its full activation by autophosphorylation or phosphorylation in *trans*, as suggested by Rigby et al. [151]. Yet, since SYK activation in T cells can occur in a CD45 and LCK independent fashion [34], it is conceivable that this concept also applies to ITK-SYK. SRC kinase independency would support the observation that even without regular TCR stimulation ITK-SYK conveys its enzymatic activity (Section 6.2). Once phosphorylated and positioned within the proximity of lipid raft associated kinases and scaffold proteins, ITK-SYK activity results in phosphorylation of key signaling proteins. Since SYK derived tyrosine residues are retained in the fusion kinase, direct binding to PI3K, VAV1, PLC $\gamma$ 1, LCK and SLP-76 seem possible. Next to conveying protein phosphorylation, ITK-SYK might also participate in LAT/SLP-76 signalosome stabilization, promoting signal relay. Subsequently, once activated, PLC $\gamma$ 1 generates the second messengers DAG and IP3, engaging Ca<sup>2+</sup>-dependent and MAPK signaling pathways. Expression of IL-2 eventually would induce T cell proliferation through autocrine stimulatory JAK/STAT signaling [152]. ITK-SYK mediated activation of VAV1 would affect cytoskeletal reorganization, necessary for T cell activation through raft clustering and synapse formation [77]. Thus, on several levels ITK-SYK could promote signal initiation similarly as induced upon T cell stimulation.

Following signal initiation, several factors could be involved in sustaining ITK-SYK induced signal transduction. One critical point might stem from ITK-SYK mediated PI3K activation. Subsequent increased PIP3 availability would establish a positive feedback loop for continued membrane recruitment of the fusion kinase. Besides ITK-SYK accumulation, high PIP3 levels would also lead to an increased recruitment of other PH domain carrying signaling molecules present in the T cell, such as ITK, AKT, PDK1 or PLC $\gamma$ 1. Constitutive recruitment of PLC $\gamma$ 1 and endogenous ITK, indeed, was observed in JurkatE T cells and as later stated (Section 6.4) also in primary cells upon ITK-SYK expression. Thus, PI3K activation could present a key mechanism for ITK-SYK to amplify signaling events independently from the CD28 provided costimulatory signal, regularly needed for PI3K activation in T cells [90]. Another important factor in signal amplification might

result from ITAM phosphorylation. In T cells it has been shown, that SYK can phosphorylate ITAM tyrosine residues of CD3 receptor associated chains [105, 26]. Thus, the fusion kinase might also target ITAMs when recruited to lipid rafts and positioned within the proximity of the TCR/CD3 receptor complex. As a consequence, SYK and ZAP70 could interact with dp-ITAMs via their tandem SH2 domains and upon activation engage familiar signaling cascades downstream of the TCR/CD3 complex [171]. Since LCK is phosphorylated upon ITK-SYK expression, the fusion kinase might further establish a positive feedback loop by TCR independent LCK activation, resulting in sustained ITAM phosphorylation.

All in all, the structural composition of ITK-SYK, its enzymatic activity together with the opportunities for interacting with key signaling components, offers many opportunities to promote T cell activation and proliferation. In what way ITK-SYK activity affects primary T cells and whether the fusion kinase is able to cause malignant cell growth

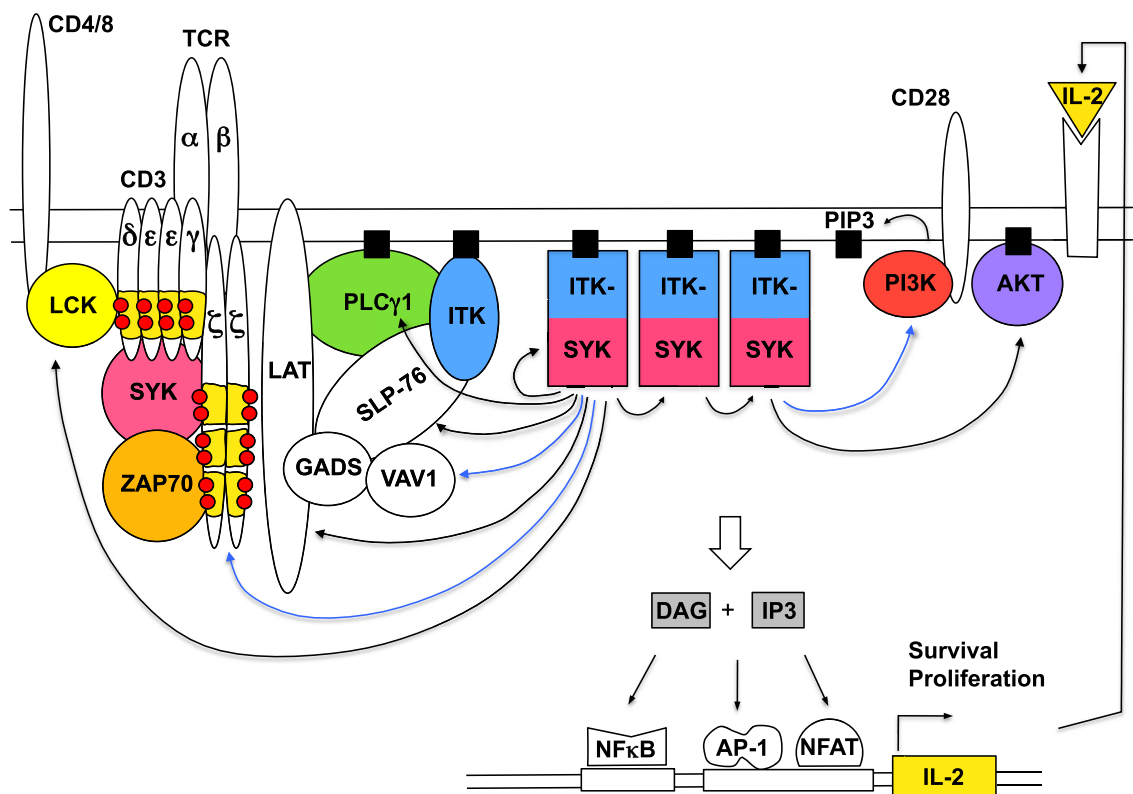


**Figure 6.1: Model of ITK-SYK induced TCR signaling.** Within this scheme, ITK-SYK targets are depicted (arrows). It is theorized that through activation of both TCR proximal molecules and costimulatory signaling components, ITK-SYK engages cell survival and proliferation pathways. Autocrine IL-2 stimulation sustains cell proliferation in a TCR receptor independent manner promoting T cell transformation. Blue arrows indicate potential ITK-SYK targets, which still need experimental verification. Details are given in Section 6.3.

has been addressed by *in vivo* investigations as discussed in the following.

## 6.4 Pathological Outcome of ITK-SYK Expression

The conclusion drawn from *in vitro* experiments that ITK-SYK has the potential to mimic a TCR signal, was indeed reflected in young ITK-SYK<sup>CD4-Cre</sup> mice. Depending on the cellular context, ITK-SYK expression resulted, on the one hand, in a severe loss of DP thymocytes, and, on the other hand, in activation of mature peripheral T cells. Deletion of thymocytes at the DP stage is part of a naturally occurring process, referred to as negative selection [31]. DP thymocytes which bind MHC/self peptide complexes too strongly via their TCR are not rescued from apoptosis, and die. Through this mechanism, potentially autoreactive T cells are eliminated before maturation is even completed [31]. Thus, the observation that ITK-SYK expression correlates with increased cell death at the DP stage, strongly supports the hypothesis that ITK-SYK induces intracellular signaling events similar to those provided by a strong TCR stimulation. Low DP thymocyte numbers resulted in reduced numbers of SP thymocytes as well as reduced numbers of mature peripheral T cells. However, those cells which eventually enter the periphery, either CD4<sup>+</sup> or CD8<sup>+</sup> T cells, do so in an activated state. Cells are enlarged, show upregulation of the activation marker CD44, and downregulation of the naive homing receptor CD62L. In line with an activated status, reduced TCR $\beta$  surface expression is also observed. Immunohistological analysis (performed in collaboration with Leticia Quintanilla-Fend) further depicted that T cells were positive for the proliferation marker Ki-67, and no signs of increased apoptosis were observed. On a molecular level, T cell activation was reflected by constitutive recruitment of phosphorylated PLC $\gamma$ 1 and ITK into lipid rafts, as was already observed for JurkatE T cells. Again, CD3/CD28 stimulation of control T cells resulted in PLC $\gamma$ 1 recruitment to a similar extent as was seen for ITK-SYK expressing T cells. Therefore, not only *in vitro* but also *in vivo* ITK-SYK expression induced an activated T cell phenotype.

The final question to be answered was, whether this state of T cell activation promotes T cell transformation. Interestingly, gene expression profiling studies on PTCL-NOS samples have shown that malignant cells most closely resemble mature activated CD4<sup>+</sup> or CD8<sup>+</sup> T cells [139]. General characterization showed that the majority of PTCL-NOS cases are derived from CD4<sup>+</sup> T cells [154] and strongly express the proliferation marker Ki-67 [163]. To investigate the outcome of ITK-SYK induced T cell activation, longterm observations of ITK-SYK<sup>CD4-Cre</sup> mice were conducted. Although initially reduced in cell numbers, mature T cells expanded steadily. Histological investigations confirmed their proliferative nature by Ki-67 positivity and further demonstrated abnormal nuclear features. Evenmore, T cells grew invasively into both lymphoid and non lymphoid areas. All three aspects are highly indicative of a neoplastic phenotype. Clonal T cell expansion

as well as the fact that malignant T cells could elicit a phenotypically equal disease in recipient mice, further substantiated the neoplastic character of the lymphoproliferative disease, allowing it to be classified as PTCL. The lymphoma showed full penetrance with a medium latency of 20.6 weeks. In the majority of cases expanded T cell clones originated from CD4<sup>+</sup> T cells. Fewer cases showed outgrowth of CD8<sup>+</sup> clones or a parallel expansion of both cell types. Next to the pathological features, such as extranodal involvement and the high proliferative index, the preferred clonal outgrowth of mature CD4<sup>+</sup> tumors is also in line with features described for human PTCL. In conclusion, ITK-SYK expression ultimately was able to induce PTCL with 100% penetrance, resembling aspects of the human disease. Since individual T cell clones expanded in ITK-SYK<sup>CD4-Cre</sup> mice, it is likely that cooperating events next to ITK-SYK contribute to their proliferative advantage.

Due to the fact that SYK is the main non receptor tyrosine kinase acting downstream of the BCR, and that strong similarities between AgR proximal as well as distal signaling events exist, it was further of interest to investigate possible effects of ITK-SYK activity on B cells. Quite astoundingly, B cell specific expression of ITK-SYK *in vivo* neither affected B cell development nor B cell activation. *In vitro* investigations by Dierks et al. [48] also showed that ITK-SYK was not able to transform the pre-B cell line BaF/3. In agreement, ITK-SYK<sup>CD19-Cre</sup> mice remained healthy until 30 weeks of age, while ITK-SYK<sup>CD4-Cre</sup> mice already succumbed to T cell lymphoma at that age. On a molecular level it became clear that whereas ITK-SYK is constitutively associated with lipid rafts in T cells, the fusion kinase was not detected in lipid rafts isolated from B cells. This observation would be in line with data gathered from JurkatE T cells, that membrane recruitment is necessary for ITK-SYK mediated cell activation. Even though this observation could explain why ITK-SYK does not affect B cell physiology, it still remains unclear why ITK-SYK is selectively recruited into lipid rafts of T cell but not of B cells. Both TEC kinases ITK and its B cell homolog BTK contain the N-terminally located PH domain, conveying membrane recruitment upon PIP3 interaction [129, 12]. The PIP3 generating kinase PI3K is expressed in both T cells [171] and B cells [102]. Thus, PIP3 in principle should be available for PH domain mediated membrane recruitment of ITK-SYK in either cell type. Yet, as differences are observed, it is hypothesized that ITK-SYK recruitment and activity are dependent on a T cell characteristic signaling environment, and that selective PH and TH domain mediated protein interactions are necessary for ITK-SYK activity. The strong presence of endogenous ITK in lipid rafts of T cells might also hint at an important involvement of ITK in conveying sustained ITK-SYK signaling. Additionally, it could also be possible that ITK-SYK is exposed to a tighter negative regulatory control in B cells than in T cells, preventing its full establishment at the B cell membrane.

An interesting observation concerning ITK-SYK membrane recruitment has been presented by Dierks et al. [48]. The authors performed bone marrow transplantation

experiments and demonstrated that recipient mice expressing the PH domain mutated version of ITK-SYK showed an earlier onset of disease symptoms compared to recipients expressing wildtype ITK-SYK. In order to understand the potential mechanism behind this observation, the authors investigated the opposite scenario, namely enforced membrane recruitment, and detect an increased phosphorylation of ITK-SYK on Tyr183. As outlined in Section 6.3, Tyr183 corresponds to Tyr323 in the wildtype SYK molecule. It is known, that Tyr323 acts as negative regulatory residue. Upon phosphorylation it recruits the ubiquitin ligase Cbl and leads to proteasomal degradation of SYK [118]. Thus Dierks et al. [48] argue that by loss of membrane localization, ITK-SYK escapes this regulatory aspect. Interestingly, these observations might point to a first negative regulatory control mechanism for ITK-SYK. Notably, these data might also have implications in composing treatment strategies. Mere blocking of ITK-SYK membrane recruitment thus might lead to a contrary effect as expected from *in vitro* observations. It remains open whether in a T cell specific mouse model, expression of a cytoplasmically located ITK-SYK version would result in the same observation as depicted in the bone marrow transplantation model.

Since no immediate effect of ITK-SYK on B cell development or B cell activation was observed, ITK-SYK<sup>CD19-Cre</sup> mice were continued to be monitored in order to rule out possible long term consequences of ITK-SYK activity on B cells. By doing so, quite unexpectedly, the ITK-SYK<sup>CD19-Cre</sup> mouse model complemented the observations gathered from the ITK-SYK<sup>CD4-Cre</sup> model, which does hold restrictions in its comparison to the human disease scenario. Firstly, since Cre expression is controlled by the CD4 promoter, deletion of the STOP cassette and subsequent ITK-SYK transcription occurs as early as in DP thymocytes. Hence, for the vast majority of T cells, the onset of ITK-SYK expression is not limited to the mature cell stage, as expected to be the case in human PTCL. Secondly, ITK-SYK expression is engaged in over 80% of all T cells present in ITK-SYK<sup>CD4-Cre</sup> mice. This is contrary to the human situation where the translocation is a rare event expected to affect a single or only a few T cells. Therefore, it was interesting to observe that ITK-SYK<sup>CD19-Cre</sup> mice eventually also developed a fatal form of PTCL. They showed a comparable phenotyp to ITK-SYK<sup>CD4-Cre</sup> mice, except for a prolonged latency. It is hypothesized that the rare event of sporadic CD19 promoter activity within T cells results in a Cre mediated deletion of the STOP cassette, allowing T cell specific ITK-SYK expression in ITK-SYK<sup>CD19-Cre</sup> mice. Analysis of TCRV $\beta$  chain distributions indicated that expanded T cells originated from a single or only a few T cell clones. Thus, sporadic ITK-SYK expression in single T cells drives PTCL development even in ITK-SYK<sup>CD19-Cre</sup> mice, emphasizing the oncogenic nature of the fusion kinase. As discussed for the ITK-SYK<sup>CD4-Cre</sup> model, secondary oncogenic events might also contribute to lymphoma development in ITK-SYK<sup>CD19-Cre</sup>. Whether ITK-SYK solely acts as tumor initiator, or whether clonal expansion and tumor maintenance still rely on ITK-SYK

activity is still a matter of investigation. First *in vivo* therapeutic approaches have been performed by Dierks et al. [48] in a bone marrow transplantation model. The authors observed a milder lymphoproliferative phenotype in recipient mice after treatment with the SYK inhibitor curcumin. In agreement, the ITK-SYK<sup>KD</sup> mutant did not lead to disease development at all. These data would support a scenario where not only disease initiation but also disease development is at least partially dependent on ITK-SYK kinase activity. Thus, blocking of SYK enzymatic activity might prove to be a successful therapeutic approach. The orally available SYK inhibitor R788 has already been investigated in clinical trials for inflammatory autoimmune [196] and malignant diseases, such as B cell NHL [58]. Currently, R788 is also under evaluation for treatment of refractory or relapse PTCL (NIH, unpublished data).

# Chapter 7

## Summary and Outlook

Aberrant tyrosine kinase activity is known to be related to tumor development [17]. Often enzymatic deregulation is a result of irregular chromosomal recombination, leading to the generation of chimeric fusion tyrosine kinases [124]. The identification of recurrent translocation events and the molecular understanding of new gene products has been especially valuable in understanding the pathogenesis of hematopoietic malignancies [157]. Even if restricted to a limited number of cases, translocations may point to a more commonly applied mechanism causing cell transformation. Recently, the translocation  $t(5;9)(q33;q22)$  was identified as the first recurrent event in a subgroup of PTCL-NOS [178]. The translocation affects the gene loci of two non receptor tyrosine kinases, SYK and ITK, leading to the expression of the fusion kinase ITK-SYK. Due to the aggressiveness of PTCL and its dismal treatment options, insights into tumor promoting events are needed.

To investigate *in vivo* consequences of ITK-SYK expression in a cell type specific manner, and to clarify its oncogenic potential in PTCL development, conditional gene targeting of the ROSA26 locus has been employed. In combination with *in vitro* analysis, it was shown that ITK-SYK constitutively activates signaling pathways which are regularly engaged upon TCR stimulation. Phosphorylation of key TCR signaling molecules such as LAT, SLP-76, and PLC $\gamma$ 1 were observed. Additional activation of AKT, as well as the MAPK proteins p38 and ERK1/2 was seen. *In vitro* ITK-SYK expression resulted in IL-2 production and CD69 expression, both being classical signs of early T cell activation. Notably, ITK-SYK was constitutively recruited into T cell lipid rafts. A general enrichment of tyrosine phosphorylated raft proteins was also observed. Since ITK-SYK structurally lacks dimerization domains to mediate self activation, constitutive membrane association could present a common activation strategy for a new set of fusion tyrosine kinases. Indeed, mutational *in vitro* analysis demonstrated that ITK-SYK induced T cell activation is dependent on PH domain mediated membrane recruitment as well as on its functional kinase activity. However, since a contradictory role of ITK-SYK membrane localisation has been ascertained in bone marrow transplantation experiments [48], the

inconsistency with the here presented *in vitro* data necessitates further investigation.

In order to answer the question whether ITK-SYK can also drive T cell transformation, longterm *in vivo* investigations were performed. Indeed, ITK-SYK<sup>CD4-Cre</sup> mice developed highly malignant PTCLs with 100% penetrance. Flow cytometric as well as histological analysis confirmed expansion of neoplastic T cells, and showed their aggressive nature. Infiltrations were detected in all analyzed organs, lymphoid as well as non lymphoid. Finally, clonally expanded T cells were transplantable, and induced a similar disease phenotype in recipient mice. Together, the described clinical and pathological features of ITK-SYK<sup>CD4-Cre</sup> mice were reminiscent of human PTCL [38]. Interestingly, ITK-SYK selectively activated T cells, yet not B cells as was observed in ITK-SYK<sup>CD19-Cre</sup>. Different outcomes may originate from ITK-SYK being constitutively recruited into lipid rafts of T cells but not B cells. The reason for this behavior, however, is still unknown. Even if ITK-SYK<sup>CD19-Cre</sup> mice did not show a B cell phenotype, it was observed that sporadic ITK-SYK expression in single T cells, eventually also led to the development of fatal PTCL in these mice. This observation presumably stems from rare CD19 promoter activity occurring in few T cells. Cre expression results in the deletion of the STOP cassette, ITK-SYK expressing T cells expand and cause PTCL to occur. Thus, the ITK-SYK<sup>CD19-Cre</sup> model strongly supports that ITK-SYK can drive T cell oncogenesis. The fact that ITK-SYK<sup>CD4-Cre</sup> as well as ITK-SYK<sup>CD19-Cre</sup> mice showed clonal T cell outgrowth, suggests that in both models cooperating events contribute to the proliferative advantage of ITK-SYK expressing T cells. Currently, it still remains a matter of investigation whether constitutive ITK-SYK signaling is predominantly responsible for tumor initiation or whether it is also essential for disease maintenance. The aspect of so-called oncogene addiction [187] will have critical implications on the development of successful treatment strategies. Insights into this matter could be obtained by treating affected mice with the orally available SYK inhibitor R788, which has already shown potential in treating B cell malignancies [58] and rheumatoid arthritis [196].

Concludingly, the work at hand presents first conditional mouse models of ITK-SYK driven PTCL development and suggests that constitutively enforced AgR signals are in principle able to induce oncogenesis in an *in vivo* setting. Since aberrant AgR signaling is frequently observed in human lymphoid malignancies [98, 40], it will be interesting to see whether deregulated TCR signaling in general or abnormal SYK activity specifically is a common mechanism found in PTCL pathogenesis. Concerning later aspect, Feldman et al. [55] demonstrated that over 90% of analyzed PTCL-NOS cases showed SYK overexpression. Thus, while the translocation t(5;9)(33;22) affects a limited percentage of PTCL-NOS cases, aberrant SYK activity might indeed be a common driver in PTCL pathogenesis. Since ITK-SYK induces activation of various signaling components the here presented mouse models will be of use in understanding the role of individual signaling

molecules in ITK-SYK mediated oncogenesis. The question can be approached on a genetic basis by crossing ITK-SYK transgenic mice with knockout mouse strains deficient for the signaling molecule of interest. In combination with *in vivo* inhibitor experiments these investigations will be helpful in identifying signaling molecules or pathway showing the most potential as candidates for therapeutic intervention.

# Bibliography

- [1] Abraham, R.T. and Weiss, A., “Jurkat T Cells and Development of the T-Cell Receptor Signalling Paradigm,” *Nature Reviews Immunology*, Vol. 4, No. 4, 2004, pp. 301–308.
- [2] Acuto, O., Bartolo, V.D., and Michel, F., “Tailoring T-Cell Receptor Signals by Proximal Negative Feedback Mechanisms,” *Nature Reviews Immunology*, Vol. 8, No. 9, 2008, pp. 699–712.
- [3] Adachi, T., Wienands, J., Tsubata, T., and Kurosaki, T., “Interdomain A is Crucial for ITAM-Dependent and -Independent Regulation of Syk,” *Biochemical and Biophysical Research Communications*, Vol. 364, No. 1, 2007, pp. 111–117.
- [4] Aifantis, I., Buer, J., von Boehmer, H., and Azogui, O., “Essential Role of the Pre-T Cell Receptor in Allelic Exclusion of the T Cell Receptor  $\beta$  Locus,” *Immunity*, Vol. 7, No. 5, 1997, pp. 601–607.
- [5] Aifantis, I., Raetz, E., and Buonamici, S., “Molecular Pathogenesis of T-Cell Leukaemia and Lymphoma,” *Nature Reviews Immunology*, Vol. 8, No. 5, 2008, pp. 380–390.
- [6] Albritton, L.M., Tseng, L., Scadden, D., and Cunningham, J.M., “A Putative Murine Ecotropic Retrovirus Receptor Gene Encodes a Multiple Membrane-Spanning Protein and Confers Susceptibility to Virus Infection,” *Cell*, Vol. 57, No. 4, 1989, pp. 659–666.
- [7] Almire, C., Bertrand, P., Ruminy, P., Maingonnat, K., Wlodarska, I., Martin-Subero, J.I., Siebert, R., Tilly, H., and Bastard, C., “PVRL2 is Translocated to the TRA@ Locus in t(14;19)(q11;q13)-Positive Peripheral T-Cell Lymphomas,” *Genes, Chromosomes & Cancer*, Vol. 46, No. 11, 2007, pp. 1011–1018.
- [8] Andreotti, A.H., Schwartzberg, P.L., Joseph, R.E., and Berg, L.J., “T-Cell Signaling Regulated by the Tec Family Kinase, Itk,” *Cold Spring Harbor Perspectives in Biology*, Vol. 2, No. 7, 2010, pp. 1–21.

- [9] Arias-Palomo, E., Recuero-Checa, M.A., Bustelo, X.R., and Llorca, O., "3D Structure of Syk Kinase Determined by Single-Particle Electron Microscopy," *Biochimica et Biophysica Acta (BBA) - Proteins & Proteomics*, Vol. 1774, No. 12, 2007, pp. 1493–1499.
- [10] Asano, N., Suzuki, R., Kagami, Y., Ishida, F., Kitamura, K., Fukutani, H., Morishima, Y., Takeuchi, K., and Nakamura, S., "Clinicopathologic and Prognostic Significance of Cytotoxic Molecule Expression in Nodal Peripheral T-Cell Lymphoma, Unspecified," *The American Journal of Surgical Pathology*, Vol. 29, No. 10, 2005, pp. 1284–1293.
- [11] Au-Yeung B.B., Deindl, S., Hsu, L.-Y., Palacios, E.H., Levin, S.E., Kuriyan, J., and Weiss, A., "The Structure, Regulation, and Function of ZAP-70," *Immunological Reviews*, Vol. 228, No. 1, 2009, pp. 41–57.
- [12] August, A., Sadra, A., Dupont, B., and Hanafusa, H., "Src-Induced Activation of Inducible T Cell Kinase (ITK) Requires Phosphatidylinositol 3-Kinase Activity and the Pleckstrin Homology Domain of Inducible T Cell Kinase," *Proceedings of the National Academy of Sciences of the United States of America (PNAS)*, Vol. 94, No. 21, 1997, pp. 11227–11232.
- [13] Ballester, B., Ramuz, O., Gisselbrecht, C., Doucet, G., Loi, L., Llorca, B., Bertucci, F., Bouabdallah, R., Devillard, E., Carbuccia, N., Mozziconacci, M.J., Birnbaum, D., Brousset, P., Berger, F., Salles, G., Briere, J., Houlgatte, R., Gaulard, P., and Xerri, L., "Gene Expression Profiling Identifies Molecular Subgroups among Nodal Peripheral T-Cell Lymphomas," *Oncogene*, Vol. 25, No. 10, 2006, pp. 1560–1570.
- [14] Bar-Nun, S., Shneyour, Y., and Beckmann, J.S., "G-418, an Elongation Inhibitor of 80S Ribosomes," *Biochimica et Biophysica Acta (BBA) - Gene Structure and Expression*, Vol. 741, No. 1, 1983, pp. 123–127.
- [15] Beck, E., Ludwig, G., Auerswald, A.E., Reiss, B., and Schaller, H., "Nucleotide Sequence and Exact Localization of the Neomycin Phosphotransferase Gene from Transposon Tn5," *Gene*, Vol. 19, No. 3, 1982, pp. 327–336.
- [16] Blonska, M., Pappu, B.P., Matsumoto, R., Li, H., Su, B., Wang, D., and Lin, X., "The CARMA1-Bcl10 Signaling Complex Selectively Regulates JNK2 Kinase in the T Cell Receptor-Signaling Pathway," *Immunity*, Vol. 26, No. 1, 2007, pp. 55–66.
- [17] Blume-Jensen, P. and Hunter, T., "Oncogenic Kinase Signalling," *Nature*, Vol. 411, No. 6835, 2001, pp. 355–365.

- [18] Bogin, Y., Ainey, C., Beach, D., and Yablonski, D., "SLP-76 Mediates and Maintains Activation of the Tec Family Kinase ITK via the T Cell Antigen Receptor-Induced Association between SLP-76 and ITK," *Proceedings of the National Academy of Sciences of the United States of America (PNAS)*, Vol. 104, No. 16, 2007, pp. 6638–6643.
- [19] Boomer, J.S. and Green, J.M., "An Enigmatic Tail of CD28 Signaling," *Cold Spring Harbor Perspectives in Biology*, Vol. 2, No. 8, 2010, pp. 1–20.
- [20] Boussiotis, V.A., Freeman, G.J., Gribben, J.G., Daley, J., Gray, G., and Nadler, L.M., "Activated Human B Lymphocytes Express Three CTLA-4 Counterreceptors that Costimulate T-Cell Activation," *Proceedings of the National Academy of Sciences of the United States of America (PNAS)*, Vol. 90, No. 23, 1993, pp. 11059–11063.
- [21] Bradford, M.M., "A Rapid and Sensitive Method for the Quantitation of Microgram Quantities of Protein Utilizing the Principle of Protein-Dye Binding," *Analytical Biochemistry*, Vol. 72, No. 1-2, 1976, pp. 248–254.
- [22] Bradshaw, J.M., "The Src, Syk, and Tec family kinases: Distinct Types of Molecular Switches," *Cellular Signalling*, Vol. 22, No. 8, 2010, pp. 1175–1184.
- [23] Braiman, A., Barda-Saad, M., Sommers, C.L., and Samelson, L.E., "Recruitment and Activation of PLC $\gamma$ 1 in T Cells: A New Insight into Old Domains," *The EMBO Journal*, Vol. 25, No. 4, 2006, pp. 774–784.
- [24] Braselmann, S., Taylor, V., Zhao, H., Samelson, L.E., Wang, S., Sylvain, C., and Baluom, M., "R406, an Orally Available Spleen Tyrosine Kinase Inhibitor Blocks Fc Receptor Signaling and Reduces Immune Complex-Mediated Inflammation," *Journal of Pharmacology and Experimental Therapeutics*, Vol. 319, No. 3, 2006, pp. 998–1008.
- [25] Brown, D.A. and Rose, J.K., "Sorting of GPI-Anchored Proteins to Glycolipid-Enriched Membrane Subdomains during Transport to the Apical Cell Surface," *Cell*, Vol. 68, No. 3, 1992, pp. 533–544.
- [26] Bu, J.Y., Shaw, A.S., and Chan, A.C., "Analysis of the Interaction of ZAP-70 and Syk Protein-Tyrosine Kinases with the T-Cell Antigen Receptor by Plasmon Resonance," *Proceedings of the National Academy of Sciences*, Vol. 92, No. 11, 1995, pp. 5106–5110.
- [27] Budd, R.C., Cerottini, J.C., Horvath, C., Bron, C., Pedrazzini, T., Howe, R.C., and MacDonald, H.R., "Distinction of Virgin and Memory T Lymphocytes. Stable

- Acquisition of the Pgp-1 Glycoprotein Concomitant with Antigenic Stimulation," *The Journal of Immunology*, Vol. 138, No. 10, 1987, pp. 3120–3129.
- [28] Bunnell, S.C., Diehn, M., Yaffe, M.B., Findell, P.R., Cantley, L.C., and Berg, L.J., "Biochemical Interactions Integrating Itk with the T Cell Receptor-Initiated Signaling Cascade," *The Journal of Biological Chemistry*, Vol. 275, No. 3, 2000, pp. 2219–2230.
- [29] Burnette, N.V., "Western Blotting: Electrophoretic Transfer of Proteins from Sodium Dodecyl Sulfate-Polyacrylamide Gels to Unmodified Nitrocellulose and Radiographic Detection with Antibody and Radioiodinated Protein A," *Analytical Biochemistry*, Vol. 112, No. 2, 1981, pp. 195–203.
- [30] Cantrell, D.A. and Smith, K.A., "The Interleukin-2 T-Cell System: A New Cell Growth Model," *Science*, Vol. 224, No. 4655, 1984, pp. 1312–1316.
- [31] Carpenter, A.C. and Bosselut, R., "Decision Checkpoints in the Thymus," *Nature Immunology*, Vol. 11, No. 8, 2010, pp. 666–673.
- [32] Chalet, L. and Wolf, F.J., "The Properties of Steptavidin, a Biotin-Binding Protein Produced by *Streptomyces*," *Archives of Biochemistry and Biophysics*, Vol. 106, No. 0, 1964, pp. 1–5.
- [33] Cheng, A.M., Rowley, B., Pao, W., Hayday, A., Bolen, J.B., and Pawson, T., "Syk Tyrosine Kinase Required for Mouse Viability and B-Cell Development," *Nature*, Vol. 378, No. 6554, 1995, pp. 303–306.
- [34] Chu, D.H., Spits, H., Peyron, J.F., Rowley, R.B., Bolen, J.B., and Weiss, A., "The Syk Protein Tyrosine Kinase can Function Independently of CD45 or Lck in T Cell Antigen Receptor Signaling," *The EMBO Journal*, Vol. 15, No. 22, 1996, pp. 6251–6261.
- [35] Coffin, J.M., Hughes, S.H., and Varmus, H.E., *Retroviruses*, Cold Spring Harbor Laboratory Press, Cold Spring Harbor (NY), USA, 1997.
- [36] Colbère-Garapin, F., Horodniceanu, F., Kourilsky, P., and Garapin, A.C., "A New Dominant Hybrid Selective Marker for Higher Eukaryotic Cells," *Journal of Molecular Biology*, Vol. 150, No. 1, 1981, pp. 1–14.
- [37] Cornall, R.J., Cheng, A.M., Pawson, T., and Goodnow, C.C., "Role of Syk in B-Cell Development and Antigen-Receptor Signaling," *Proceedings of the National Academy of Sciences of the United States of America (PNAS)*, Vol. 97, No. 4, 2000, pp. 1713–1718.

- [38] Cotta, C.V. and Hsi, E.D., "Pathobiology of Mature T-Cell Lymphomas," *Clinical Lymphoma and Myeloma*, Vol. 8, No. Suppl. 5, 2008, pp. S168–S179.
- [39] Davis, H.E., Morgan, J.R., and Yarmush, M.L., "Polybrene Increases Retrovirus Gene Transfer Efficiency by Enhancing Receptor-Independent Virus Adsorption on Target Cell Membranes," *Biophysical Chemistry*, Vol. 97, No. 2-3, 2002, pp. 159–172.
- [40] Davis, R.E., Ngo, V.N., Lenz, G., Tolar, P., Young, R.M., Romesser, P.B., Kohlhammer, H., Lamy, L., Zhao, H., Yang, Y., Xu, W., Shaffer, A.L., Wright, G., Xiao, W., Powell, J., Jiang, J.-k., Thomas, C.J., Rosenwald, A., Ott, G., Muller-Hermelink, H.K., Gascoyne, R.D., Connors, J.M., Johnson, N.A., Rimsza, L.M., Campo, E., Jaffe, E.S., Wilson, W.H., Delabie, J., Smeland, E.B., Fisher, R.I., Braziel, R.M., Tubbs, R.R., Cook, J. R., Weisenburger, D.D., Chan, W.C., Pierce, S.K., and Staudt, L.M., "Chronic Active B-Cell-Receptor Signaling in Diffuse Large B-Cell Lymphoma," *Nature*, Vol. 463, No. 7277, 2010, pp. 88–92.
- [41] De Grendele, H.C., Kosfiszter, M., Estess, P., and Siegelman, M.H., "CD44 Activation and Associated Primary Adhesion is Inducible via T Cell Receptor Stimulation," *The Journal of Immunology*, Vol. 159, No. 6, 1997, pp. 2549–2553.
- [42] De Klein, A., van Kessel, A.G., Grosveld, G., Bartram, C.R., Hagemeijer, A., Bootsma, D., Spurr, N.K., Heisterkamp, N., Groffen, J., and Stephenson, J.R., "A Cellular Oncogene is Translocated to the Philadelphia Chromosome in Chronic Myelocytic Leukaemia," *Nature*, Vol. 300, No. 5894, 1982, pp. 765–767.
- [43] De Leval, L., Bisig, B., Thielen, C., Boniver, J., and Gaulard, P., "Molecular Classification of T-Cell Lymphomas," *Critical Reviews in Oncology/Hematology*, Vol. 72, No. 2, 2009, pp. 125–143.
- [44] De Leval, L. and Gaulard, P., "Pathology and Biology of Peripheral T-Cell Lymphomas," *Histopathology*, Vol. 58, No. 1, 2011, pp. 49–68.
- [45] Deckert, M., Tartare-Deckert, S., Couture, C., Mustelin, T., and Altman, A., "Functional and Physical Interactions of Syk Family Kinases with the Vav Proto-Oncogene Product," *Immunity*, Vol. 5, No. 6, 1996, pp. 591–604.
- [46] Deindl, S., Kadlecsek, T.A., Brdicka, T., Cao, X., Weiss, A., and Kuriyan, J., "Structural Basis for the Inhibition of Tyrosine Kinase Activity of ZAP-70," *Cell*, Vol. 129, No. 4, 2007, pp. 735–746.

- [47] Dhein, J., Walczak, H., Baumler, C., Debatin, K.M., and Krammer, P.H., “Autocrine T-Cell Suicide Mediated by APO-1/(Fas/CD95),” *Nature*, Vol. 373, No. 6513, 1995, pp. 438–441.
- [48] Dierks, C., Adrian, F., Fisch, P., Ma, H., Maurer, H., Herchenbach, D., Forster, C.U., Sprissler, C., Liu, G., Rottmann, S., Guo, G.-R., Katja, Z., Veelken, H., and Warmuth, M., “The ITK-SYK Fusion Oncogene Induces a T-Cell Lymphoproliferative Disease in Mice Mimicking Human Disease,” *Cancer Research*, Vol. 70, No. 15, 2010, pp. 6193–6204.
- [49] Dombroski, D., Houghtling, R.A., Labno, C.M., Precht, P., Takesono, A., Caplen, N.J., Billadeau, D.D., Wange, R.L., Burkhardt, J.K., and Schwartzberg, P.L., “Kinase-Independent Functions for Itk in TCR-Induced Regulation of Vav and the Actin Cytoskeleton,” *The Journal of Immunology*, Vol. 174, No. 3, 2005, pp. 1385–1392.
- [50] Drevot, P., Langlet, C., Guo, X.-J., Bernard, A.-M., Colard, O., Chauvin, J.-P., Lasserre, R., and He, H.-T., “TCR Signal Initiation Machinery is pre-Assembled and Activated in a Subset of Membrane Rafts,” *The EMBO Journal*, Vol. 21, No. 8, 2002, pp. 1899–1908.
- [51] Dustin, M.L. and Depoil, D., “New Insights into the T Cell Synapse from Single Molecule Techniques,” *Nature Reviews Immunology*, Vol. 11, No. 10, 2011, pp. 672–684.
- [52] Eisinger, J. and Shulman, R.G., “Excited Electronic States of DNA,” *Science*, Vol. 161, No. 3848, 1968, pp. 1311–1319.
- [53] Engels, N., Engelke, M., and Wienands, J., “Conformational Plasticity and Navigation of Signaling Proteins in Antigen-Activated B Lymphocytes,” Vol. 97 of *Advances in Immunology*, Academic Press, x, 2008, pp. 251–281.  
doi:10.1016/S0065-2776(08)00005-9
- [54] Feldman, A.L., Law, M., Remstein, E.D., Macon, W.R., Erickson, L.A., Grogg, K.L., Kurtin, P.J., and Dogan, A., “Recurrent Translocations Involving the IRF4 Oncogene Locus in Peripheral T-Cell Lymphomas,” *Leukemia*, Vol. 23, No. 3, 2009, pp. 574–580.
- [55] Feldman, A.L., Sun, D.X., Law, M.E., Novak, A.J., Attygalle, A.D., Thorland, E.C., Fink, S.R., Vrana, J.A., Caron, B.L., Morice, W.G., Remstein, E.D., Grogg, K.L., Kurtin, P.J., Macon, W.R., and Dogan, A., “Overexpression of Syk Tyrosine Kinase in Peripheral T-Cell Lymphomas,” *Leukemia*, Vol. 22, No. 6, 2008, pp. 1139–1143.

- [56] Flanagan, S.P., “‘Nude’, a New Hairless Gene with Pleiotropic Effects in the Mouse,” *Genetical Research*, Vol. 8, No. 3, 1966, pp. 295–309.
- [57] Foss, F.M., Zinzani, P.L., Vose, J.M., Gascoyne, R.D., Rosen, S.T., and Tobinal, K., “Peripheral T-Cell Lymphoma,” *Blood*, Vol. 117, No. 25, 2011, pp. 6756–6767.
- [58] Friedberg, J.W., Sharman, J., Sweetenham, J., Johnston, P.B., Vose, J.M., LaCasce, A., Schaefer-Cuttillo, J., De Vos, S., Sinha, R., Leonard, J.P., Cripe, L.D., Gregory, S.A., Sterba, M.P., Lowe, A.M., Levy, R., and Shipp, M.A., “Inhibition of Syk with Fostamatinib Disodium has Significant Clinical Activity in Non-Hodgkin Lymphoma and Chronic Lymphocytic Leukemia,” *Blood*, Vol. 115, No. 13, 2010, pp. 2578–2585.
- [59] Friedrich, G. and Soriano, P., “Promoter Traps in Embryonic Stem Cells: A Genetic Screen to Identify and Mutate Developmental Genes in Mice,” *Genes & Development*, Vol. 5, No. 9, 1991, pp. 1513–1523.
- [60] Fu, C., Turck, C.W., Kurosaki, T., and Chan, A.C., “BLNK: a Central Linker Protein in B Cell Activation,” *Immunity*, Vol. 9, No. 1, 1998, pp. 93–103.
- [61] Fuetterer, K., Wong, J., Grucza, R.A., Chan, A.C., and Waksman, G., “Structural Basis for Syk Tyrosine Kinase Ubiquity in Signal Transduction Pathways Revealed by the Crystal Structure of its Regulatory SH2 Domains Bound to a Dually Phosphorylated ITAM Peptide,” *Journal of Molecular Biology*, Vol. 281, No. 3, 1998, pp. 523–537.
- [62] Fuller, W. and Waring, M.J., “A Molecular Model for the Interaction of Ethidium Bromide with Deoxyribonucleic Acid,” *Berichte der Bunsengesellschaft für physikalische Chemie*, Vol. 68, No. 8-9, 1964, pp. 805–808.
- [63] Furlong, M.T., Mahrenholz, A.M., Kim, K.H., Ashendel C.L., Harrison M.L., and Geahlen, R.L., “Identification of the Major Sites of Autophosphorylation of the Murine Protein-Tyrosine Kinase Syk,” *Biochimica et Biophysica Acta (BBA) - Molecular Cell Research*, Vol. 1355, No. 2, 1997, pp. 177–190.
- [64] Gaertner, F., Alt, F.W., Monroe, R., Chu, M., Sleckman, B.P., Davidson, L., and Swat, W., “Immature Thymocytes Employ Distinct Signaling Pathways for Allelic Exclusion versus Differentiation and Expansion,” *Immunity*, Vol. 10, No. 5, 1999, pp. 537–546.
- [65] Gauld, S.B., Dal Porto, J.M., and Cambier, J.C., “B Cell Antigen Receptor Signaling: Roles in Cell Development and Disease,” *Science*, Vol. 296, No. 5573, 2002, pp. 1641–1642.

- [66] Geissinger, E., Bonzheim, I., Roth, S., Rosenwald, A., Mueller-Hermelink, H.K., and Ruedinger, T., "CD52 Expression in Peripheral T-Cell Lymphomas Determined by Combined Immunophenotyping Using Tumor Cell Specific T-Cell Receptor Antibodies," *Leukemia&Lymphoma*, Vol. 50, No. 6, 2009, pp. 1010–1016.
- [67] Gille, H., Kortenjann, M., Thomae, O., Moomaw, C., Slaughter, C., Cobb, M.H., and Shaw, P.E., "ERK Phosphorylation Potentiates Elk-1-Mediated Ternary Complex Formation and Transactivation," *The EMBO Journal*, Vol. 14, No. 5, 1995, pp. 951–962.
- [68] Golde, W.T., Gollobin, P., and Rodriguez, L.L., "A Rapid, Simple, and Humane Method for Submandibular Bleeding of Mice Using a Lancet," *Lab Animal*, Vol. 34, No. 9, 2005, pp. 39–43.
- [69] Graham, F.L. and van der Eb, A.J., "A New Technique for the Assay of Infectivity of Human Adenovirus 5 DNA," *Virology*, Vol. 52, No. 2, 1973, pp. 456–467.
- [70] Greenwald, R.J., Freeman, G.J., and Sharpe, A.H., "The B7 Family Revisited," *Annual Review of Immunology*, Vol. 23, No. 1, 2005, pp. 515–548.
- [71] Groesch, T.D., Zhou, F., Mattila, S., Geahlen, R.L., and Post, C.B., "Structural Basis for the Requirement of Two Phosphotyrosine Residues in Signaling Mediated by Syk Tyrosine Kinase," *Journal of Molecular Biology*, Vol. 356, No. 5, 2006, pp. 1222–1236.
- [72] Gu, H., Zou, Y.R., and Rajewsky, K., "Independent Control of Immunoglobulin Switch Recombination at Individual Switch Regions Evidenced Through Cre-loxP-Mediated Gene Targeting," *Cell*, Vol. 73, No. 6, 1993, pp. 1155–1164.
- [73] Hamann, J., Fiebig, H., and Strauss, M., "Expression Cloning of the Early Activation Antigen CD69, a Type II Integral Membrane Protein with a C-Type Lectin Domain," *The Journal of Immunology*, Vol. 150, No. 11, 1993, pp. 4920–4927.
- [74] Hara, T., Jung, L.K.L., Bjorndahl, J.M., and Fu, S.M., "Human T Cell Activation. III. Rapid Induction of a Phosphorylated 28 kD/32 kD Disulfide-Linked Early Activation Antigen (EA 1) by 12-o-Tetradecanoyl Phorbol-13-Acetate, Mitogens, and Antigens," *Journal of Experimental Medicine*, Vol. 164, No. 6, 1986, pp. 1988–2005.
- [75] Heyeck, S.D., Wilcox, H.M., Bunnell, S.C., and Berg, L.J., "Lck Phosphorylates the Activation Loop Tyrosine of the Itk Kinase Domain and Activates Itk Kinase Activity," *Journal of Biological Chemistry*, Vol. 272, No. 40, 1997, pp. 25401–25408.

- [76] Hitoshi, Y., Lorens, J., Kitada, S., Fisher, J., LaBarge, M., Ring, H.Z., Francke, U., Reed, J.C., Kinoshita, S., and Nolan, G.P., "Toso, a Cell Surface, Specific Regulator of Fas-Induced Apoptosis in T Cells," *Immunity*, Vol. 8, No. 4, 1998, pp. 461–471.
- [77] Hornstein, I., Alcover, A., and Katzav, S., "Vav Proteins, Masters of the World of Cytoskeleton Organization," *Cellular Signalling*, Vol. 16, No. 1, 2004, pp. 1–11.
- [78] Houtman, J.C.D., Houghtling, R.A., Barda-Saad, M., Toda, Y., and Samelson, L.E., "Early Phosphorylation Kinetics of Proteins Involved in Proximal TCR-Mediated Signaling Pathways," *The Journal of Immunology*, Vol. 175, No. 4, 2005, pp. 2449–2458.
- [79] Howman, R.A. and Prince, H.M., "New Drug Therapies in Peripheral T Cell Lymphoma," *Expert Reviews Anticancer Therapy*, Vol. 11, No. 3, 2011, pp. 457–472.
- [80] Huang, Y.H., Grasis, J.A., Miller, A.T., Xu, R., Soonthornvacharin, S., Andreotti, A.H., Tsoukas, C.D., Cooke, M.P., and Sauer, K., "Positive Regulation of Itk PH Domain Function by Soluble IP4," *Science*, Vol. 316, No. 5826, 2007, pp. 886–889.
- [81] Huck, K., Feyen, O., Niehues, T., Rueschendorf, F., Huebner, N., Laws, H.J., Telieps, T., Knapp, S., Wacker, H.H., Meindl, A., Jumaa, H., and Borkhardt, A., "Girls Homozygous for an IL-2Inducible T Cell Kinase Mutation that Leads to Protein Deficiency Develop Fatal EBV-Associated Lymphoproliferation," *The Journal of Clinical Investigation*, Vol. 119, No. 5, 2009, pp. 1350–1358.
- [82] Hussain, A., Faryal, R., Nore, B.F., Mohamed, A.J., and Smith, C.I.E., "Phosphatidylinositol-3-Kinase-Dependent Phosphorylation of SLP-76 by the Lymphoma-Associated ITK-SYK Fusion-Protein," *Biochemical and Biophysical Research Communications*, Vol. 390, No. 3, 2009, pp. 892–896.
- [83] Iqbal, J., Weisenburger, D.D., Greiner, T.C., Vose, J.M., McKeithan, T., Kucuk, C., Geng, H., Deffenbacher, K., Smith, L., Dybkaer, K., Nakamura, S., Seto, M., Delabie, J., Berger, F., Loong, F., Au, W.Y., Ko, Y.H., Sng, I., Armitage, J.O., Chan, W.C., and for the International Peripheral T-Cell Lymphoma Project, "Molecular Signatures to Improve Diagnosis in Peripheral T-Cell Lymphoma and Prognostication in Angioimmunoblastic T-cell Lymphoma," *Blood*, Vol. 115, No. 5, 2010, pp. 1026–1036.
- [84] Jain, J., Burgeon, E., Badalian, T.M., Hogan, P.G., and Rao, A., "A Similar DNA-binding Motif in NFAT Family Proteins and the Rel Homology Region," *Journal of Biological Chemistry*, Vol. 270, No. 8, 1995, pp. 4138–4145.

- [85] Jern, P. and Coffin, J.M., “Effects of Retroviruses on Host Genome Function,” *Annual Review of Genetics*, Vol. 42, No. 1, 2008, pp. 709–732.
- [86] Jordan, M.S., Smith, J.E., Burns, J.C., Austin, J.E.T., Nichols, K.E., Aschenbrenner, A.C., and Koretzky, G.A., “Complementation in Trans of Altered Thymocyte Development in Mice Expressing Mutant Forms of the Adaptor Molecule SLP76,” *Immunity*, Vol. 28, No. 3, 2008, pp. 359–369.
- [87] Joseph, R.E. and Andreotti, A.H., “Conformational Snapshots of Tec Kinases during Signaling,” *Immunological Reviews*, Vol. 228, No. 1, 2009, pp. 74–92.
- [88] Joseph, R.E., Fulton, D.B., and Andreotti, A.H., “Mechanism and Functional Significance of Itk Autophosphorylation,” *Journal of Molecular Biology*, Vol. 373, No. 5, 2007, pp. 1281–292.
- [89] Kawamoto, H., Ikawa, T., Ohmura, K., Fujimoto, S., and Katsura, Y., “T Cell Progenitors Emerge Earlier than B Cell Progenitors in the Murine Fetal Liver,” *Immunity*, Vol. 12, No. 4, 2000, pp. 441–450.
- [90] Kenneth, M.P., *Janeway’s Immunobiology*, Garland Science, Taylor & Francis Group, LLC, New York (NY), USA, 2012.
- [91] Keshvara, L.M., Isaacson, C., Harrison, M.L., and Geahlen, R.L., “Syk Activation and Dissociation from the B-Cell Antigen Receptor Is Mediated by Phosphorylation of Tyrosine 130,” *Journal of Biological Chemistry*, Vol. 272, No. 16, 1997, pp. 10377–10381.
- [92] Kim, J.W., Closs, E.I., Albritton, L.M., and Cunningham, J.M., “Transport of Cationic Amino Acids by the Mouse Ecotropic Retrovirus Receptor,” *Nature*, Vol. 352, No. 6337, 1991, pp. 725–728.
- [93] Kneba, M., Bolz, I., Linke, B., and Hiddemann, W., “Analysis of Rearranged T-Cell Receptor Beta-Chain Genes by Polymerase Chain Reaction (PCR) DNA Sequencing and Automated High Resolution PCR Fragment Analysis,” *Blood*, Vol. 86, No. 10, 1995, pp. 3930–3937.
- [94] Kolanus, W., Romeo, C., and Seed, B., “T Cell Activation by Clustered Tyrosine Kinases,” *Cell*, Vol. 74, No. 1, 1993, pp. 171–183.
- [95] Koschmieder, S. and Schemionek, M., “Mouse Models as Tools to Understand and Study BCR-ABL1 Diseases,” *American Journal of Blood Research*, Vol. 1, No. 1, 2011, pp. 65–75.

- [96] Kozak, M., "Compilation and Analysis of Sequences Upstream From the Translational Start Site in Eukaryotic mRNAs," *Nucleic Acids Research*, Vol. 12, No. 2, 1984, pp. 857–872.
- [97] Krishnan, S., Warke, V.G., Nambiar, M.P., Tsokos, G.C., and Farber, D.L., "The FcR $\gamma$  Subunit and Syk Kinase Replace the CD3 $\zeta$ -Chain and ZAP-70 Kinase in the TCR Signaling Complex of Human Effector CD4 T Cells," *The Journal of Immunology*, Vol. 170, No. 8, 2003, pp. 4189–4195.
- [98] Kueppers, R., "Mechanisms of B-Cell Lymphoma Pathogenesis," *Nature Reviews Cancer*, Vol. 5, No. 4, 2005, pp. 251–262.
- [99] Kulathu, Y., Hobeika, E., Turchinovich, G., and Reth, M., "The Kinase Syk as an Adaptor Controlling Sustained Calcium Signalling and B-Cell Development," *The EMBO Journal*, Vol. 27, No. 9, 2008, pp. 1333–1344.
- [100] Kunder, S., Calzada-Wack, J., Hoelzlwimmer, G., Mueller, J., Kloss, C., Howat, W., Schmidt, J., Hoefler, H., Warren, M., and Quintanilla-Martinez, L., "A Comprehensive Antibody Panel for Immunohistochemical Analysis of Formalin-Fixed, Paraffin-Embedded Hematopoietic Neoplasms of Mice: Analysis of Mouse Specific and Human Antibodies Cross-Reactive with Murine Tissue," *Toxicologic Pathology*, Vol. 35, No. 3, 2007, pp. 366–375.
- [101] Kuno, Y., Abe, A., Emi, N., Iida, M., Yokozawa, T., Towatari, M., Tanimoto, M., and Saito, H., "Constitutive Kinase Activation of the TEL-Syk Fusion Gene in Myelodysplastic Syndrome with t(9;12)(q22;p12)," *Blood*, Vol. 97, No. 4, 2001, pp. 1050–1055.
- [102] Kurosaki, T. and Hikida, M., "Tyrosine Kinases and Their Substrates in B Lymphocytes," *Immunological Reviews*, Vol. 228, No. 1, 2009, pp. 132–148.
- [103] Kurosaki, T., Shinohara, H., and Baba, Y., "B Cell Signaling and Fate Decision," *Annual Review of Immunology*, Vol. 28, No. 1, 2010, pp. 21–55.
- [104] Laemmli, U.K., "Cleavage of Structural Proteins during the Assembly of the Head of Bacteriophage T4," *Nature*, Vol. 227, No. 5259, 1970, pp. 680–685.
- [105] Latour, S., Fournel, M., and Veillette, A., "Regulation of T-Cell Antigen Receptor Signalling by Syk Tyrosine Protein Kinase," *Molecular and Cellular Biology*, Vol. 17, No. 8, 1997, pp. 4434–4441.
- [106] Latour, S. and Veillette, A., "Proximal Protein Tyrosine Kinases in Immunoreceptor Signaling," *Current Opinion in Immunology*, Vol. 13, No. 3, 2001, pp. 299–306.

- [107] Law, C.L., Chandran, K.A., Sidorenko, S.P., and Clark, E.A., “Phospholipase C-gamma1 Interacts with Conserved Phosphotyrosyl Residues in the Linker Region of Syk and is a Substrate for Syk,” *Molecular and Cellular Biology*, Vol. 16, No. 4, 1996, pp. 1305–1315.
- [108] Lee, P.P., Fitzpatrick, D.R., Beard, C., Jessup, H.K., Lehar, S., Makar, K.W., Prez-Melgosa, M., Sweetser, M.T., Schlissel, M.S., Nguyen, S., Cherry, S.R., Tsai, J.H., Tucker, S.M., Weaver, W.M., Kelso, A., Jaenisch, R., and Wilson, C.B., “A Critical Role for Dnmt1 and DNA Methylation in T Cell Development, Function, and Survival,” *Immunity*, Vol. 15, No. 5, 2001, pp. 763–774.
- [109] Lemmon, M.A., “Membrane Recognition by Phospholipid-Binding Domains,” *Nature Reviews Molecular Cell Biology*, Vol. 9, No. 2, 2008, pp. 99–111.
- [110] Lemmon, M.A. and Schlessinger, J., “Cell Signaling by Receptor Tyrosine Kinases,” *Cell*, Vol. 141, No. 7, 2010, pp. 1117–1134.
- [111] Lenardo, M.J., “Interleukin-2 Programs Mouse  $\alpha\beta$  T lymphocytes for Apoptosis,” *Nature*, Vol. 353, No. 6347, 1991, pp. 858–861.
- [112] Liao, W., Lin, J.-X., and Leonard, W.J., “IL-2 Family Cytokines: New Insights Into the Complex Roles of IL-2 as a Broad Regulator of T Helper Cell Differentiation,” *Current Opinion in Immunology*, Vol. 23, No. 5, 2011, pp. 598–604.
- [113] Lingwood, D. and Simons, K., “Lipid Rafts As a Membrane-Organizing Principle,” *Science*, Vol. 327, No. 5961, 2010, pp. 46–50.
- [114] Liu, K.Q., Bunnell, S.C., Gurniak, C.B., and Berg, L.J., “T Cell Receptor-Initiated Calcium Release Is Uncoupled from Capacitative Calcium Entry in Itk-Deficient T Cells,” *The Journal of Experimental Medicine*, Vol. 187, No. 10, 1998, pp. 1721–1727.
- [115] Liu, S.K., Fang, N., Koretzky, G.A., and McGlade, C.J., “The Hematopoietic-Specific Adaptor Protein Gads Functions in T-Cell Signaling via Interactions with the SLP-76 and LAT Adaptors,” *Current Biology*, Vol. 9, No. 2, 1999, pp. 67–75.
- [116] Loken, M.R. and Herzenberg, L.A., “Analysis of Cell Populations with a Fluorescence-Activated Cell Sorter,” *Annals of the New York Academy of Sciences*, Vol. 254, No. 1, 1975, pp. 163–171.
- [117] Love, P.E. and Hayes, S.M., “ITAM-Mediated Signaling by the T-Cell Antigen Receptor,” *Cold Spring Harbor Perspectives in Biology*, Vol. 2, No. 6, 2010, pp. 1–11.

- [118] Lupher, M.L., Rao, N., Lill, N.L., Andoniou, C.E., Miyake, S., Clark, E.A., Druker, B., and Band, H., "Cbl-Mediated Negative Regulation of the Syk Tyrosine Kinase," *Journal of Biological Chemistry*, Vol. 273, No. 52, 1998, pp. 35273–35281.
- [119] Luthman, H. and Magnusson, G., "High Efficiency Polyoma DNA Transfection of Chloroquine Treated Cells," *Nucleic Acids Research*, Vol. 11, No. 5, 1983, pp. 1295–1308.
- [120] Mallis, R.J., Brazin, K.N., Fulton, D.B., and Andreotti, A.H., "Structural Characterization of a Proline-Driven Conformational Switch within the Itk SH2 Domain," *Nature Structural Biology*, Vol. 9, No. 12, 2002, pp. 900–905.
- [121] Martin-Subero, J.I., Wlodarska, I., Bastard, C., Picquenot, J-M., Hoepfner, J., Giefing, M., Klapper, W., and Siebert, R., "Chromosomal Rearrangements Involving the BCL3 Locus are Recurrent in Classical Hodgkin and Peripheral T-Cell Lymphoma," *Blood*, Vol. 108, No. 1, 2006, pp. 401–402.
- [122] Martinez-Delgado, B., Cuadros, M., Honrado, E., Ruiz de la Parte, A., Roncador, G., Alves, J., Castrillo, J.M., Rivas, C., and Benitez, J., "Differential Expression of NF- $\kappa$ B Pathway Genes among Peripheral T-Cell Lymphomas," *Leukemia*, Vol. 19, No. 12, 2005, pp. 2254–2263.
- [123] Matsumoto, R., Wang, D., Blonska, M., Li, H., Kobayashi, M., Pappu, B., Chen, Y., Wang, D., and Lin, X., "Phosphorylation of CARMA1 Plays a Critical Role in T Cell Receptor-Mediated NF- $\kappa$ B Activation," *Immunity*, Vol. 23, No. 6, 2005, pp. 575–585.
- [124] Medves, S. and Demoulin, J.-B., "Tyrosine Kinase Gene Fusions in Cancer: Translating Mechanisms into Targeted Therapies," *Journal of Cellular and Molecular Medicine*, Vol. 16, No. 2, 2012, pp. 237–248.
- [125] Melo, J.V., "The Diversity of BCR-ABL Fusion Proteins and their Relationship to Leukemia Phenotype," *Blood*, Vol. 88, No. 7, 1996, pp. 2375–2384.
- [126] Michie, A.M. and Zúñiga-Pfluecker, J.C, "Regulation of Thymocyte Differentiation: Pre-TCR Signals and  $\beta$ -Selection," *Seminars in Immunology*, Vol. 14, No. 5, 2002, pp. 311–323.
- [127] Miller, J.F.A.P., "The Golden Anniversary of the Thymus," *Nature Reviews Immunology*, Vol. 11, No. 7, 2005, pp. 489–495.
- [128] Mocsai, A, Ruland, J., and Tybulewicz, V. L. J., "The SYK Tyrosine Kinase: A Crucial Player in Diverse Biological Functions," *Nature Reviews Immunology*, Vol. 10, No. 6, 2010, pp. 387–402.

- [129] Mohamed, A.J., Yu, L., Bckesj, C.M., Vargas, L., Faryal, R., Aints, A., Christensson, B., Bergloef, A., Vihinen, M., Nore, B.F., and Smith, C.I.E, "Brutons Tyrosine Kinase (Btk): Function, Regulation, and Transformation with Special Emphasis on the PH Domain," *Immunological Reviews*, Vol. 228, No. 1, 2009, pp. 58–73.
- [130] Montixi, C., Langlet, C., Bernard, A.-M., Thimonier, J., Dubois, C., Wurbel, M.-A., Chauvin, J.-P., Pierres, M., and He, H.-T., "Engagement of T cell Receptor Triggers its Recruitment to Low-Density Detergent-Insoluble Membrane Domains," *The EMBO Journal*, Vol. 17, No. 18, 1998, pp. 5334–5348.
- [131] Moon, K.D., Post, C.B., Durden, D.L., Zhou, Q., De, P., Harrison, M.L., and Geahlen, R.L., "Molecular Basis for a Direct Interaction between the Syk Protein-Tyrosine Kinase and Phosphoinositide 3-Kinase," *Journal of Biological Chemistry*, Vol. 280, No. 2, 2005, pp. 1543–1551.
- [132] Mullis, K.B. and Faloona, A., "Specific Synthesis of DNA in Vitro via a Polymerase-Catalyzed Chain Reaction," *Methods in Enzymology*, Vol. 155, 1987, pp. 335–350.
- [133] Neumann, E. and Rosenheck, K., "Permeability Induced by Electric Impulses in Vesicular Membranes," *Journal of Membrane Biology*, Vol. 10, No. 1, 1972, pp. 279–290.
- [134] O'Connor, O.A., Horwitz, S., Hamlin, P., Portlock, C., Moskowitz, C.H., Sarasohn, D., Neylon, E., Mastrella, J., Hamelers, R., MacGregor-Cortelli, B., Patterson, M., Seshan, V.E., Sirotnak, F., Fleisher, M., Mould, D.R., Saunders, M., and Zelenetz, A.D., "Phase II-I-II Study of Two Different Doses and Schedules of Pralatrexate, a High-Affinity Substrate for the Reduced Folate Carrier, in Patients with Relapsed or Refractory Lymphoma Reveals Marked Activity in T-Cell Malignancies," *Journal of Clinical Oncology*, Vol. 27, No. 26, 2009, pp. 4357–4364.
- [135] Palacios, E.H. and Weiss, A., "Distinct Roles for Syk and ZAP-70 during Early Thymocyte Development," *The Journal of Experimental Medicine*, Vol. 204, No. 7, 2007, pp. 1703–1715.
- [136] Pantelouris, E.M., "Absence of Thymus in a Mouse Mutant," *Nature*, Vol. 217, No. 5126, 1968, pp. 370–371.
- [137] Pear, W.S., Miller, J.P., Xu, L., Pui, J.C., Soffer, B., Quackenbush, R.C., Pendergast, A.M., Bronson, R., Aster, J.C., Scott, M.L., and Baltimore, D., "Efficient and Rapid Induction of a Chronic Myelogenous Leukemia-Like Myeloproliferative Disease in Mice Receiving P210 bcr/abl-Transduced Bone Marrow," *Blood*, Vol. 92, No. 10, 1998, pp. 3780–3792.

- [138] Pertoft, H., Laurent, T.C., Ls, T., and Kgedal, L., “Density Gradients Prepared from Colloidal Silica Particles Coated by Polyvinylpyrrolidone (Percoll),” *Analytical Biochemistry*, Vol. 88, No. 1, 1978, pp. 271–282.
- [139] Piccaluga, P.P., Agostinelli, C., Califano, A., Rossi, M., Basso, K., Zupo, S., Went, P., Klein, U., Zinzani, P.L., Baccarani, M., Dalla Favera, R., and Pileri, S.A., “Gene Expression Analysis of Peripheral T Cell Lymphoma, Unspecified, Reveals Distinct Profiles and New Potential Therapeutic Targets,” *The Journal of Clinical Investigation*, Vol. 117, No. 3, 2007, pp. 823–834.
- [140] Porter, A.G. and Jaenicke, R.U., “Emerging Roles of Caspase-3 in Apoptosis,” *Cell Death and Differentiation*, Vol. 6, No. 2, 1999, pp. 99–104.
- [141] Putney, J.W., “Calcium Signaling: Deciphering the Calcium-NFAT Pathway,” *Current Biology*, Vol. 22, No. 3, 2012, pp. R87–R89.
- [142] Qi, Q., Sahu, N., and August, A., “Tec Kinase Itk Forms Membrane Clusters Specifically in the Vicinity of Recruiting Receptors,” *Journal of Biological Chemistry*, Vol. 281, No. 50, 2006, pp. 38529–38534.
- [143] Raffer, N.A., Rivera-Nieves, J., and Ley, K., “L-Selectin in Inflammation, Infection and Immunity,” *Drug Discovery Today: Therapeutic Strategies*, Vol. 2, No. 3, 2005, pp. 1740–6773.
- [144] Rassidakis, G.Z., Jones, D., Lai, R., Ramalingam, P., Sarris, A.H., McDonnell, T.J., and Medeiros, L.M., “BCL-2 Family Proteins in Peripheral T-Cell Lymphomas: Correlation with Tumour Apoptosis and Proliferation,” *The Journal of Pathology*, Vol. 200, No. 2, 2003, pp. 240–248.
- [145] Readinger, J.A., Mueller, K.L., Venegas, A.M., Horai, R., and Schwartzberg, P.L., “Tec Kinases Regulate T-Lymphocyte Development and Function: New Insights into the Roles of Itk and Rlk/Txk,” *Immunological Reviews*, Vol. 228, No. 1, 2009, pp. 93–114.
- [146] Reimer, P.C., “Impact of Autologous and Allogeneic Stem Cell Transplantation in Peripheral T-Cell Lymphomas,” *Advances in Hematology*, Vol. 2010, No. x, 2010, pp. 1–12.
- [147] Reth, M., “Antigen Receptor Tail Clue,” *Nature*, Vol. 338, No. 6214, 1989, pp. 383–384.
- [148] Rhee, I. and Vielle, A., “Protein Tyrosine Phosphatases in Lymphocyte Activation and Autoimmunity,” *Nature Immunology*, Vol. 13, No. 5, 2012, pp. 439–447.

- [149] Rhee, S.G., "Regulation of Phosphoinositide-Specific Phospholipase C\*," *Annual Review of Biochemistry*, Vol. 70, No. 1, 2001, pp. 281–312.
- [150] Rickert, R.C., Roes, J., and Rajewsky, K., "B Lymphocyte-Specific, Cre-Mediated Mutagenesis in Mice," *Nucleic Acids Research*, Vol. 25, No. 6, 1997, pp. 1317–1318.
- [151] Rigby, S., Huang, Y., Streubel, B., Chott, A., Du, M.Q., Turner, S.D., and Bacon, C.M., "The Lymphoma-Associated Fusion Tyrosine Kinase ITK-SYK Requires Pleckstrin Homology Domain-Mediated Membrane Localization for Activation and Cellular Transformation," *The Journal of Biological Chemistry*, Vol. 284, No. 36, 2009, pp. 26871–26881.
- [152] Rochman, Y., Spolski, R., and Leonard, W.J., "New Insights Into the Regulation of T Cells by  $\gamma$ c Family Cytokines," *Nature Reviews Immunology*, Vol. 9, No. 7, 2009, pp. 480–490.
- [153] Rodgers, W. and Rose, J.K., "Exclusion of CD45 Inhibits Activity of p56lck Associated with Glycolipid-Enriched Membrane Domains," *The Journal of Cell Biology*, Vol. 135, No. 6, 1996, pp. 1515–1523.
- [154] Rodriguez-Abreu, D., Filho, B.V., and Zucca, E., "Peripheral T-Cell Lymphomas, Unspecified (or Not Otherwise Specified): A Review," *Hematological Oncology*, Vol. 26, No. 1, 2007, pp. 8–20.
- [155] Rolli, V., Gallwitz, M., Wossning, T., Flemming, A., Schamel, W.W.A., Zuern, C., and Reth, M., "Amplification of B Cell Antigen Receptor Signaling by a Syk/ITAM Positive Feedback Loop," *Molecular Cell*, Vol. 10, No. 5, 2002, pp. 1057–1069.
- [156] Rowley, J.D., "A New Consistent Chromosomal Abnormality in Chronic Myelogenous Leukaemia Identified by Quinacrine Fluorescence and Giemsa Staining," *Nature*, Vol. 243, No. 5405, 1973, pp. 290–293.
- [157] Rowley, J.D., "Chromosome Translocations: Dangerous Liaisons Revisited," *Nature Reviews Cancer*, Vol. 1, No. 3, 2001, pp. 245–250.
- [158] Salvador, J.M., Mittelstadt, P.R., Guszczynski, T., Copeland, T.D., Yamaguchi, H., Appella, E., Fornace, A.J., and Ashwell, J.D., "Alternative p38 Activation Pathway Mediated by T Cell Receptor-Proximal Tyrosine Kinases," *Nature Immunology*, Vol. 6, No. 4, 2005, pp. 390–395.
- [159] Sambrook, J. and Russell D.W., *Molecular Cloning, 3rd Edition*, Cold Spring Harbor Laboratory Press, Cold Spring Harbor (NY), USA, 2001.

- [160] Sasaki, Y., Derudder, E., Hobeika, E., Pelanda, R., Reth, M., Rajewsky, K., and Schmidt-Supprian, M., "Canonical NF- $\kappa$ B Activity, Dispensable for B Cell Development, Replaces BAFF-Receptor Signals and Promotes B Cell Proliferation upon Activation," *Immunity*, Vol. 24, No. 6, 2006, pp. 729–739.
- [161] Sato, S., Steeber, D.A., Jansen, P.J., and Tedder, T.F., "CD19 Expression Levels Regulate B Lymphocyte Development: Human CD19 Restores Normal Function in Mice Lacking Endogenous CD19," *The Journal of Immunology*, Vol. 158, No. 10, 1997, pp. 4662–4669.
- [162] Savage, K., "Peripheral T-Cell Lymphomas," *Blood Reviews*, Vol. 21, No. 4, 2007, pp. 201–216.
- [163] Savage, K., Ferreri, A.J.M., Zinzani, P.L., and Pileri, S.A., "Peripheral T Cell Lymphoma-Not Otherwise Specified," *Critical Reviews in Oncology/Hematology*, Vol. 79, No. 3, 2010, pp. 321–329.
- [164] Scholzen, T. and Gerdes, J., "The Ki-67 Protein: From the Known and the Unknown," *Journal of Cellular Physiology*, Vol. 182, No. 3, 2000, pp. 311–322.
- [165] Schweneker, M., Favre, D., Martin, J.N., Deeks, S.G., and McCune, J.M., "HIV-Induced Changes in T Cell Signaling Pathways," *The Journal of Immunology*, Vol. 180, No. 10, 2008, pp. 6490–6500.
- [166] Shan, X. and Czar, M.J. and Bunnell, S.C. and Liu, P. and Liu, Y. and Schwartzberg, P.L. and Wange, R.L., "Deficiency of PTEN in Jurkat T Cells Causes Constitutive Localization of Itk to the Plasma Membrane and Hyperresponsiveness to CD3 Stimulation," *Molecular and Cellular Biology*, Vol. 20, No. 18, 2000, pp. 6945–6957.
- [167] Shaulian, E. and Karin, M., "AP-1 as a Regulator of Cell Life and Death," *Nature Cell Biology*, Vol. 4, No. 5, 2002, pp. E131–E136.
- [168] Simons, K. and Toomre, D., "Lipid Rafts and Signal Transduction," *Nature Reviews Molecular Cell Biology*, Vol. 1, No. 1, 2000, pp. 31–39.
- [169] Simpson, E.M., Linder, C.C., Sargent, E.E., Davisson, M.T., Mobraaten, L.E., Sharp, J.J., Okkenhaug, K., Hagenbeek, T.J., Spits, H., and Cantrell, D.A., "Genetic Variation among 129 Substrains and its Importance for Targeted Mutagenesis in Mice," *Nature Genetics*, Vol. 16, No. 1, 1997, pp. 19–27.
- [170] Sinclair, L.V., Finlay, D., Feijoo, C., Cornish, G.H., Gray, A., Ager, A., Okkenhaug, K., Hagenbeek, T.J., Spits, H., and Cantrell, D.A., "Phosphatidylinositol-3-OH Kinase and Nutrient-Sensing mTOR Pathways Control T Lymphocyte Trafficking," *Nature Immunology*, Vol. 9, No. 5, 2008, pp. 513–521.

- [171] Smith-Garvin, J.E., Koretzky, G.A., and Jordan, M.S., "T Cell Activation," *Annual Review of Immunology*, Vol. 27, No. 1, 2009, pp. 591–619.
- [172] Sojka, D.K., Bruniquel, D., Schwartz, R.H., and Singh, N.J., "IL-2 Secretion by CD4+ T Cells In Vivo Is Rapid, Transient, and Influenced by TCR-Specific Competition," *The Journal of Immunology*, Vol. 172, No. 10, 2004, pp. 6136–6143.
- [173] Sommer, K., Guo, B., Pomerantz, J.L., Bandaranayake, A.D., Moreno-Garcia, M.E., Ovechkina, Y.L., and Rawlings, D.J., "Phosphorylation of the CARMA1 Linker Controls NF- $\kappa$ B Activation," *Immunity*, Vol. 23, No. 6, 2005, pp. 561–574.
- [174] Soriano, P., "Generalized lacZ Expression with the ROSA26 Cre Reporter Strain," *Nature Genetics*, Vol. 21, No. 1, 1999, pp. 70–71.
- [175] Southern, E. M., "Detection of Specific Sequences among DNA Fragments Separated by Gel Electrophoresis," *Journal of Molecular Biology*, Vol. 98, No. 3, 1975, pp. 503–517.
- [176] Srinivas, S., Watanabe, T., Lin, C.-S., Williams, C., Tanabe, Y., Jessell, T., and Costantini, F., "Cre Reporter Strains Produced by Targeted Insertion of EYFP and ECFP into the ROSA26 Locus," *BMC Developmental Biology*, Vol. 1, No. 1, 2001, pp. 1–4.
- [177] Steele, R.E., Stover, N.A., and Sakaguchi, M., "Appearance and Disappearance of Syk Family Protein-Tyrosine Kinase Genes during Metazoan Evolution," *Gene*, Vol. 239, No. 1, 1999, pp. 91–97.
- [178] Streubel, B., Vinatzer, U., Willheim, M., Raderer, M., and Chott, A., "Novel t(5;9)(q33;q22) Fuses ITK to SYK in Unspecified Peripheral T-Cell Lymphoma," *Leukemia*, Vol. 20, No. 2, 2006, pp. 313–318.
- [179] Sutcliffe, J.G., "Nucleotide Sequence of the Ampicillin Resistance Gene of Escherichia Coli Plasmid pBR322," *Proceedings of the National Academy of Sciences of the United States of America (PNAS) Natl. Acad. Sci. USA*, Vol. 75, No. 8, 1978, pp. 3737–3741.
- [180] Takahama, Y., "Journey through the Thymus: Stromal Guides for T-Cell Development and Selection," *Nature Reviews Immunology*, Vol. 6, No. 2, 2006, pp. 127–135.
- [181] Takata, M., Sabe, H., Hata, A., Inazu, T., Homma, Y., Nukada, T., and Kurosaki, T., Y., "Tyrosine Kinases Lyn and Syk Regulate B Cell Receptor-Coupled Ca<sup>2+</sup> Mobilization Through Distinct Pathways," *The EMBO Journal*, Vol. 13, No. 6, 1994, pp. 1341–1349.

- [182] Tomasz, M., Lipman, R., Chowdary, D., Pawlak, J., Verdine, G.L., and Nakanishi, K., "Isolation and Structure of a Covalent Cross-Link Adduct between Mitomycin C and DNA," *Science*, Vol. 235, No. 4793, 1987, pp. 1204–1208.
- [183] Torres, R.M. and Kuehn, R., *Laboratory Protocols for Conditional Gene Targeting*, Oxford University Press, Oxford, UK, 1997.
- [184] Tsang, E., Giannetti, A.M., Shaw, D., Dinh, M., Tse, J.K.Y., Gandhi, S., Ho, H., Wang, S., Papp, E., and Bradshaw, J.M., "Molecular Mechanism of the Syk Activation Switch," *Journal of Biological Chemistry*, Vol. 283, No. 47, 2008, pp. 32650–32659.
- [185] Turner, J.M., Brodsky, M.H., Irving, B.A., Levin, S.D., Perlmutter, R.M., and Littman, D.R., "Interaction of the Unique N-Terminal Region of Tyrosine Kinase p56lck with Cytoplasmic Domains of CD4 and CD8 is Mediated by Cysteine Motifs," *Cell*, Vol. 60, No. 5, 1990, pp. 755–765.
- [186] Turner, M., Mee, P.J., Costello, P.S., Williams, O., Price, A.A., Duddy, L.P., Furlong, M.T., Geahlen, R.L., and Tybulewicz, V.L., "Perinatal Lethality and Blocked B-Cell Development in Mice Lacking the Tyrosine Kinase Syk," *Nature*, Vol. 378, No. 6554, 1995, pp. 298–302.
- [187] Turner, S.D. and Alexander, D.R., "Fusion Tyrosine Kinase Mediated Signalling Pathways in the Transformation of Haematopoietic Cells," *Leukemia*, Vol. 20, No. 4, 2006, pp. 572–582.
- [188] Underhill, D.M. and Goodridge, H.S., "The Many Faces of ITAMs," *Trends in Immunology*, Vol. 28, No. 2, 2007, pp. 66–73.
- [189] Valitutti, S., Mueller, S., Salio, M., and Lanzavecchia, A., "Degradation of T Cell Receptor (TCR)-CD3- $\zeta$  Complexes after Antigenic Stimulation," *The Journal of Experimental Medicine*, Vol. 185, No. 10, 1997, pp. 1859–1864.
- [190] Vallabhapurapu, S. and Karin, M., "Regulation and Function of NF- $\kappa$ B Transcription Factors in the Immune System," *Annual Review of Immunology*, Vol. 27, No. 1, 2009, pp. 693–733.
- [191] van Dongen, J.J., Langerak, A.W., Brueggemann, M., Evans, P.A.S., Hummel, M., Lavender, F.L., Delabesse, E., Davi, F., Schuurink, E., Garca-Sanz, R., van Krieken, J.H.J.M., Droese, J., Gonzalez, D., Bastard, C., White, H.E., Spaargaren, M., Gonzalez, M., Parreira, A., Smith, J.L., Morgan, G.J., Kneba, M., and Macintyre, E.A., "Design and Standardization of PCR Primers and Protocols for Detection

- of Clonal Immunoglobulin and T-Cell Receptor Gene Recombinations in Suspect Lymphoproliferations: Report of the BIOMED-2 Concerted Action BMH4-CT98-3936," *Leukemia*, Vol. 17, No. 12, 2003, pp. 2257–2317.
- [192] van Heyningen, S., "Cholera Toxin: Interaction of Subunits with Ganglioside GM1," *Science*, Vol. 183, No. 4125, 1974, pp. 656–657.
- [193] Vose, J., Armitage, J., and Weisenburger, D., "International Peripheral T-Cell and Natural Killer/ T-Cell Lymphoma Study: Pathology Findings and Clinical Outcomes," *Journal of Clinical Oncology*, Vol. 26, No. 25, 2008, pp. 4124–4130.
- [194] Wang, C., Deng, L., Hong, M., Akkaraju, G. R., Inoue, J.-i., and Chen, Z.J., "TAK1 is a Ubiquitin-Dependent Kinase of MKK and IKK," *Nature*, Vol. 412, No. 6844, 2001, pp. 346–351.
- [195] Wang, H., Kavanaugh, M.P., North, R.A., and Kabat, D., "Cell-Surface Receptor for Ecotropic Murine Retroviruses is a Basic Amino-Acid Transporter," *Nature*, Vol. 352, No. 3, 1991, pp. 729–731.
- [196] Weinblatt, M.E., Kavanaugh, A., Burgos-Vargas, R., Dikranian, A.H., Medrano-Ramirez, G., Morales-Torres, J.L., Murphy, F.T., Musser, T.K., Straniero, N., Vicente-Gonzales, A.V., and Grossbard, E., "Treatment of Rheumatoid Arthritis with a Syk Kinase Inhibitor: a Twelve-Week, Randomized, Placebo-Controlled Trial," *Arthritis and Rheumatism*, Vol. 58, No. 11, 2008, pp. 3309–3318.
- [197] Wienands, J., Schweikert, J., Wollscheid, B., Jumaa, H., Nielsen, P.J., and Reth, M., "SLP-65: A New Signaling Component in B Lymphocytes which Requires Expression of the Antigen Receptor for Phosphorylation," *The Journal of Experimental Medicine*, Vol. 188, No. 4, 1998, pp. 791–795.
- [198] Williams, R.L., Hilton, D.J., Pease, S., Willson, T., Stewart, C.L., Gearing, D.P., Wagner, E.F., Metcalf, D., Nicola, N.A., and Gough, N.M., "Myeloid Leukaemia Inhibitory Factor Maintains the Developmental Potential of Embryonic Stem Cells," *Nature*, Vol. 336, No. 6200, 1988, pp. 684–687.
- [199] World Health Organization, *WHO Classification of Tumours of Haematopoietic and Lymphoid Tissues, 4th Edition*, IARC Press, Lyon, France, 2008.
- [200] Yamaguchi, H. and Hendrickson, W.A., "Structural Basis for Activation of Human Lymphocyte Kinase Lck upon Tyrosine Phosphorylation," *Nature*, Vol. 384, No. 6608, 1996, pp. 484–489.

- [201] Zain, J. and O'Connor, O., "Targeted Treatment and New Agents in Peripheral T-Cell Lymphoma," *International Journal of Hematology*, Vol. 92, No. 1, 2010, pp. 33–44.
- [202] Zambrowicz, B.P., Imamoto, A., Fiering, S., Herzenberg, L. A., Kerr, W. G., and Soriano, P., "Disruption of Overlapping Transcripts in the ROSA $\beta$ geo 26 Gene Trap Strain Leads to Widespread Expression of  $\beta$ -Galactosidase in Mouse Embryos and Hematopoietic Cells," *Proceedings of the National Academy of Sciences of the United States of America (PNAS)*, Vol. 94, No. 8, 1997, pp. 3789–3794.
- [203] Zhang, J., Billingsley, M.L., Kincaid, R., and Siraganian, R.P., "Phosphorylation of Syk Activation Loop Tyrosines Is Essential for Syk Function," *Journal of Biological Chemistry*, Vol. 275, No. 45, 2000, pp. 35442–35447.
- [204] Zhang, J., Salojin, K.V., Gao, J.-X., Cameron, M.J., Bergerot, I., and Delovitch, T.L., "p38 Mitogen-Activated Protein Kinase Mediates Signal Integration of TCR/CD28 Costimulation in Primary Murine T Cells," *The Journal of Immunology*, Vol. 162, No. 7, 1999, pp. 3819–3829.
- [205] Zhang, J., Yang, P.L., and Gray, N.S., "Targeting Cancer with Small Molecule Kinase Inhibitors," *Nature Reviews Cancer*, Vol. 9, No. 1, 2009, pp. 28–39.
- [206] Zhang, W., Tribble, R.P., and Samelson, L.E., "LAT Palmitoylation: Its Essential Role in Membrane Microdomain Targeting and Tyrosine Phosphorylation during T Cell Activation," *Immunity*, Vol. 9, No. 2, 1998, pp. 1074–7613.
- [207] Zhang, Y., Oh, H., Burton, R.A., Burgner, J.W., Geahlen, R.L., and Post, C.B., "Tyr130 Phosphorylation Triggers Syk Release from Antigen Receptor by Long-Distance Conformational Uncoupling," *Proceedings of the National Academy of Sciences of the United States of America (PNAS)*, Vol. 105, No. 33, 2008, pp. 11760–11765.